THE NATURE OF FLUORINATED OXIDE CATALYSTS: A NUCLEAR MAGNETIC RESONANCE INVESTIGATION

Thesis by

John Robert Schlup

In Partial Fulfillment of the Requirements

for the Degree of

Doctor of Philosophy

California Institute of Technology
Pasadena, California

1981

(Submitted May 8, 1981)

This thesis is dedicated to Robert W. Vaughan, and to Gil Gazanian, Roger Bosch and Carl Garbe.

"Not only was the Teacher wise, but also he imparted knowledge to the people. He pondered and searched out and set in order many proverbs. The teacher searched to find just the right words, and what he wrote was upright and true. The words of the wise are like goads, their collected sayings like firmly embedded nails - given by one shepard."

Ecclesiastes 12:9-11

Acknowledgments

There are many individuals who have contributed directly and indirectly to my growth during my graduate studies. It is inevitable that some of their names will be omitted here and I ask forgiveness for any omissions in advance.

Professor Vaughan's guidance during the first 3½ years of my graduate study has been invaluable. His availabiliy to his students and his desire to help us learn how to approach scientific problems will always be an example for me. Gil Gazanian, Carl Garbe, and Roger Bosch have complemented Bob Vaughan well. Just as Bob Vaughan invested in my professional growth, Gil, Roger, and Carl have invested in my personal and spiritual growth. My growth in these areas directly reflect their contributions. These four men have been my teachers in every sense of the word.

This period of my life will be memorable because I have been able to be a part of Lake Avenue Congregational Church. The people there who have shared in my life are responsible for nurturing my excitement for God. Their prayer support and love have brought me much peace and joy.

One particular individual who I met at Lake Avenue Congregational Church has beome very important to me...my wife, Jody. I cannot thank her enough for the patience and the love she has shown to me during the time we have shared while this thesis was being completed.

Professors S. I. Chan and W. H. Weinberg have been instrumental

in the completion of my graduate studies. Professor Chan's assistance in helping to maintain my financial support was invaluable. I will always remember the investment of time made by both of these men. Their support and the support of other members of the Caltech community following Professor Vaughan's death has been very encouraging.

The staff at Caltech has been wonderful. The technical support provided by John Yehle and George Griffith was essential in building and maintaining the equipment needed for my experiments. I also want to thank Lori Rudee and Sharon ViGario for typing this manuscript.

My stay in California has been made very pleasant by many people who have become my good friends. Graduate study enabled Russ Bone and me tocontinue a friendship that began at Kansas State. My relationship with Jeff Reimer encouraged my professional and spiritual growth, especially as we grew together in the knowledge of our God. Several families (the Newtons, Carol and Ernie Boehr, and the Schicketanzs) have seen that my holidays were with "family" and they have truly allowed their homes to become my home.

The contributions made by my parents began long before I came to Caltech. I have only begun recently to appreciate the way in which they allowed me to pursue the opportunities that have come my direction. Their love has been everpresent.

The Department of Energy has provided the financial support during my graduate studies. I am especially grateful for their continuing support following Professor Vaughan's death.

Abstract

Fluorination of oxide catalysts has been shown to drastically change the catalytic properties of these materials. The catalytic activity of these materials has been studied using a wide variety of reactions. Research on fluorinated oxides has focused upon improving product yields and product selectivity and upon obtaining a better understanding of the unmodified oxide catalyst as changes due to fluorination are observed. The purpose of this investigation has been to demonstarate the utility of pulsed nuclear magnetic resonance (NMR) spectroscopy as a direct spectroscopic probe of the local chemical environment of the hydroxyl groups and the fluorine atoms of these materials.

Quantitative analysis of the hydroxyl group and fluorine atom concentrations of these materials is difficult. Most techniques used previously require temperatures in excess of 1200 K and result in destruction of the sample. NMR has been shown to be an effective non-destructive quantitative tool. Precision of 5% has been demonstrated with samples containing as few as 5×10^{18} hydrogen or fluorine atoms.

The chemical shift interaction has shown that the fluorine forms covalent bonds to the silicon and aluminum atoms of silica, alumina, and various aluminosilicates. If an aluminosilicate contains 11 wt% alumina, only SiF and SiOH species are observed. SiF, SiOH, AlF, and AlOH species are observed for aluminosilicates containing 48 wt% alumina. The SiF bond is identical for all fluorinated silicas and aluminosilicates calcined at 873 K. The Carr-Purcell-Meiboom-Gill

data show that the hydroxyl groups are well isolated from one another for all samples. The same is true for the fluorine atoms.

The decay constants of the hydrogen and fluorine 90^{o}-τ-180^{o} and Carr-Purcell-Meiboom-Gill experiments differ by at least a factor of ten. Therefore, the nuclei are experiencing fluctuations in their local magnetic fields, probably as a result of anisotropic motion or diffusion. The behavior of the spectra observed at temperatures between 110 K and 290 K is very dependent upon the type of oxide, the degree of fluorination, and the calcining temperature.

Table of Contents

CHAPTER I

INTRODUCTION

An understanding of catalysis has been the goal of many chemical engineering investigations. One goal of catalytic research has been the development of catalysts which have better product yields or improved product selectivity or which allow less severe reactor conditions. The development of fluorinated oxide catalysts is a good example of this type of research. The number of patents issued on these materials demonstrates their usefulness. Among the catalytic oxides used to prepare these materials are alumina (1, 6), zirconia (2, 3), silica-alumina-zirconia (4), silica-magnesia (5), and crystalline aluminosilicates (7, 8). These materials have been reported to catalyze isomerization (1, 2, 6, 7), alkylation (1, 3, 4, 5), and skeletal rearrangement (6, 8) reactions of hydrocarbons. The patents mentioned above are only a sample of the industrial uses of fluorinated oxides. A comprehensive review article that provides further information about the patent literature and that summarizes the research literature about fluorinated oxide catalysts has been prepared by V. R. Choudhary **(9)**. This investigation focused on the properties of amorphous silica, alumina, and aluminosilicates which have been treated with aqueous ammonium fluoride solutions.

The fluorination of zeolitic materials has been reported as early as 1958. Cannon has demonstrated that chlorodifluoromethane and dichlorodifluoromethane adsorb irreversibly on various zeolites (10, 11, 12). Cannon focused on the adsorption properties of the zeolites and the fluorinated zeolites. Their catalytic properties were not studied. The desorption isotherms of these fluorinated methanes are similar to those observed for carbon dioxide. Carbon dioxide is the only product

observed during desorption. Although there is a decrease in the surface area of the material, X-ray diffraction indicates no gross changes in the surface structure. Analysis of the modified zeolite showed that fluorine atoms were present in the zeolite.

The catalytic activity of α- and β-aluminum trifluoride for cracking reactions has been studied also (13). The catalysts were prepared by thermal decomposition of NH_4AlF_4. The hexagonal β-structure has significant cracking activity at temperatures below 700 K. This is not true of the rhombic α-structure. The catalytic activity of aluminum hydroxyfluorides has been studied also (14, 15, 16).

The catalytic activity of fluorinated silica, alumina, and aluminosilicates have been studied using a wide variety of reactions. The conversion of propylene during propylene polymerization using a fluorinated alumina catalyst increases from 0 to 0.03%/m^2 as the fluorine content of the catalyst increases from 0 to 4 wt% (17, 18). Peri reported that fluorinated alumina and aluminosilicates readily dimerized butene (19). However, fluorinated aluminosilicates were never more active than similarly calcined unmodified aluminosilicates. Fluorinated silica showed no activity for butene polymerization.

Several isomerization reactions have been studied using fluorinated alumina and aluminosilicate catalysts. The rate of isomerization of o-xylene (17), cyclopropane (20), and C_{11} to C_{14} hydrocarbons (21) is higher for fluorinated alumina catalysts than for the unmodified alumina. Maximum activity as a function of catalyst fluorine concentration is usually observed for catalysts containing less than 10 wt% fluorine. The butene isomerization reaction is used often in evaluating the isomerization

activity of catalysts. Choudhary and Doraiswamy (22) demonstrated that fluorination of η-alumina increased the conversion of n-butene to isobutene from 4.1% to greater than 20% with a catalyst containing 0.85% fluorine having maximum activity. Fluorinated alumina was the most active of the catalysts studied. Finch and Clark (23) studied the reactions of 1-butene on fluorinated alumina using ammonia-blocking and isotropic tracer experiments. The butene formed a polymeric complex. Maximum activity occurred at a fluoride concentration of 12.4×10^{14} F^-/cm^2. All fluorinated aluminas were more active than the unmodified alumina.

Fluorination of cracking catalysts significantly influences their reactivity and selectivity. Hall and co-workers (20, 24) have shown that fluorination of alumina catalysts increases the reaction rate for 2, 3-dimethylbutane cracking and maximum activity is observed for fluorine contents of 2.7%. The catalytic activity of an aluminosilicate, a fluorinated aluminosilicate, and silica-magnesia have been compared for methylcyclohexane and n-decane cracking reactions (25). The fluorinated aluminosilicate had the highest activity and the least coke formation. Komarov et. al. (26) reported reduced coke formation during the cracking of petroleum gas-oil fractions when fluorinated aluminosilicate catalysts were used. Fluorination increases the activity for cracking n-octane and the molar ratios of the products change as the fluorine content of the catalyst increases (17). The most significant changes occur with catalysts containing 1.6% to 3% fluorine.

Several investigators have studied cumene cracking using fluorinated oxide catalysts. Fluorinated silica gel has been shown to have lower

catalytic activity than silicas prepared using other halogens (27). However, the rate constants measured for fluorinated silica are over ten times larger than those observed using unmodified silica. Chapman and Hair (28) showed that the conversion of cumene to benzene catalyzed by a fluorinated silica glass approached the conversion reported for an aluminosilicate. A maximum in cumene cracking activity occurs when fluorinated aluminosilicates contain 0.5 to 1.0 wt% fluorine (29). Covini et al. (30) observed maximum cumene conversion per gram of catalyst for a fluorinated alumina containing 10 wt% fluorine. The activity per unit surface area has maxima at 10 wt% fluorine and at 50 wt% fluorine.

Although the usefulness of fluorinated oxide catalysts has been demonstrated, an understanding of how these materials influence a reaction has not been obtained. That understanding is necessary if a prediction of the performance of a reactor for a variety of feedstocks and operating conditions is needed.

Measurements of the surface acidity of fluorinated oxides have been made attempting to explain the activity of these catalysts. Katsuo and co-workers reported that the acid sites of fluorinated silica were weak and that the number of strong acid sites was less for fluorinated silica than for other halogenated silicas (27). The acidity of fluorinated alumina has been measured by a variety of techniques and a variety of interpretations of the results have been reported. Results from butylamine titration have been interpreted as showing only the presence of Lewis acid sites with a maximum acidity for catalysts containing 10 wt% fluorine (30). Data acquired from the infrared spectrum of adsorbed pyridine (31)

and from titrations using indicators forming stable surface carbonium ions (32) have been interpreted as resulting from the existence of both Lewis and Bronsted acid sites. Ammonia adsorption experiments have been performed. An increase in the acid strength upon fluorination has been reported while the number of acid sites is not affected (33). A maximum in the ammonia adsorption has been reported at $4 \times 10^{14}/Fcm^2$ (20). The Hammett acidities reported for fluorinated aluminosilicates have shown a maximum at fluorine concentrations of approximately 2 weight percent (29).

The data mentioned above contain much information about the catalytic activity and the acidity of fluorinated oxides. However, using these data to understand the properties of the catalyst at the molecular level requires developing a model of the catalyst at the molecular level so that macroscopic properties can be predicted. An unambiguous interpretation of the data is difficult to obtain. It is more desirable to obtain information about the catalyst at the molecular level by using spectroscopic probes specific for the chemical environments of interest.

Several questions are basic to an understanding of catalytic materials at the molecular level. The surface area of the catalyst and the concentration of the chemical species of interest must be known. An understanding of the geometry and chemical nature of the catalyst surface is needed. A knowledge of the specific properties of the surface species is needed to determine if a specific spectroscopic technique can be used as a direct probe of the chemical environment of interest.

X-ray photoelectron spectroscopy (XPS), X-ray diffraction, infrared (IR) spectroscopy, and nuclear magnetic resonance (NMR) spectroscopy have

been used to study fluorinated silica, alumina, and aluminosilicates. XPS has shown that the fluorine 1s binding energy changes as a function of fluorine concentration and calcining conditions (34). Results from combined XPS and X-ray diffraction studies have demonstrated the formation of surface fluorine-containing compounds (35, 36). Isolated fluorine atoms exist at low fluorine concentrations. As the fluorine concentration increases, $(NH_3)_3$ AlF_6 crystallites form which are transformed into a low surface area α-AlF_3 phase on calcination. Aluminum hydroxyfluorides and β-AlF_3 have been reported at fluorine concentrations greater than 10 wt% fluorine.

Infrared spectroscopy has been the spectroscopic tool used most extensively. Several investigators have studied the infrared spectrum of fluorinated silica (28, 37, 38 39). A band at 3745 cm^{-1} is attributed to isolated hydroxyl groups. The intensity of this band decreased after the adsorption of the fluorine atoms. This band disappeared upon calcining at temperatures above 773 K. These vibrations are observed at temperatures above 1273 K for unmodified silicas. An asymmetric band is observed at 3690 cm^{-1} and its intensity is less affected by fluorination. The species causing this vibration is stable at temperatures as high as 773 K. Deuterium exchange experiments suggest that it results from hydroxyl groups which have formed hydrogen bonds. The effects of rehydration of the fluorinated silicas on their infrared spectrum depends upon the hydration conditions.

The infrared spectrum of fluorinated alumina has been reported by Peri (38) and by Antipina and co-workers (14). Peri treated alumina and aluminosilicate aerogel plates with NH_4F vapor. Evacuation of the alumina

plates for one hour at 873 K resulted in aluminas with two weak hydroxyl groups with stretching vibrations at 3690 cm^{-1} and 3745 cm^{-1}. Further heat treatment at 873 K resulted in the disappearance of these bands from the spectrum. No hydroxyl groups vibrations were observed in the infrared spectrum of fluorinated aluminosilicates containing 32.7% alumina and calcined in the same manner as the fluorinated alumina.

The effects of fluorination of the oxide upon the infrared spectra of small molecules adsorbed onto the fluorinated and the unmodified oxide have been studied also. Carbon monoxide (38), carbon dioxide (38), butene (38), pyridine (14, 16, 36, 38), dioxane (36), benzene (36), and t-butylcyanide (36) have been used as probe molecules. The infrared spectrum of pyridine adsorbed on fluorinated alumina was used to detect the Lewis and Bronsted acid sites of the catalyst (31). Although several aluminum-fluorine surface species were discussed, direct observation of the fluorine species by infrared spectroscopy was not reported.

Infrared spectroscopy has two limitations as a spectroscopic tool for fluorinated oxides. Infrared spectroscopy is not a quantitative technique. The use of IR spectroscopy for quantitative analysis requires the assumption that the oscillator strength of the vibration of interest is the same for each sample and for the reference sample. The second limitation is that direct observations of fluorine-containing species have not been reported. For example, fluorine-silicon infrared bands are expected to be in the 800-1100 cm^{-1} region (40). The vibrations of the silica lattice are in this region of the spectrum and obscure the fluorine-silicon vibrations. Therefore, infrared spectra will provide information only about the local chemical environments of the hydroxyl

groups.

The usefulness of a specific spectroscopic technique depends upon the catalytic system being investigated and upon the questions to be answered. For example, the techniques used in studying fluorinated oxides which have been discussed to this point either have not been useful for studying hydroxyl groups or have not been able to study the chemical environment of the fluorine atoms due to interference from the oxide lattice. It is difficult to study molecular motion of the hydroxyl groups and fluorine atoms using the above techniques.

The chemical species of interest on fluorinated oxide catalysts are hydroxyl groups and fluorine atoms. A spectroscopic technique that can detect both of these environments is nuclear magnetic resonance. Golovanova and co-workers obtained the hydrogen NMR spectrum of fluorinated silica at 83 K (39). Fluorine did not replace all of the hydroxyl groups. A two component spectrum was reported following heat treatment at 373 K. The narrow component was similar to that of unmodified silica and its intensity decreased with increasing pretreatment temperatures. It had disappeared by 723 K. The line width of the broad component following heat treatment at 373 K was 12 G and it narrowed to 8 G after heat treatment at 723 K.

The fluorine NMR spectrum of fluorinated alumina was reported by Golovanova and co-workers (41) and by O'Reilly (42). Golovanova and co-workers reported that a two component hydrogen spectrum was observed for fluorinated aluminas containing 6 wt% fluorine. Hydroxyl groups were reported on fluorinated alumina containing 11 wt% fluorine. The fluorine atoms were not mobile at 290 K. Golovanova postulated that two

populations of fluorine atoms existed and that their relative populations changed as a function of the fluroine concentration and the calcining temperature.

O'Reilly (42) observed the fluorine resonance of fluorinated aluminas with fluorine concentrations ranging from 0.3 to 12.5 wt%. Surface fluorine atoms were differentiated from bulk fluoride species by studying the effect of adsorbed water on the fluorine spin-lattice relaxation times. Surface fluorine atoms were present at low fluorine concentrations. A bulk fluoride phase began to appear at fluorine concentrations greater than 5 wt%.

The NMR data reported above were obtained using wide line spectrometers. The first derivative of the absorption curve is reported. Details of the line shape are difficult to see in such spectra. The fluorine spectrum of fluorinated silica has not been reported and no spectra of fluorinated aluminosilicates have been obtained.

The objective of this investigation is to understand further the chemical nature of fluorinated silica, alumina, and aluminosilicates using nuclear magnetic resonance techniques. Report techniques for the quantitative analysis of the hydroxyl group and fluorine atom concentrations are difficult. Temperatures in excess of 1200 K usually are required and the sample is destroyed during the analysis. Quantitative NMR is a non-destructive technique and the hydrogen and fluorine concentrations have been obtained for a number of fluorinated oxides prepared under a variety of conditions. The NMR chemical shift interaction is caused by the distortion of the magnetic field at a particular nuclear site by the distribution of electrons about the nucleus. Therefore, the chemical

shift interaction can be used to describe the chemical bonding experienced by that nucleus. This is especially important since the manner in which the fluorine bonds to the oxide has not been determined.

Molecular motion causes fluctuations in the physical parameters which determine the contribution to the spectrum from the chemical shift and the dipolar interactions. NMR can be a useful tool in describing the motion of the hydroxyl groups and the fluorine atoms of fluorinated oxides. Several investigators have suggested that increased mobility of the hydrogen atoms of the hydroxyl groups are responsible for the increased catalytic activity. However, no direct observation of this mobility has been reported previously.

The dipolar interaction is useful of describing the local environment about the resonant nuclei. This will provide information about the proximity of neighboring hydroxyl groups and fluorine atoms. The existence of hydrogen bonds between neighboring hydroxyl groups and fluorine will cause the NMR spectrum to have a large contribution from the dipolar interaction.

A review of the various interactions and NMR techniques pertinent to this investigation is given in Chapter 2. Chapter 3 discusses the hydrogen and fluorine NMR spectra of fluorinated silicas prepared under a variety of conditions. The hydrogen and fluorine NMR spectra of fluorinated aluminas and aluminosilicates are discussed in Chapter 4. Appendix A presents butene isomerization data obtained using a fluorinated aluminosilicate catalyst and relates the kinetic data to the material properties of the fluorinated aluminosilicate.

References

1. Sobel, J. E. (to Universal Oil Products Co.) U. S. Patent 3 763 261 (Oct. 2, 1973).
2. Hervert, G. L., and Lin, C. B., U. S. Patent 3 217 059 (Nov. 9, 1965).
3. Hervert, G. L., Linn, C. B., U. S. Patent 3 054 834 (Sept. 18, 1962).
4. Hervert, G. L., Linn, C. B., U. S. Patent 3 054 835 (Sept. 18, 1962).
5. Hervert, G. L., Linn, C. B., U. S. Patent 3 050 570 (Aug. 21, 1962).
6. Moore, L. D., Odioso, R. C., U. S. Patent 3 217 057 (Nov. 9, 1965).
7. Hervert, G. L., U. S. Patent 3 467 728 (Sept. 16, 1969).
8. Fishel, N. A., U. S. Patent 3 413 370 (Nov. 26, 1968).
9. Choudhary, V. R., Ind. Eng. Chem., Product Res.and Develop. 16, 12 (1977).
10. Cannon, P., J. Amer. Chem. Soc. 80, 1766 (1958).
11. Cannon, P., J. Phys. Chem. 63, 160 (1959).
12. Cannon, P., in "Solid Surfaces and the Gas-Solid Interface," Advances in Chemistry Series (R. F. Gould, Ed.). Vol. 33, p. 122. American Chemical Society, Washington, D. C., 1961.
13. Moerkerken, A., Behr, B., Noordeloos-Maas, M. A., and Boelhouwer, C., J. Catal. 24, 177 (1972).
14. Antipina, T. V., Bulgakov, O. V., and Uvarov, A. V., in "Proceedings of the Fourth International Congress on Catalysis (Moscow), 1968" (J. W. Hightower, Ed.). Vol. 4, p.1387. Rice

University Printing and Reproduction Dept., Houston, 1969.

15. Antipina, T. V., Bulgakov, O. V., and Yushchenko, V. V., Kinet. Katal. 9, 196 (1968).
16. Antipina, T. V., and Bulgakov, O. V., Dokl. Akad, Nauk SSSR, 179, 845 (1968).
17. Holm, V. C. F., and Clark, A., Ind. Eng. Chem., Product Res. and Develop. 2, 38 (1963).
18. Holm, V. C. F., and Clark, A., J. Catal. 8, 286 (1967).
19. Peri, J. B., J. Phys. Chem. 72, 2917 (1968).
20. Gerberich, H. R., Lutinski, F. E., and Hall, W. K., J. Catal. 6, 209 (1966).
21. Orkin, B. A., Ind. Eng. Chem., Product Res. and Develop. 8, 154 (1969).
22. Choudhary, V. R., and Doraiswamy, L. K., J. Catal. 23, 54 (1971).
23. Finch, J. N., and Clark, A., J. Catal. 19, 292 (1970).
24. Hall, W. K., Lutinski, F. E., and Gerberich, H. R., J. Catal. 3, 512 (1964).
25. Plank, C. J., Sibbett, D. J., and Smith, R. B., Ind. Eng. Chem. 49, 742 (1957).
26. Komarov, V. S., Varlamov, V. I., Semyachko, R. Ya., and others, Russ. J. Phys. Chem. 45, 41 (1971).
27. Katsuo, T., Satohiro, Y., and Kimio, T., Bull. Jap. Petrol. Inst. 12, 136 (1970).
28. Chapman, I. D., and Hair, M. L., J. Catal. 2, 145 (1963).
29. Sano, M., Hosino, T., Yotsuyanagi, T., and Aomura, K., Kogyo Kogaku Zasshi 73, 2541 (1970).

30. Covini, R., Fattore, V., and Giordano, N., J. Catal. 7, 126 (1967).

31. Hughes, T. R., White, H. M., and White, R. J., J. Catal. 13, 58 (1969).

32. Hirschler, A. E., J. Catal. 2, 428 (1963).

33. Webb, A. N., Ind. Eng. Chem. 49, 261 (1957).

34. Evans, H. E., Ph.D. thesis, California Institute of Technology, 1980.

35. Kerkhof, F. P. J. M., Moulijn, J. A., Thomas, R., and Oudejans, J. C., in "Preparations of Catalysts II, Studies in Surface Science and Catalysis" (B. Delmon, P. Grange, P. Jacobs, and G. Poncelet, Eds.). Vol. 3, p. 77. Elsevier Scientific Publishing Co., New York, 1979.

36. Scokart, P. D., Selim, S. A., Damon, J. P., and Rouxhet, P. G., J. Coll. Interf. Sci. 70, 209 (1979).

37. Sidorov, A. N., and Neimark, I. E., Russ. J. Phys. Chem. 38, 1518 (1964).

38. Peri, J. B., J. Phys. Chem. 72, 2917 (1968).

39. Golovanova, G. F., Ivanova, N. N., and others, Theor. Exp. Chem., USSR 9, 301 (1973).

40. "Silicon Compounds: Register and Review" (B. C. Arkles and W. R. Peterson, Jr., Eds.). p. 110. Petrarch Systems, Inc., Levittown, Pa., 1979.

41. Golovanova, G. F., Kvlividze, V. I., and Kiselev, V. F., Kinet. Katal. 16, 761 (1975).

42. O'Reilly, D. E., in "Advances in Catalysis" (D. D. Eley, H. Pines, and P. B. Weiss, Eds.). Vol. 12, P. 31. Academic Press, New York, 1960.

CHAPTER II

AN OVERVIEW OF THE NUCLEAR MAGNETIC RESONANCE TECHNIQUES USED IN THIS INVESTIGATION

The use of nuclear magnetic resonance (NMR) as a spectroscopic probe of catalysts was discussed briefly in the previous chapter. The goal of this chapter is to assist the reader in visualizing the experiments and equipment that are involved in this investigation.

Several conventions will be followed throughout this discussion. The direction of the equilibrium magnetization is parallel to the applied magnetic field and that direction is defined to be the z-axis of the coordinate system. A 90^{o} pulse is defined as a radio frequency pulse which, when applied to the sample, can rotate the magnetization through 90^{o} (rotating the equilibrium magnetization from the z-axis into the xy-plane for example). A 180^{o} pulse rotates the magnetization through 180^{o}. Two-pulse sequences will be described by expressions of the form $\alpha\text{-}\tau\text{-}\beta_{\phi}$, where α is the pulse length of the initial pulse, β is the pulse length of the second pulse, τ is the pulse separation, and ϕ is the relative phase difference between the two pulses. Resonant spins will be designated as the I-spin system. The non-resonant spins are designated as the S-spin system.

A. An Overview of the NMR Interactions

The samples being investigated contain both hydrogen and fluorine. A simplified spin Hamiltonian in frequency units for a solid containing hydrogen and fluorine can be expressed as

$$H = H_o + H_1 \qquad (1)$$

where

$$H_o = -\gamma_I \Sigma_i B_o I_{iz} - \gamma_S \Sigma_j B_o S_{jz} \qquad (2)$$

= Zeeman interactions with the external field, B_o, for both spin systems.

The perturbation Hamiltonian, H_1, is defined as below.

$$H_1 = H_{II} + H_{SS} + H_{IS} + H_\sigma \tag{3}$$

In this expression, H_{II} and H_{SS} are the truncated homonuclear dipolar Hamiltonians for the interactions between resonant and non-resonant spins. These Hamiltonians can be expressed as

$$H_{II} = \frac{1}{4}\gamma_I^2\hbar\,\Sigma_{j,k}\left(\frac{-(1-3\cos^2\theta_{jk})}{r_{jk}^3}\,\underset{\sim}{I_j}\underset{\sim}{I_k} + \frac{3(1-3\cos^2\theta_{jk})}{r_{jk}^3}\,I_{jz}I_{kz}\right) \tag{4}$$

$$H_{SS} = \frac{1}{4}\gamma_S^2\hbar\,\Sigma_{m,n}\left(\frac{-(1-3\cos^2\theta_{mn})}{r_{mn}^3}\,\underset{\sim}{S_m}\cdot\underset{\sim}{S_n} + \frac{3(1-3\cos^2\theta_{mn})}{r_{mn}^3}\,S_{mz}S_{nz}\right) \tag{5}$$

H_{IS} is the truncated diploar Hamiltonian for the heteronuclear interaction. It is described by

$$H_{IS} = \frac{1}{4}\gamma_I\gamma_S h\,\Sigma_{j,m}\frac{(1-3\cos^2\theta_{jm})}{r_{jm}^3}\,I_{jz}S_{mz} \tag{6}$$

θ_{ij} is the angle between the internuclear vector of two nuclei, i and j, and the direction of the external magnetic field. (r_{ij}) is the distance between the nuclei i and j.

H_σ is the chemical shift Hamiltonian. It can be described as

$$H_\sigma = \gamma\Sigma_i(\underset{\sim}{I_i}\cdot\underset{\approx}{\sigma_i}\cdot\underset{\sim}{B_0}) \tag{7}$$

where $\underset{\approx}{\sigma}$ is the chemical shift tensor.

The chemical shift interaction is due to the distortion of the magnetic field at a nuclear site by the distribution of electrons about the nucleus. The electronic environment about a nucleus is normally non-isotropic. Therefore, the field experienced by a nucleus in a solid will have an angular dependence described by the chemical shift tensor.

The interactions mentioned above yield much information about the

local chemical environment of a nucleus. The dipolar Hamiltonians describe the local geometry between neighboring nuclei through the parameters θ_{ij} and r_{ij}. The chemical shift Hamiltonian describes the electronic environment about a given nucleus. Chemical shift parameters are quite sensitive to the local bonding, and the magnitude of the chemical shift interaction is directly proportional to the strength of the external magnetic field, B_o. Changes in various interactions as a function of temperature can be used to describe the molecular motion of the observed species.

The acquisition and analysis of the NMR data for the samples considered in this study are complicated by a number of factors. Since the oxides used in this investigation were amorphous materials, a superposition of all molecular orientations relative to the external magnetic field will be observed in their spectra. The dilute spin concentration of the samples will cause their signal-to-noise ratio to be small. The fluorine modified oxides contain two spin species, both of which are 100% naturally abundant and have large gyromagnetic ratios. Therefore, a large contribution from the heteronuclear dipolar Hamiltonian is a possibility. The aluminum-fluorine heteronuclear dipolar interaction is expected to broaden the spectra considerably when oxides containing aluminum are studied.

B. The Free Induction Decay (FID) Experiment

In this experiment a 90^o pulse is applied to the sample such that the equilibrium magnetization is rotated from the z-axis into the xy-plane (see Figure 1). After the radio frequency field is removed, the magnitude of the magnetization in the xy-plane is observed as the

component of the magnetization in the xy-plane returns to equilibrium. The individual magnetic moment vectors precess at slightly different rates about the z-axis. This component of the magnetization decays as the individual magnetic moment vectors dephase due to their different precession rates. The transverse relaxation time (T_2^*) is the time constant for the decay. The frequency spectrum is the Fourier transform of the free induction decay (1,2).

C. Variable Temperature Experiments

The fluctuations in the magnetic field which a nucleus experiences are often temperature dependent phenomena. This is especially true if the fluctuations are caused by chemical exchange or by changes in the dipolar Hamiltonian resulting from some sort of molecular motion. There are several ways of studying molecular motion. One obvious means is to observe changes in the spectrum as a function of temperature. Changes in the line width, the chemical shift parameters, or the appearance (or disappearance) of structure in the resonance line are commonly observed whenever the observation temperature is varied.

Molecular motion causes fluctuations in the physical parameters which determine the contribution to the spectrum from a particular Hamiltonian. Examples would be changes in the dipolar Hamiltonian due to fluctuations in the internuclear distance and the angle the internuclear vector makes with the applied field. Motion can cause the nucleus to experience various degrees of magnetic shielding which alters the chemical shift Hamiltonian. Chemical exchange and hydrogen bonding can cause changes in the electronic environment about the nucleus. These

effects alter the chemical shifts observed in the spectrum.

D. Obtaining FID's at Different External Field Strengths

The Hamiltonian expressed in Eqs. (2) and (3) can be separated into contributions which are independent and dependent of the strength of the external magnetic field, B_0. The Zeeman and chemical shift Hamiltonians are directly proportional to the strength of the magnetic field. If the magnitude of the static field is changed, a change in the RF frequency would be required in order to obtain resonance at that magnetic field. Changes in the chemical shift anisotrophy and the isotropic chemical shift expressed in energy units are directly proportional to changes in the external field strength. If these parameters are expressed in parts per million with respect to the external field strength, their reported values are constant regardless of the field strength. There is no effect on the contribution from the secular part of the dipolar Hamiltonians when the strength of the external field changes. Therefore, by obtaining spectra at two or more fields, it is possible to separate the contributions to the spectrum from various interactions.

E. Measurement of Spin-Lattice Relaxation Times (T_1)

When the magnetization has been displaced from equilibrium, the z-component of the magnetization will decay to its equilibrium value with a time constant, T_1. Since the magnetic dipoles are in equilibrium with the lattice, T_1 is called the spin-lattice relaxation time. Two techniques can be employed for measuring T_1. The most commonly used technique is the $180^0-\tau-90^0$ sequence. In this experiment a 180^0 pulse inverts the equilibrium magnetization to a value of $(-M_0)$ along the z-axis. As it returns to equilibrium following the 180^0 pulse, it goes

from a value of $(-M_o)$ through zero to its equilibrium value M_o. At some time τ after the initial pulse, a 90^o pulse is applied which rotates the magnetization into the xy-plane. The initial height of the resulting FID is proportional to the magnetization along the z-axis at time τ. By allowing the magnetization to return to equilibrium and repeating the experiment for various values of τ, the decay rate of M_z can be determined.

Bloch et. al. (3,4) derived the following equation of motion for the macroscopic magnetization in the presence of an applied magnetic field using phenomenological differential equations.

$$\frac{d\underset{\sim}{M}}{dt} = \gamma \underset{\sim}{M} \times \underset{\sim}{B} \qquad (8)$$

Bloch then assumed that spin-lattice relaxation could be considered as a first-order process characterized by a relaxation time T_1. Since $M_x = M_y = 0$, the decay of M_z is described by

$$\frac{dM_z}{dt} = -\frac{(M_z - M_o)}{T_1} \quad . \qquad (9)$$

Integrating Eq. 9 with the initial condition that $M_z = -M_o$ at t=0 yields the following description for the magnetization observed during the $180^o - \tau - 90^o$ experiment.

$$M_z = M_o\,(1-2\,\exp\,(-t/T_1)) \quad . \qquad (10)$$

A problem in using this technique occurs when the sample has a long T_1 and a small signal-to-noise ratio. Then signal averaging must be used with a time interval of $5T_1$ between measurements. If this is the case, measurement of T_1 can become very time consuming. These problems can be avoided if the FID decays to zero much more rapidly than M_z

returns to equilibrium. If this is the case, a sequence of repeated 90^{o} pulses is useful for measuring T_1. The first 90^{o} pulse rotates the equilibrium magnetization into the xy-plane. After a time τ during which the FID has decayed to zero, a second 90^{o} pulse is applied. The value of M_z at the time τ is proportional to the initial height of the second FID. If a series of pulses separated by a constant time interval τ is applied, a steady state value for the magnetization following the 90^{o} pulse is rapidly reached. The magnetization is dependent on τ and T_1. T_1 can be determined by using the steady state magnetizations observed for various values of τ. The analysis is based on the Bloch equations, but now using $M_z = 0$ at $t = 0$ for the initial condition. In this case,

$$M_z = M_o(1-\exp(-t/T_1)) \ . \qquad (11)$$

The samples used in this investigation had long spin-lattice relaxation times (5-40 sec) and they required extensive averaging. In all cases T_1 was 10000 times greater than the decay constant for the FID. Therefore, the sequence of 90^{o} pulses was used to measure T_1.

F. Spin Echo Experiments

Spin echo experiments consist of applying a pulse to the sample in order to rotate the magnetization into the xy-plane. After a time interval τ, a second pulse is applied in order to restore phase coherence to the spins. The ability of a given pulse scheme to reestablish phase coherence to the spins provides information about the nature of the interactions determining the local environment of the nuclei. Descriptions of the three spin echo experiments used in this

investigation are given below. The experiments are shown schematically in Figure 1.

1. 90^{o}-τ-180^{o} Echo

The initial step in this experiment is the use of a 90^{o} pulse to rotate the magnetization into the xy-plane. After the radio frequency field is removed, the magnetization will decay as in the FID experiment. After a time τ, the 180^{o} pulse is applied. The effect of this pulse is to reverse the direction in which the individual magnetic moment vectors were precessing. The vectors will now precess in such a way that they will refocus at time 2τ. After the spins have refocused they will continue to precess causing them to dephase with a time constant of T_2^*, as in the FID experiment (see Figure 2).

The 90^{o}-τ-180^{o} experiment was used for two purposes in this investigation. The decay of the echo amplitudes as a function of 2τ can be described by a time constant, T_2. Any interaction which has the same symmetry as the homonuclear dipolar Hamiltonian ($\underset{\sim}{I}_i \cdot \underset{\sim}{I}_j$ or $I_{iz}\ I_{jz}$) or which results in fluctuations in Hamiltonians with I_z symmetry is unaffected by the 180^{o} pulse. The 180^{o} pulse inverts the sign of all interactions which have the same symmetry as the spin operator I_z. The effects of these interactions are reversed causing the magnetization to refocus at time 2τ. Therefore, the time constant T_2 measures the effects of the homonuclear dipolar Hamiltonian and of the fluctuations in the field experienced by the nuclei. If the effects due to fluctuations are neglected, Mansfield (5) has shown that the echo response to second order in time is

$$E(2\tau) = 1-M_2^{II}(2\tau)^2\ /2! \qquad (12)$$

where M_2^{II} is the contribution to the second moment from the homonuclear dipolar Hamiltonian.

Secondly, the probe electronics require several microseconds to recover from the high power radio frequency pulses. The FID cannot be observed during this recovery time. The spin echo experiment can be used to observe the initial portion of the FID. The value of τ must be long enough so that the echo maximum at 2τ is beyond the recovery time for the 180^o pulse, but τ must be sufficiently short so that components of the spectrum with short values of T_2 will refocus ($\tau<T_2$).

2. 90^o-τ-$90^o_{90^o}$ Experiment

In this experiment a 90^o pulse is applied to the sample. After that radio frequency field has been removed, the individual magnetic moment vectors are allowed to dephase as in the FID experiment. After a time interval, τ, has elapsed, another 90^o pulse is applied. However, this pulse has a relative phase shift of 90^o with respect to the initial pulse.

The classical picture used conveniently to describe the behavior of the magnetization during a 90^o-τ-180^o sequence is not adequate for the 90^o-τ-$90^o_{90^o}$ sequence. A quantum mechanical approach needs to be applied to describe the interactions. The theory has been treated by Mansfield (5) and by Boden and Levine (6). Mansfield demonstrated that contributions due to Hamiltonians with the same symmetry as the homonuclear dipolar Hamiltonian will refocus at time 2τ. The decay constant (referred to in this investigation as T_2^{IS}) results from dephasing of the magnetic moment vectors due to interactions with the same symmetry as the operator I_z. Mansfield has shown that the echo response at time 2τ

to second order in time is

$$E(2\tau) = 1-M_2^{IS}(2\tau^2)/2! \qquad (13)$$

where M_2^{IS} is the contribution to the second moment due to Hamiltonians with the same symmetry as the heteronuclear dipolar Hamiltonian.

3. The Carr-Purcell-Meiboom-Gill (CPMG) Experiment

This experiment consists of a 90^0 pulse followed by a series of 180^0 pulses which have a relative phase shift of 90^0 with respect to the initial 90^0 pulse. The 90^0 pulse and the initial 180^0 pulse are separated by a time interval τ and the time interval between 180^0 pulses is 2τ. The effect of this sequence on individual magnetic moment vectors is illustrated in Figure 2. The result is the same as for a 90^0-τ-180^0 experiment with a relative phase shift of 90^0 between the two pulses, except that following the dephasing of the magnetic moment vectors shown in Figure 2.f another 180^0 pulse is applied at 3τ (as Figure 2.c). This causes a rephasing of the magnetic moment vectors along the y-axis at time 4τ. Repeated 180^0 pulses at 5τ, 7τ, etc. cause continued rephasing of the magnetic moment vectors at 6τ, 8τ, etc.

Carr and Purcell (7) have demonstrated that diffusion of the nuclei with spin can drastically influence the results of the 90^0-τ-180^0 experiment. They have shown that the echo response for a pulse separation of τ is given by

$$E(2\tau) \alpha \exp\left(-\frac{2\tau}{T_2} - \frac{2}{3}\gamma^2 G^2 D \tau^3\right) \qquad (14)$$

where γ= gyromagnetic ratio

G = spatial magnetic field gradient

$\mathscr{D}$ = diffusion coefficient.

By modifying the pulse cycle proposed by Carr and Purcell, Meiboom and Gill (8) developed the pulse cycle discussed here which eliminates cumulative pulse errors in the Carr-Purcell cycle as well as reducing the effects due to diffusion. For 180^{o} pulse spacings of 2τ and stroboscopic observation at time intervals of $2n\tau$, the echo response observed the $2n\tau$ windows is

$$E(2n\tau) \alpha \exp\left(-\frac{t}{T_2} - \frac{2n}{3}\gamma^2 G^2 \mathscr{D}\tau^3\right) \qquad (15)$$

The true decay constant resulting from the effects of the homonuclear dipolar Hamiltonian can be measured since the contribution from the diffusion term will be negligible for sufficiently small values of τ.

The Carr-Purcell-Meiboom-Gill experiment has one additional advantage when compared to the 90^{o}-τ-180^{o} sequence. In the 90^{o}-τ-180^{o} experiment separate measurements must be performed to obtain data at each value of τ. However, the CPMG experiment obtains the entire decay with one measurement. If N averages are required for a given signal-to-noise ratio, the total decay can be obtained after N averages using the CPMG experiment. The 90^{o}-τ-180^{o} experiment requires that N averages be taken for each value of τ observed.

G. Quantitative Analysis by NMR

The net magnetization observed for a given sample is proportional to the number of resonant nuclei present in the sample. The total magnetization of the sample can be obtained from the area under the absorption curve in the frequency spectrum or from the amplitude of the

FID at time zero. When the magnetization of the sample being measured is compared with the magnetization of a sample where the number of resonant nuclei is known, the absolute number of nuclei present in the sample can be determined.

In order to obtain reliable values for quantitative analysis of solid samples, several factors must be considered. The reduction in magnetization due to the spin-lattice relaxation time must be considered if the time between FID experiments is not greater than $5T_1$. The FID must be extrapolated to zero time since there might be a significant reduction in magnetization during the recovery time of the probe and receiver. Care must be used so that any component of the spectrum with a short T_2^* is not omitted during quantitative analysis. Since the standard sample is usually external to the sample whose spin concentration is being determined, the two spectra must be obtained in the same manner. The sample tubes should be identical and any differences in bulk magnetic susceptibilities of the samples should be considered.

The number of spins in these samples were obtained by determining the initial amplitudes of the FID's. Reference samples were prepared in such a way that differences in bulk magnetic susceptibility and in the sample tubes could be neglected.

H. Comments on Multiple-Pulse Techniques

Two multiple-pulse NMR techniques might have application to the study of fluorine modified oxide catalysts. One of these techniques involves reducing the contribution from the homonuclear dipolar Hamiltonian using the MREV-8 (9,10,11) or BR-24 (12) pulse cycles. The other is use of various schemes for reducing the contributions from heteronuclear dipolar

effects. These methods were not employed for a variety of reasons.

The use of line-narrowing experiments with samples having dilute spin concentrations needs to be considered thoughtfully. At 24 kG the fluorine chemical shift anisotropy is sufficiently large that the principal values of the chemical shift anisotrophy can be obtained from the FID powder pattern. Little would be gained from performing a fluorine-fluorine decoupling experiment. Even the hydrogen spectra observed in this study were not dominated by homonuclear dipolar effects. Although removal of the hydrogen homonuclear dipolar broadening should reduce the observed hydrogen line widths substantially, the quality factor, Q, of the probe would have to be reduced from 115 to approximately 30 in order to obtain sufficiently short cycle times. In doing so the signal-to-noise ratio would be reduced by a factor of 2. Therefore, using a low Q probe to obtain spectra with the same signal-to-noise ratio as that obtained using the high Q probe would increase the signal averaging required by a least a factor of four. This increase in the required signal averaging and the long T_1's observed for the samples used in this investigation limit the usefulness of multiple-pulse experiments.

Hydrogen-fluorine decoupling experiments could provide useful information about such phenomena as OH---F hydrogen bonds. These experiments have been performed with other materials such as potassium bifluoride (13) and 4,4'-difluorobiphenyl (14). However, a number of instrumental difficulties are involved in performing these experiments with fluorine modified oxides. A double resonance probe for pulsed decoupling of the hydrogen and fluorine spins would have to be constructed.

Since there is a difference of 6 MHz between the resonance frequencies of hydrogen and fluorine at 24 kG, the Q of the probe would have to be reduced in order to irradiate at both radio/frequencies simultaneously. Since a bandwidth of 6 MHz would require a Q of 16 or less at 96.7 MHz, the signal-to-noise ratio would be decreased by at least a factor of 7. The signal averaging required for the samples used in this investigation would make the experiments very difficult. Also, the low Q of the probe would make it quite difficult to isolate the receiver from RF leakage from the probe circuitry due to irradiation of the sample at the S-spin radio frequency.

I. Description of the NMR Spectrometers Used in This Investigation

An NMR spectrometer similar to the ones used in this work has been described elsewhere (15). Here only the particulars of these spectrometers which differ from the earlier spectrometer and the details necessary for operation at 24 kG will be discussed. The low field spectrometer (13 kG) was used in the configuration previously described (15). The radio frequency electronics were tuned at 56.4 MHz for both hydrogen and fluorine and the field was increased in order to obtain fluorine spectra. The sample coil had a diameter of 5 mm. A small hydrogen background signal was subtracted from the hydrogen spectra.

The high field spectrometer (24 kG) was used in the configuration shown in Figure 3. The spectrometer was operated at 24 kG for all nuclei and the probe was retuned for the nuclei of interest. The Q factor of the probe was 115 and the coil diameter was 5.5 mm. A quartz dewar surrounded the coil. Low temperature data were obtained by cooling the

sample area with a stream of nitrogen gas at 100^{o} K. Temperatures were regulated by varying the flowrate of the nitrogen gas. A small hydrogen background signal due to the quartz dewar about the sample area was subtracted from the hydrogen spectra.

Operating frequencies greater than 70 MHz present problems since electrical connections and cables begin to behave like inductors and capacitors. Probes with construction similar to those used at lower frequencies become difficult or impossible to tune. Probes used for frequencies of 90 MHz or greater were constructed with sidewalls of thin copper rather than aluminum plates. The narrow gap of the 24 kG electromagnet required the coil to be 20 cm from the rest of the probe electronics. Co-axial cable took on capacitive properties when used in the circuitry, which prevented proper tuning of the probe. Use of a flattened copper wire (approximately one centimeter wide and 1.5 millimeters thick) to conduct the radio frequency pulses to the coil resulted in the desired tuning for the probe. Separate grounds for the two branches of the tuning circuit were used to keep the length of electrical connectors used in the probe to a minimum.

A second problem is background noise. Cables used to transfer signals between components of the spectrometer act as antennas for FM radio signals. This problem was minimized by using solid co-axial cables with copper shielding for connections between the amplifier, probe, receiver, and DC amplifier.

The probe recovery time was 12 μsec. A typical value for the radiofrequency field was 40 G (approximately 165 kHz for hydrogen). Typical pulse lengths were 1.5 μsec for 90 pulses and 3.0 μsec for 180 pulses.

References

1. Ernst, R. R., and Anderson, W. A., Rev. Sci. Instrum. 37, 93 (1966).
2. Lowe, I. J., and Norberg, R. E., Phys. Rev. 107, 46 (1957).
3. Bloch, R., Phys. Rev. 70, 460 (1946).
4. Bloch, R., Hasen, W. W., and Packard, M., Phys. Rev. 70, 474 (1946).
5. Mansfield, P., Phys. Rev. A 137, 961 (1965).
6. Boden, N., and Levine, Y. K., J. Magn. Resonance 30, 327 (1978).
7. Carr, H. Y., and Purcell. E. M., Phys. Rev. 94, 630 (1954).
8. Meiboom, S., and Gill D., Rev. Sci. Instrum. 29, 688 (1958).
9. Rhim, W. K., Elleman, D. D., and Vaughan, R. W., J. Chem. Phys. 59, 3740 (1973).
10. Rhim, W.-K., Elleman, D. D., and Vaughan, R. W., J. Chem. Phys. 58, 1772 (1973).
11. Mansfield, P., J. Phys. C 4, 1444 (1971).
12. Burum, D. P., and Rhim, W.-K., J. Chem. Phys. 71, 944 (1979).
13. Van Hecke, P., Spiess, H. W., and Haeberlen, U., J. Magn. Resonance 22, 103, (1976).
14. Halstead, T. K., Spiess, H. W., and Haeberlen, U., Mol. Phys. 31, 1569 (1976).
15. Vaughan, R. W., Elleman, D. D., Stacey, L. M., Rhim, W.-K., and Lee, J. W., Rev. Sci. Instrum. 43, 1356 (1972).

Figure Captions

Figure 1. Schematic diagram showing the pulse sequences used in this investigation.

Figure 2. The 90^{o}-τ-$180^{o}_{90^{o}}$ experiment. (a) A 90^{o} pulse is applied along the x-axis at time 0 rotating the magnetization into the xy-plane. (b) Dephasing of the individual magnetic moment following the initial 90^{o} x pulse. (c) A 180^{o} pulse is applied along the y-axis at time τ which rotates the vectors 180^{o} about the y-axis. (d) Rephasing of the vectors following the 180^{o} pulse. (e) The magnetic moment vectors are rephased along the y-axis at time 2τ. (f) The magnetic moment vectors continue to dephase for times greater than 2τ.

Figure 3. Schematic diagram of the 23.4 kG pulse NMR spectrometer.

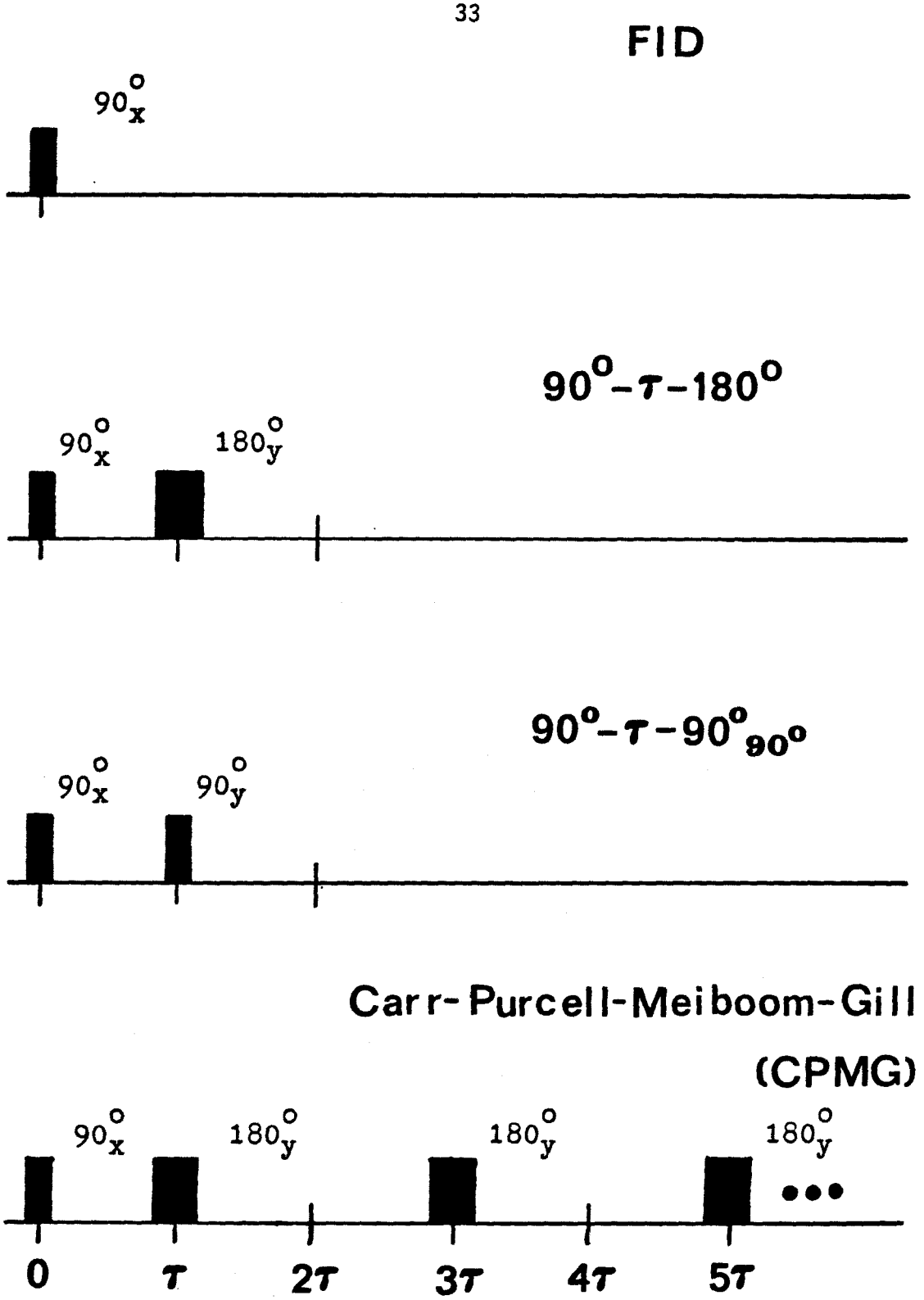
FID
90°_x
$90^\circ-\tau-180^\circ$
90°_x
180°_y
$90^\circ-\tau-90^\circ_{90^\circ}$
90°_x
90°_y
Carr-Purcell-Meiboom-Gill
(CPMG)
90°_x
180°_y
180°_y
180°_y
0
τ
2τ
3τ
4τ
5τ

Figure 1

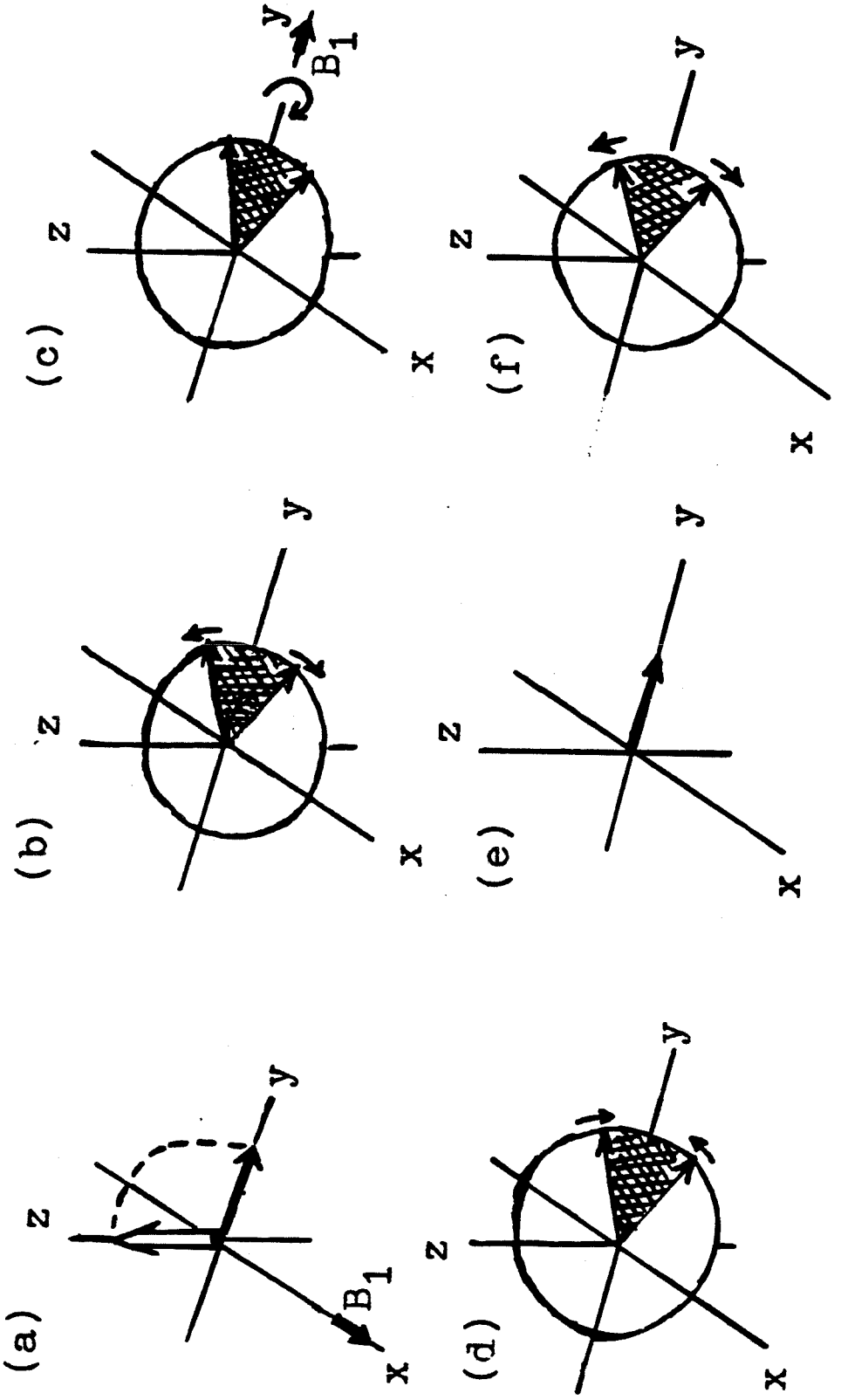

Figure 2

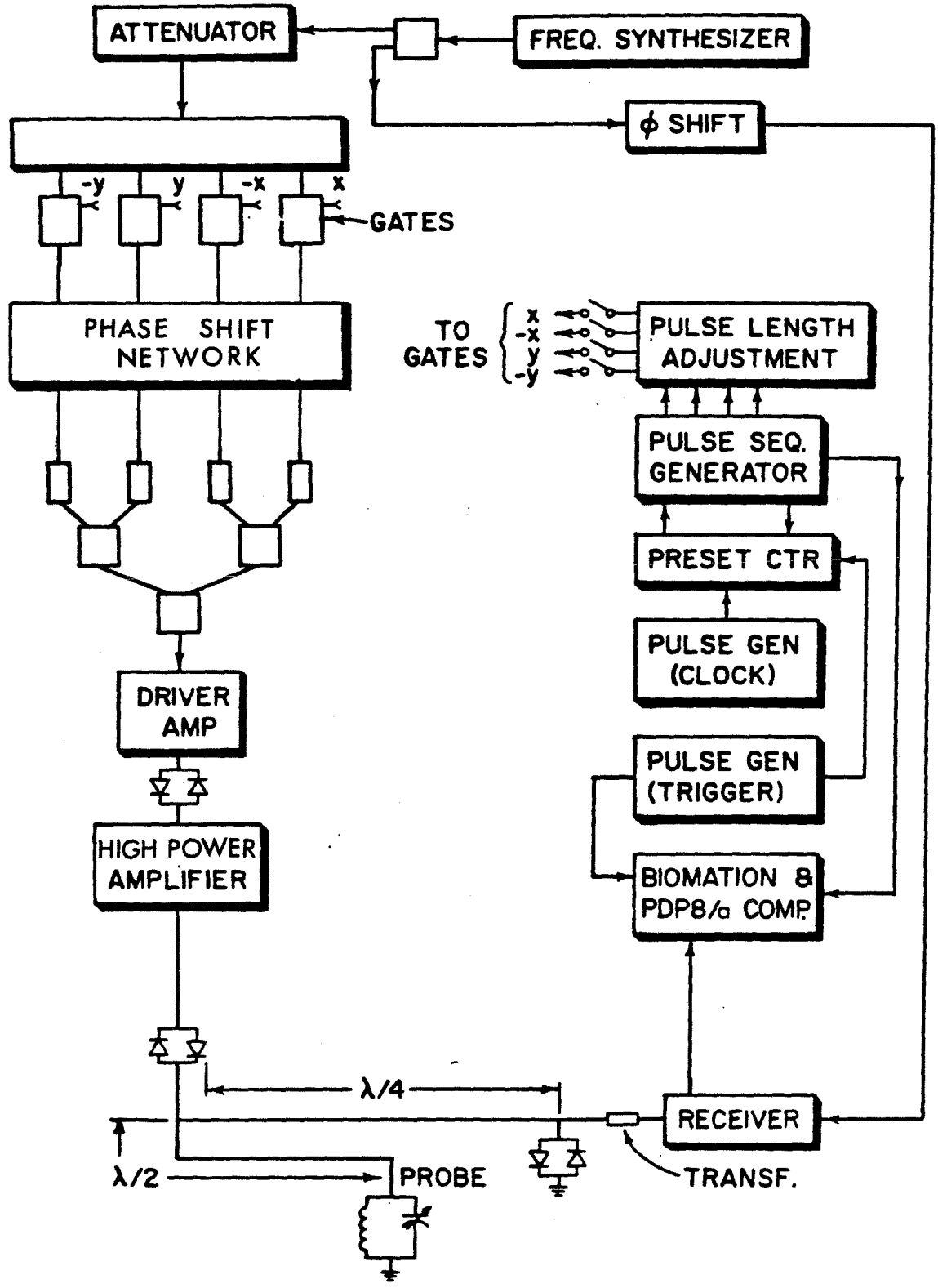
ATTENUATOR
FREQ. SYNTHESIZER
ϕ SHIFT
-y
y
-x
x
GATES
PHASE SHIFT NETWORK
TO GATES
x
-x
y
-y
PULSE LENGTH ADJUSTMENT
PULSE SEQ. GENERATOR
PRESET CTR
PULSE GEN (CLOCK)
DRIVER AMP
PULSE GEN (TRIGGER)
HIGH POWER AMPLIFIER
BIOMATION 8 PDP8/a COMP
λ/4
RECEIVER
λ/2
PROBE
TRANSF.

Figure 3

CHAPTER III

A NUCLEAR MAGNETIC RESONANCE INVESTIGATION OF FLUORINATED OXIDE CATALYSTS

Part 1: Fluorinated Silica

(Chapter III is essentially an article by J. R. Schlup and R. W. Vaughan, entitled "A Nuclear Magnetic Resonance Investigation of Fluorinated Oxide Catalysts. Part 1: Fluorinated Silica." This article has been submitted to the Journal of Catalysis.)

INTRODUCTION

The catalytic properties of fluorinated oxides have been studied extensively and Choudhary has prepared a review of the literature (1). Most of the information focuses on the activity of fluorinated alumina and aluminosilicates. The relative absence of catalytic date for fluorinated silica reflects the differences in the catalytic behavior of unmodified silica, alumina, and aluminosilicates. Peri (2) reported that fluorinated silica showed no activity for butene polymerization. Fluorination of silica does increase the cumene cracking rate (3,4) so that its activity approaches that of an aluminosilicate.

Infrared spectroscopy has been used in a number of studies to understand the effects of fluorination on silica (2,3,5,6). The behavior of isolated and hydrogen-bonded hydroxyl groups has been reported for several fluorine treatments and calcining temperatures. Adsorption of simple probe molecules (such as ammonia, chloroform, carbon monoxide, and carbon dioxide) on silica and monitoring the effects of fluorination of the oxide upon the infrared spectrum of the adsorbed molecules has been a standard tool for attempting to understand the changes that occur on the oxide surface as a result of fluorination. However, infrared spectroscopy has not provided direct information about the interaction between fluorine and silica since vibrations below 1250 cm^{-1} are obscured by the vibrations of the silica lattice. The fluorine-silicon stretching vibrations are expected to be in the 800-1100 cm^{-1} region (7).

A spectroscopic technique which allows direct observation of both hydrogen and fluorine atoms is nuclear magnetic resonance (NMR). The only previously reported use of NMR as a spectroscopic tool for studying

fluorinated silica was done by Golovanova and co-workers (6). However, they reported only the wide-line spectrum of hydrogen at 83 K on samples prepared at 373, 653, and 723 K. The present work represents the only attempt to use NMR to study both fluorine and hydrogen on fluorinated silica.

The use of silica for studying fluorine modified oxides is advantageous for a number of reasons. Silica can be made as a high surface area material. Since it contains both oxygen atoms and acidic hydroxyl groups, it is a simple, useful model for oxide catalysts. An understanding of the interaction of fluorine with silica under several different preparation conditions will help to prepare other fluorinated oxides uniformly since many fluorine-silicon compounds are volatile and thermal degradation of fluorinated silicas can be expected. Since only 4.7% of the silicon nuclei have nuclear spin ($I=\frac{1}{2}$), the hydrogen and fluorine NMR spectra of fluorinated silica will not be complicated by dipolar interactions involving the oxide.

EXPERIMENTAL DETAILS

Sample Preparation

The silica samples were prepared from Grace/Davison Grade 62 silica gel. The particle size was 60 to 200 mesh. The initial surface area was reported to be 340 m^2/g. The silica gel was cleaned by calcining under flowing oxygen at 773 K for three hours.

The fluorinated silicas were prepared using aqueous ammonium fluoride solutions with fluoride concentrations of 5 mM and 18 mM. Preparation of samples using aqueous ammonium fluoride solutions have been reported to

have better reproducibility than other methods of fluorine atom addition (1). The cleaned silica was placed in the aqueous ammonium fluoride solution for four hours. Then the excess ammonium fluoride solution was removed by evaporation. The dried modified silica was sub-divided and each portion was calcined under flowing oxygen at the desired temperature for three hours. A sample of unmodified silica was prepared using cleaned silica and the above procedure except that the exposure to fluoride was omitted.

A heavily modified silica was prepared using an aqueous ammonium fluoride solution that was five weight percent fluoride. It was exposed to fluoride for 70 hours. The excess ammonium fluoride solution was removed by evaporation and the modified silica was calcined at 773 K under flowing oxygen for three hours.

NMR Apparatus

A Fourier transform NMR spectrometer similar to the ones used in this investigation has been described elsewhere (8). Two spectrometers were used in this investigation, operating at field strengths of 13 kG and 24 kG. The quality factor (the ratio of the energy stored to the energy dissipated), Q, of the probes was 120. The recovery time for the overload effects resulting from the high power radio frequency pulses for the probe and receiver was 12 μsec.

The NMR measurements were made at temperatures from 105 K to 290 K. The probe was cooled using cold nitrogen gas and the temperature was varied by changing the flowrate of the nitrogen. The low signal-to-noise ratio of these samples required accumulating the signal from as few as

256 to as many as 4096 experiments in order to obtain the data reported.

NMR Techniques

The application of NMR techniques can furnish information about the concentration of the atoms, the nature of the bonding of the atoms, the interactions between neighboring atoms, and the motion of the atoms.

The hydrogen and fluorine concentrations were obtained by measuring the initial magnitude of the free induction decay (FID) observed after a 90^{o} pulse. The magnetization observed was calibrated using samples of known hydrogen and fluorine content. Corrections for differences in the bulk magnetic susceptibility between samples were found to be negligible in this investigation.

The nature of the chemical bonding of hydrogen and fluorine to silica was investigated using the center of mass or the isotropic chemical shift of the Fourier transform of the free induction decay and the fluorine chemical shift anisotropy. The magnetic field at a nuclear site can be distorted by the electron distribution about the nucleus. The electronic environment about a nucleus is normally non-isotropic. Therefore, the field experienced by a nucleus in a solid will have an angular dependence described by the chemical shift tensor.

In polycrystalline materials, such as the ones studied here, the sample contains crystallites with many different orientations so that the observed resonance is broadened by chemical shift effects. This is referred to as the "powder pattern" spectrum and analysis of this spectrum yields the magnitude of the three principal components of the chemical shift tensor, σ_{zz}, σ_{yy}, and σ_{xx}. The isotropic chemical shift,

$\bar{\sigma} = (1/3)(\sigma_{zz} + \sigma_{xx} + \sigma_{yy})$, is the center of mass of the chemical shift tensor.

The line width of the NMR spectra in solids normally prevents accurate chemical shift data from being obtained. Multiple-pulse sequences usually must be applied in order to remove selectively the effects of dipolar broadening. However, the samples investigated here had relatively weak dipolar interactions. Therefore, the centers of mass could be obtained for all of the samples. At 24 kG the fluorine chemical shift anisotropy was sufficiently large that the principal components of the chemical shift anisotropy could be obtained from the Fourier transform of the free induction decay.

The local arrangements of the atoms and the possibility of molecular motion were investigated using the 90^{o}-τ-180^{o} (spin echo) and 90^{o}-τ-90^{o} (solid echo) experiments (where the second pulse has a relative phase shift of 90^{o} with respect to the first pulse) and the Carr-Purcell-Meiboom-Gill (CPMG) pulse sequence (9).

The two-pulse experiments were used to study these materials for a number of reasons. The solid echo formed by a 90^{o}-τ-90^{o} sequence is the result of contributions from the homonuclear dipolar interactions. During the spin echo experiment the echo is formed from contributions from the heteronuclear dipolar interactions and from the chemical shift interaction. Molecular motion (or other phenomena which can cause fluctuations in interactions with the same symmetry as the spin operator I_z) can cause discrepancies in the relaxation times observed from the spin echo and the CPMG experiments.

All three experiments mentioned above were used to investigate hydrogen on fluorinated silica. The fluorine spectra of these samples were dominated at 24 kG by a large chemical shift anisotropy. Therefore, only the CPMG sequence was used to investigate the dipolar interactions of the fluorine atoms on these samples.

RESULTS and DISCUSSION

Quantitative Analysis

Quantitative analysis of hydrogen and fluorine contained in silica is difficult. Elevated temperatures are usually required (often in excess of 1200 K) and the sample is destroyed by most techniques. Quantitative analysis of the acid site concentrations has been attempted using infrared spectroscopy (10). However, the results of quantitative analysis based upon infrared spectroscopic techniques are complicated by changes in the oscillator strengths of the absorption bands and by the interpretation of results involving adsorbed molecules.

NMR can be used as a quantitative tool. The total magnetization is directly proportional to the number of resonant nuclei present. It is a non-destructive analytical tool. In this investigation, hydrogen and fluorine atom concentrations were obtained from the initial amplitudes of the free induction decays (FIDs). Even when as few as 2×10^{19} nuclei are present (less than one atom per 100 $\mathring{A}^2$), relative standard deviations of 10% are obtained routinely.

The nitrogen BET surface areas and the hydrogen atom concentrations for the silicas studied are found in Table 1. Although the removal of hydroxyl groups from the silica surface upon fluorination has been

reported, hydrogen was present on all samples treated with aqueous 5 mM and 18 mM F^- solutions and for calcining temperatures up to 873 K. The hydrogen concentration of the unmodified silica and the fluorine modified silicas calcined at 573 and 673 K (regardless of fluorination conditions) are the same, and the hydrogen concentration of the modified silica remains constant through 673 K. Hydrogen was removed from the catalyst by calcining at 773 K. Calcining at 873 K reduces the hydrogen atom concentration to 1.2 per 100 Å^2 (less than one-half the hydrogen atom concentration when the sample was calcined at 573 K). The hydrogen concentrations of modified silicas prepared using 5 mM and 18 mM F^- solutions and calcined at 873 K are the same.

The unmodified silica and the modified silica prepared using a 5 mM F^- solution and calcined at 753 K have hydrogen atom surface concentrations of 2.4 and 1.8 hydrogen atoms per 100 Å^2, respectively. Their ratios of hydrogen atoms to total silicon atoms are 0.0082 and 0.0045, respectively. Using NMR techniques to measure the hydrogen content of silicas calcined at 773 K, surface concentrations of 2.4, 1.6, 1.4, and 0.87 per 100 Å^2 have been reported by Hall et. al. (11), Schreiber and Vaughan (12), Freude et. al. (13), and Oehme (14), respectively. Using deuterium exchange experiments, Davydov and co-workers (15) measured hydroxyl group concentrations of 1.6-2.3 hydrogen atoms per 100 Å^2 for silica calcined at 773 K.

The nitrogen BET surface areas and fluorine concentrations for the modified silica samples investigated are found in Table 1. After calcining at 573 K, the fluorine concentration of the silica prepared with an 18 mM F^- solution has three times the fluorine concentration of

silica prepared using a 5 mM F^- solution. However, the fluorine modified silicas calcined at 873 K have identical fluorine concentrations within experimental error. Samples with fluoride treatment using a 5 mM F^- solution have a constant fluorine atom concentration when calcined at 573, 673 and 773 K. The ratio of fluorine atoms to total silicon atoms for the modified silica with prepared with a 5 mM F^- solution and calcined at 773 K is 0.0062. The fluorine atom concentration is reduced by 40% when the silica is calcined at 873 K. The hydrogen and fluorine concentrations are the same within experimental error for modified silicas prepared from 5 and 18 mM F^- solutions and calcined at 873 K.

The modified silica prepared using an aqueous solution of ammonium fluoride which is five weight percent fluoride is very different from silicas prepared using an 18 mM F^- solution. Treatment with aqueous fluoride solutions with fluoride concentrations less than 20 mM result in a modified silica with the same surface area as an unmodified silica. Use of a five weight percent fluoride solution reduced the surface area of the modified silica by 50%. A volatile product was formed at calcining temperatures of 573 K or higher.

The volatile product condensed on the quartz tubing at the cool end of the tube furnace as the sample was being calcined. The condensed material was a white solid at room temperature. It is stable on glass and on Tygon tubing. The condensed material was scraped from the quartz tube and analyzed by mass spectrometry. Preliminary investigation showed that the sublimate volatilized at 473 K and 523 K. The material evolved at 473 K has a mass spectrum characteristic of SiH_4 and SiF_4. The material evolved at 523 K is more complex. Species characteristic of

SiH_4 amd SiF_4 have been identified. SiF_2O has been observed in the spectrum. Disiloxane, meta-silicic acid, and siloxane were also present.

Spin-Lattice Relaxation Time Measurements (T_1)

A complete study of the spin-lattice relaxation times (T_1) of these materials was not performed. There were two objectives in obtaining the room temperature T_1's for the samples. Knowledge of the T_1 for a given sample is necessary if efficient signal averaging is to be performed. Secondly, since the net magnetization is proportional to the number of resonant nuclei (16), NMR can be used as a quantitative tool. However, the magnetization observed during an NMR experiment depends upon the T_1 for the sample. Therefore, knowing the T_1 of the sample is required for accurate quantitative analysis.

Data were obtained only at room temperature. The line shape was independent of the time interval used in signal averaging. Since $T_1 >> T_2$, the 90^0-τ-90^0 method was used to measure T_1. This method acquired data more efficiently than the 180^0-τ-90^0 method since the signal-to-noise ratio of these samples is small.

The results of the T_1 measurements for both fluorine and hydrogen are found in Table 2. The spin-lattice relaxation times for hydrogen ranged from 6 to 17 seconds. Unmodified silica exhibited the shortest T_1. However, changes in the relaxation times for the fluorine modified silica appear to have no particular trend based on the data available.

The T_1 values of fluorine are constant for the silicas prepared with a 5 mM F^- solution and calcined at temperatures of 773 K or less. The T_1 decreases by a factor of two when the silica was calcined at 873 K.

For modified silicas calcined at 573 K, the T_1 of the silica prepared with a 18 mM F^- solution is one-half the T_1 of the silica prepared with a 5 mM F^- solution. There is an increase in T_1 as the calcining temperature is increased for silicas treated with an 18 mM F^- solution. The silica prepared using a 5 weight percent fluoride solution had the shortest fluorine T_1 measured, 10 seconds.

Room Temperature Free Induction Decays (FID's)

The hydrogen spectrum for unmodified silica is shown in Figure 1. The hydrogen spectra of the fluorine modified silicas are shown in Figure 2. The centers of mass, full widths at half heights, and second moments calculated from the room temperature spectra are given in Table 3. The centers of mass are reported in parts per million (ppm) with respect to tetramethylsilane. The center of mass (σ_{Av}) is calculated using the following convention:

$$\sigma_{Av} = \left(\frac{\nu_{ref} - \nu_{cm}}{\nu_{ref}}\right) \times 10^6 \qquad (1)$$

ν_{ref} = resonance frequency of the chemical shift reference

ν_{cm} = frequency of the center of mass of the spectrum.

The values reported in Tables 3, 4, and 5 are not corrected for the effects of bulk magnetic susceptibility. The volume susceptibility for these materials has not been measured. However, if a volume susceptibility of (-1.13×10^{-6}) for silica is used (13), an estimate can be made of the necessary susceptibility correction. The sample can be approximated as an ellipsoid with b=c=0.5a, where a, b, and c are the semiaxes with the

magnetic field being along axis b. Using the values tabulated by Osborn (17) and the estimated volume susceptibility, a bulk susceptibility correction of 1.1 ppm to higher field is obtained. Since this correction is less than or equal to the experimental error in the data and the estimated correction would be uniformly applied to all of the fluorine and hydrogen room temperature spectra, the observed chemical shifts are reported and not the chemical shifts corrected for bulk susceptibility.

The hydrogen spectrum of an unmodified silica has a full width at half intensity of 1.8 kHz at 24 kG. The second moment (M_2) is 0.05 G^2 and is independent of the strength of the external magnetic field. Therefore, the major contribution to the linewidth is the homonuclear dipolar interaction.

The parameters obtained from the hydrogen spectra of fluorine modified silicas are found in Table 3 also. The centers of mass range from 0 ppm to -8 ppm relative to tetramethylsilane (TMS) with the exception of fluorinated silica prepared using a 5 mM F^- solution and calcined at 573 K. Although the chemical environment of the hydrogen atom is reflected in its chemical shift, the data cannot distinguish unambiguously between silane and hydroxyl hydrogens. The values reported in the literature for σ_{SiH} are -6 ppm < σ_{SiH} < -3 ppm. Reimer, Vaughan, and Knights (18) report the isotropic chemical shift of hydrogen in plasma-deposited Si:H films to be -18 ppm which becomes -12.6 ppm when corrected using a chemical sift scaling factor of 0.7 (19). The range of isotropic chemical shifts of organic alcohols is -6 ppm < σ_{OH} < -1.4 ppm. Therefore, silane and hydroxyl groups cannot be distinguished

unambiguously using their isotropic chemical shifts alone.

The center of mass reported here for the unmodified silica is in excellent agreement with respect to the isotropic chemical shift (uncorrected for the bulk magnetic susceptibility) of -2.8 ppm relative to TMS reported by Schreiber and Vaughan (12). In that study infrared spectroscopy identified the hydrogen as surface hydroxyl groups. Since the center of mass for unmodified silica is 10 ppm upfield from the isotropic chemical shift of the hydrogen in a plasma-deposited Si:H film and is in excellent agreement with the spectrum reported for surface hydroxyl groups, it may be concluded that the center of mass for the silanol groups on the unmodified silica is at -3. ppm with respect to TMS.

The field strength, calcining temperature, and fluoride treatment have significant effects on the line widths and second moments observed for the hydrogen spectra of fluorinated oxides. In all cases the full width at half height increases with an increase in the field strength. Similar behavior is exhibited by the second moments of the spectra. Samples calcined at 873 K and prepared with aqueous solutions with fluoride concentrations less than 20 mM F^- have line widths dominated by the dipolar interactions. Line widths for the hydrogen NMR spectrum of silica have been reported by several researchers. Schreiber and Vaughan (12) reported a full width at half height of 1600 Hz and Freude et. al. (13) reported a second moment of 0.05 G^2 for the room temperature spectrum of silica calcined at 773 K. Hall and co-workers (20) reported the decay constant of the FID, T_2^*, for silica was constant over a temperature range from 63 K to 553 K (with the T_2^* reported corresponding to a full

width at half height of 1770 Hz). Oehme (14) reported the second moment of the hydrogen spectrum of silica gel measured at 77 K to be 0.04 G^2 for calcination at 773 K.

While the centers of mass for the hydrogen spectra of the modified silicas vary with the sample treatment, they are consistent with the chemical shift reported for hydroxyl groups on silica. The field dependence of the hydrogen spectra for modified silicas indicates that the chemical bonding of the hydroxyl groups of fluorinated silica differ from the hydroxyl groups of the unmodified silica. The modified silica prepared using a 5 mM F^- solution and calcined at 573 K is significantly upfield from the chemical shifts reported for silanes, or silanols, or alcohols. The line width of the hydrogen spectra for silica prepared using an 18 mM F^- solution and calcined at 573 K increases proportionally with respect to the field strength. This implies that the dominant contribution to the line width is from chemical shift interactions. The line shape cannot be described satisfactorly by chemical shift anisotropy alone. The observed spectra can be the result of anisotropic motion or the presence of two or more resonance lines.

The fluorine FID's of these modified oxides provide much information concerning the chemical environment of the fluorine atoms (see Table 4). Reported values for the chemical shift of fluorine covalently bound to silicon range from 54 ppm for $FSiH_3$ to -54 ppm for F_3SiH. Two fluorine chemical shifts reported for fluorinated disiloxanes are 8 ppm for $^{28}SiF_3$-O-$^{29}SiF_3$ and -25 ppm for $HF(CH_3)Si$-O-$Si(CH_3)HF$. The chemical shifts reported for fluoride ions range from -154 ppm to -35 ppm with

the exceptions of NaF at 62 ppm and CdF_2 at 24.8 ppm. The chemical shifts of oxyfluorides range from -454 ppm to -210 ppm. All of the fluorine chemical shifts are reported relative to hexafluorobenzene.

Figure 3 shows the fluorine spectra of the fluorinated silicas prepared using a 5 mM F^- solution. As the calcining temperature is increased, the spectral features sharpen. This would be expected if the broadening is due to dipolar interactions and if the internuclear distance increases as the calcining temperature increases. The increasing internuclear distance with increasing calcining temperature is confirmed by the decrease in the surface fluorine concentration when the samples are calcined at 873 K.

Figure 4 compares the fluorine spectra of silicas prepared with an 18 mM F^- solution but calcined at different temperatures. The spectrum of the sample calcined at 573 K not only has broader features, but the line shape varies considerably from the line shape of the sample calcined at 873 K. Figure 5 compares the fluorine spectrum of the moderately fluorinated silica calcined at 573 K at two different field strengths. The line width scales with the field and the structure of the line shape at 14.1 kG is still quite different from that observed for samples calcined at 873 K.

VanderHart and Gutowsky (21) have shown that such structure is possible in the spectrum of an amorphous or polycrystallline material when the chemical shift and dipolar interactions of an isolated dipole pair have the same magnitude. In this situation the anisotropy of the chemical shift powder pattern of the resonant spins approaches the

magnitude of the separation between the divergences of the powder pattern of the dipolar spectrum of the isolated dipole pair. One example of such isolated dipole pairs would be isolated hydrogen bonds formed between fluorine atoms and hydroxyl groups ($\underset{|}{F}$ ..... H—$\underset{|}{O}$). The theoretical line shape would vary considerably depending on the relative sizes and orientations of the chemical shift and dipolar interactions. Changes in the line shape similar to those observed between the spectra in Figure 4 can also be caused by anisotropic motion.

The centers of mass and the second moments of the room temperature fluorine spectra are found in Table 4. The centers of mass of the fluorine spectra are independent of the fluoride treatment or the calcining temperature. The chemical shift data show clearly that oxyfluoride species ($\equiv$Si-OF) are not formed. The centers of mass are at slightly higher field than one would expect for a fluoride ion. The observed centers of mass are consistent with the reported values of the chemical shifts for fluorine covalently bound to silicon (22).

Within experimental error, all samples calcined at temperatures greater than 673 K have a second moment of 0.5 G^2. The samples calcined at 573 K have second moments 40% larger than those of samples calcined at 873 K. If the line width is due to chemical shift interactions, the ratio of the second moment of spectra obtained at 90.1 MHz to that obtained at 56.4 MHz would be $(90.1/56.4)^2 = 2.6$. The measured values of this ratio range from 1.7 to 2.0. Therefore, the line width has contributions from both chemical shift and dipolar interactions.

The asymmetry observed in the spectra and the shape of the resonance

line can be described by a chemical shift powder pattern. Table 5 contains the results of fitting the expression for a chemical shift powder pattern convoluted with a Gaussian broadening function to the fluorine FID spectra. The conventions used in defining the principal components, $\bar{\sigma}$, δ, and η are given by

$$|\sigma_{zz} - \bar{\sigma}| \geq |\sigma_{xx} - \bar{\sigma}| \geq |\sigma_{yy} - \bar{\sigma}| \qquad (2)$$

$$\bar{\sigma} = (1/3)\,\mathrm{tr}\,\underset{\approx}{\sigma} \qquad (3)$$

where $\underset{\approx}{\sigma}$ is the tensor describing the chemical shift anisotropy

$$\delta = \sigma_{zz} - \bar{\sigma}$$

$$\eta = (\sigma_{yy} - \sigma_{xx})/\delta$$

All values are reported in parts per million relative to hexafluorobenzene. Positive values of the chemical shift are upfield from the reference. The agreement between the centers of mass calculated from the spectra and the isotropic chemical shifts obtained from the fits of the chemical shift tensors is excellent.

Samples treated with aqueous fluoride solutions with fluoride concentrations of 5 mM and 18 mM and calcined at temperatures of 673 K or higher can be described by chemical shift tensors which have the same principal components. Since η is small, < 0.1, it is possible to describe the spectra by an axially symmetric chemical shift tensor. Using the data for lightly modified silica calcined at 873 K, the following parameters are obtained

$$\sigma_{\perp} = \sigma_{xx} = \sigma_{yy} = -44 \text{ ppm}$$

$$\sigma_{\parallel} = \sigma_{zz} = 52 \text{ ppm}$$

$$\Delta\sigma = \sigma_{\parallel} - \sigma_{\perp} = 96 \text{ ppm}.$$

The parameters of the axially symmetric chemical shift tensors obtained from fits of the fluorine spectra for both samples calcined at 873 K are identical within experimental error. The fluorine spectrum obtained at 14.1 kG for the sample prepared using an 18 mM F^- solution and calcined at 873 K can be described by the same chemical shift parameters. Therefore, the line shape is due to the chemical shift anisotropy. The chemical bonding of the fluorine is independent of the fluoride treatment for preparation using aqueous fluoride solutions less than 20 mM F^- and calcination at 873 K.

It can be shown (23) that the second moment of a chemical shift powder pattern calculated about its center of mass is described by

$$\langle \Delta\omega^2 \rangle = (\omega_o \delta)^2 \frac{1}{15} (3 + \eta^2) \qquad (4)$$

where ω_o is the radiofrequency used

δ and η are defined above.

This expression gives the second moment in units of $(\text{rad/sec})^2$. If the parameters of the axially symmetric chemical shift powder pattern obtained for the lightly modified silica calcined at 873 K are substituted into Eq. (4), the second moment calculated for the ideal chemical shift powder pattern is $M_2 = 0.41\ G^2$. The agreement with the second moment calculated from the FID, $0.48\ G^2$, is excellent.

The fluorine chemical shift anisotropy demonstrates that the bonding of the fluorine to the surface does not depend upon the calcining temperature when the calcination occurs at temperatures above 673 K.

For modified silicas calcined at 873 K, the fluorine bonding is independent of the original fluorine atom concentration of the silica.

Relaxation Time Measurements

The hydrogen relaxation times measured at room temperature are reported in Table 6. The hydrogen spin echo, solid echo, and CPMG results for the fluorinated silicas are shown in Figures 7, 8, and 9, respectively.

Figure 6 shows the hydrogen CPMG, spin echo, and solid echo results for the unmodified silica calcined at 773 K. A comparison of the spin echo and the solid echo data shows that the relaxation data are not dominated by the homonuclear dipolar interaction. The chemical shift anisotropy makes a significant contribution to the line width. The CPMG data exhibit a two component decay, the decay constants of which differ from the measured T_2. The relaxation time obtained from the CPMG experiment, T_2^+, has an initial value that is twice as large as T_2. The CPMG data are independent of the pulse spacing for $2\tau \leq 100$ μsec.

The spin echo and CPMG data for fluorine modified silicas are similar to those obtained for the unmodified silica. All samples show contributions to the line width from interactions which refocus under both two-pulse sequences. T_2 increases as the calcining temperature increases for both fluorine modifications. There is a significant difference between T_2 and T_2^+ for all samples, which would result if fluctuations occur in the local fields experienced by the nuclei.

The results of the spin echo experiment for the fluorinated silica prepared using a 5 mM F^- solution and calcined at 873 K are qualitatively similar to those predicted for a system of diffusing nuclei (24). If the

slope of the initial spin echo data is used to obtain T_2, the decay constant is 1.6 μsec. This agrees quite well with the initial slope of the CPMG data. Diffusion of hydrogen or the existence of some other phenomenon causing fluctuations in the interactions have the same symmetry as the I_z spin operator is expected. The modified silica with moderate fluorine treatment calcined at 573 K has similar spin echo behavior but has only a single component in the CPMG data with $T_2^+ \sim 10T_2$.

The behavior described above for the lightly fluorinated silica calcined at 873 K is not apparent in all of the samples. If the fluctuations are relatively fast, the part of the decay dominated by T_2 may be quite small. In order to observe this behavior, data need to be collected for short values of τ. If the spacing between 180^o pulses is reduced, the CPMG experiment might exhibit two component behavior. If 2τ is long compared to the fluctuation rate, then only the slow decay of the magnetization due to the isolated spin system would be observed.

The long decay observed during the CPMG experiment is characteristic of stationary, well isolated nuclei. The measured values of T_2^+ for samples calcined at 873 K are in very close agreement with one another. Using a statistical approach developed by Anderson (25), the expression for the half width at half height of an absorption curve broadened by dipolar effects for a magnetically dilute material is

$$\delta = \frac{2\pi^2}{3\sqrt{3}} \gamma^2 \hbar n \qquad (5)$$

where n is the density of spins.

If two samples are compared which are identical in all ways except the spin density, then the following ratio is obtained

$$\frac{\delta_1}{\delta_2} \alpha \frac{n_1}{n_2}$$

The spin density is defined as

$$n = N/V$$

where N is the number of spins and V is the volume of the sample. If the dipoles are assumed to be distributed uniformly throughout the samples,

$$\frac{n_1}{n_2} \alpha \frac{r_{ij,2}^3}{r_{ij,1}^3} \qquad (6)$$

where r_{ij} is the internuclear distance between the dipoles. Then

$$\frac{\delta_1}{\delta_2} \alpha \frac{r_{ij,2}^3}{r_{ij,1}^3} \qquad (7)$$

The CPMG data of the fluorinated silica prepared using a 5 mM F^- solution and calcined at 873 K can be described by two exponential decays. If $2\delta_{II}$ is the contribution to the full width at half height due to homonuclear dipolar interactions, then $2\delta_{II} = \frac{1}{\pi T_2^+}$. Using $T_2^+ = 18$ msec, then $2\delta_{II} = 17.6$ Hz = 4.2 mG. When $T_2^+ = 1.5$ msec, then $2\delta_{II} = 212$ Hz = 50 mG. Since the parameters in Eq. (7) are identical for both parts of the decay except for the density of spins then

$$\frac{\delta_2}{\delta_1} = \frac{17.6}{212} = 0.083 = \frac{r_{ij,1}^3}{r_{ij,2}^3}$$

and $r_{ij,2} = 2.3\ r_{ij,1}$. Therefore, the second part of the CPMG decay

represents hydroxyl groups with twice the internuclear separation of those contributing to the first part of the decay.

The full widths at half intensity of hydrogen on fluoride modified silicas measured at 99.7 MHz ranged from 1200 Hz to 2600 Hz. If T_2^+ = 1.5 msec, then the homonuclear dipolar effects contribute significantly to the line width. When T_2^+ is greater than 10 msec, homonuclear dipolar effects have a negligble contribution to the line width.

The decay of the magnetization as a function of 2τ during the solid echo experiment is due to the chemical shift and heteronuclear dipolar interactions. For silicas prepared using a 5 mM F^- solution, the decay constant of the 90^o-τ-90^o experiment, T_2^{IS}, increased by more than a factor of two as the calcining temperature was increased. Since the chemical shift would be expected to remain constant, this increase in T_2^{IS} can be interpreted as a decrease in the heteronuclear dipolar interaction. The calcining temperature does not have an effect upon T_2^t for samples prepared using an 18 mM F^- solution.

The magnitude of the fluorine-fluorine dipolar interaction was determined from CPMG experiments. Solid echo experiments were not used since the fluorine chemical shift anisotropy could be determined from the ^{19}F FID spectrum. The heteronuclear dipolar interaction is much smaller than the chemical shift anisotropy and therefore would be difficult to obtain using solid echo data. T_2 was measured on two samples and the results compared their T_2^+'s in order to check for the possibility of diffusion.

Results from ^{19}F CPMG experiments showed that $T_2^+ > 1.5$ msec for all samples (see Table 7). The decay constant, T_2^+, for fluoride treatment

using an 18 mM F^- solution is 8.3 msec regardless of the calcining temperature. Assuming a Lorentzian line shape with T_2^+ = 8.3 msec, the contribution of the fluorine-fluorine dipolar interaction to the full width at half height is 38 Hz. The CPMG data indicate that the fluorine atoms are widely separated from one another. The results of the CPMG experiments were independent of the pulse spacing for $2\tau \leq 150$ sec.

T_2 data for samples treated with an 18 mM F^- solution show that fluorine atoms experience fluctutations of some kind in their local magnetic fields. There are two possible sources for this fluctuation. One is the diffusion of fluorine in the modified silica. The second is fluctuations arising from changes in the hydrogen-fluorine heteronuclear dipolar interaction.

Low Temperature Free Induction Decays

The relaxation studies showed significant differences between T_2 and T_2^+ for all modified silicas. The hydrogen spin echo data for lightly modified silica calcined at 873 K are qualitatively similar to the results expected if the hydrogen atoms were diffusing in the sample. Therefore, free induction decays were obtained at several temperatures. The spectra used for external chemical shift references were taken at the same temperature as the FID for temperatures above 145 K. Room temperature references were used for data below this temperature. However, no shift in the center of mass was observed for the external references used and the external magnetic field did not change as the probe was cooled from room temperature to 110 K. None of the data presented here have been corrected for bulk magnetic susceptibility

since the volumetric susceptibilities of the samples were unknown. Using the room temperature susceptibility estimated previously, 1.1 ppm to higher field, and recalling that the magnetic susceptibility is inversely proportional to the temperature, a maximum susceptibility correction of approximately 3 ppm to higher field is estimated (corresponding to a temperature of 120 K).

Two types of behavior may be expected as the temperature is lowered. If any motion is occurring, the motional averaging of the interactions broadening the line will cease as the sample temperature is lowered. This will cause the line width to increase. Slowing of anisotropic motion may cause changes in the line shape as the averaging of the chemical environment that the nuclei experiences will change. Also, if the atoms are exchanging rapidly between two or more sites, lowering the temperature will slow the rate of exchange until the resonances for each individual species are observed rather than the averaged resonance.

Figure 10 shows the hydrogen spectrum for unmodified silica as a function of temperature. Changes in the line shape occur at all temperatures. The center of mass and second moment are constant for temperatures greater than 160 K. Below this temperature, the center of mass begins to move slightly downfield. The second moment increases, reaching a value of 0.08 G^2 at 105 K. The values of the center of mass, second moment, and full width at half height are found in Table 8.

The centers of mass, second moments, and full widths at half height for the fluorine modified silicas are found in Table 8 also. In all cases, with the exception of the moderately fluorinated silica calcined

at 573 K, the centers of mass shift downfield as the temperature decreases. The maximum downfield shift is 14 ppm. Both fluorinated silicas prepared using a 5 mM F^- solution experience an increase in the second moment of at least 50%. Line shapes and second moments of samples prepared using an 18 mM F^- solution show little change as a function of temperature. No broad components appear in the spectra of any sample at any observation temperature. The asymmetries in the hydrogen spectra are retained at all observation temperatures.

The low temperature fluorine NMR spectra of modified silica calcined at 873 K do not change as a function of temperature. The spectra of fluorinated silicas prepared using a 5 mM F^- solution and calcined at 873 K have been obtained at two temperatures and are shown in Figure 11. Spectral parameters of modified silicas calcined at 873 K are given in Table 9. The principal components of the chemical shift tensors measured for the spectra obtained at 290 K and 110 K agree closely for the fluorinated silica prepared using a 5 mM F^- solution and calcined at 873 K.

The room temperature fluorine NMR spectrum of silica treated with a 5 mM F^- solution and calcined at 573 K differs little from the spectrum observed at 115 K. However, the silica treated with an 18 mM F^- solution and calcined at 573 K shows changes in its line shape when observed at these temperatures. The fluorine spectra of both samples calcined at 573 K are very similar when observed at 115 K. The centers of mass and chemical shift parameters are given in Table 9. The fluorine spectra of fluorinated silica prepared using an 18 mM F^- solution and calcined at 573 K at four observation temperatures are shown in Figure 12. The

complete spectrum is being observed in all cases. There are no large increases in the line width of the spectra as the observation temperature is lowered. However, changes in the line shape are observed as the observation temperature is changed. The room temperature spectrum cannot be described by a chemical shift powder pattern. As the temperature is lowered, the spectrum loses intensity near its center of mass. At 110 K the fluorine spectrum can be described by a chemical shift powder pattern which has the principal components σ_{xx} = -73 ppm, σ_{yy} = -49 ppm, and σ_{zz} = 41 ppm. All values are given relative to hexafluorobenzene.

CONCLUSIONS

The use of nuclear magnetic resonance spectroscopy has provided direct information concerning the local environment of hydroxyl groups and fluorine atoms on modified silicas. Fluorine does not adsorb onto silica by direct replacement of hydroxyl groups. The ammonium fluoride reacts with the oxide bridges between silicon atoms. Heating at temperatures less than 373 K eliminates excess water and ammonium fluoride. Calcining at temperatures of 573 K or higher removes the physically adsorbed ammonia and causes condensation reactions between neighboring surface species as below.

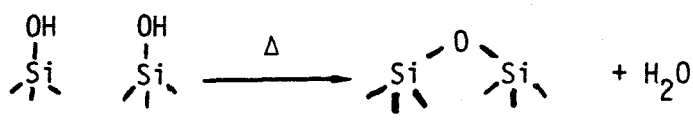

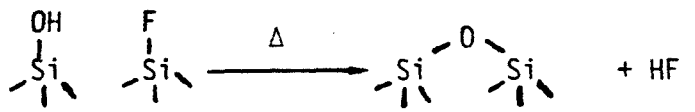

If diffusion of the surface species occurs at the temperatures used for

calcination, the condensation reactions above might occur even when the concentration of the surface species is low. The adsorbed fluorine forms covalent bonds to the silicon atoms. The fluorine bonding does not change as the calcination temperature is varied.

Reproducible fluorine modified silicas can be prepared using aqueous fluoride solutions with fluoride concentrations up to 20 mM. If aqueous ammonium fluoride solutions with fluoride concentrations of five weight percent are used, volatile silicon compounds are formed upon calcination which cause sample destruction. Therefore, the fluorine modification of oxides must be done carefully if the oxides contain silicon.

Hydrogen is present at all calcination temperatures up to 873 K unless concentrated aqueous ammonium fluoride solutions are used for sample preparation. Although the hydrogen spectra appear to contain only a single resonance, the shifts in the centers of mass and the changes in the second moments as a function of external field strength indicate that the nature of the bonding of the hydroxyl groups changes depending on the sample preparation. Maciel and co-workers (26, 27) have identified the three silicon environments shown below on a chromatographic silica gel using ^{29}Si NMR with cross-polarization and magic-angle sample planning techniques:

$(HO)_2 Si (OSi\lessgtr)_2$ $\qquad$ $HOSi(OSi\lessgtr)_3$ $\qquad$ $Si(OSi\lessgtr)_4$

Higher hydroxyl group concentrations and geminal hydroxyl groups, $\gtrless Si(OH)_2$, are expected for the chromatographic gels studied.

Hydrogen chemical shift anisotropies typically have values of 14 ppm or greater for hydroxyl groups (23, 28). Such chemical shift anisotropies

are too large to describe the hydrogen spectra obtained for fluorine modified silica. Therefore, either the chemical bonding of these hydroxyl groups must differ from that reported for other types of hydroxyl groups in the solid state or anisotropic motion causes a partial averaging of the chemical shift anisotropy.

The formation of solid echoes by hydroxyl groups means that there must be a significant contribution from the chemical shift and heteronuclear dipolar interactions. The long CPMG relaxation times, T_2^+, indicate that the hydroxyl groups are well separated from each other and that the fluorine atoms are isolated from one another. The spin echo relaxation times, T_2, are much shorter than T_2^+ for both the fluorine atoms and the hydroxyl groups. This behavior indicates that there are fluctuations in the local fields of the nuclei.

The discrepancy between T_2 and T_2^+ is usually explained by molecular diffusion. If diffusion is occurring, data taken at low temperatures should show an increase in the line width or changes in the line shape. No significant broadening of the spectra is observed in the spectra for either the hydroxyl groups or fluorine atoms for temperatures as low as 110 K. The line width of unmodified silica observed at 77 K (15) agrees with the data reported here. Staudte (29) reported that diffusion of hydroxyl groups in unmodified silica occurs at temperatures above 393 K. The presence of adsorbed molecules increases the diffusion rate of the hydroxyl groups. An increase in T_2^* was observed as the temperature increased from 148 to 423 K. This was explained by rotation of the hydroxyl protons about the Si-O axis. Schreiber and Vaughan (12) proposed

that the narrow chemical shift tensor observed for hydroxyl groups on silica could be explained by rotation of the hydroxyl proton about the Si-O axis. This rotational motion could explain the discrepancy between T_2 and T_2^+ observed in this investigation and the changes in the line shape as a function of the observation temperature.

The calcining temperature is a key variable in the preparation of fluorine modified silica. The fluorine spin-lattice relaxation time, the fluorine concentration, and the hydroxyl group concentrations of modified silicas calcined at 873 K differ significantly from samples calcined at 773 K or less. Calcination at 873 K forms a reproducible oxide for silicas which initially have very different fluorine and hydroxyl group concentrations.

The relaxation phenomena could result from a number of factors. If motional processes were very fast, the line widths would not be affected at the temperatures studied. Fluctuations in the heteronuclear dipolar or the chemical shift interactions would also cause significant differences between T_2 and T_2^+. Any motion of the fluorine atoms must be anisotropic since a large chemical shift anisotropy is observed in the fluorine FID.

The long T_2^+ values measured for both the hydrogen and fluorine spectra of all of the samples suggest that the broadening of the fluorine FID's at lower calcining temperature is due to contributions from hydrogen-fluorine dipolar interactions. Katsuo et. al. (4) propose that silanol groups interact with neighboring fluorine atoms as shown below.

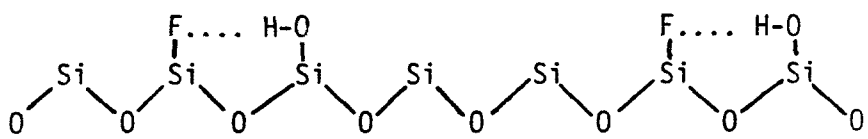

Hydrogen bonds between hydrogen and fluorine have been observed for the bifluoride ion, FHF^-, (30, 31, 32) and hydrazine fluoride, $N_2H_6F_2$, (33). The hydrogen-fluorine internuclear distances are 1.15 Å and 1.54 Å, respectively. The divergences for the powder pattern dipolar spectra for these isolated dipole pairs would be separated by 11.8 kHz and 4.9 kHz, respectively. The bond distance for hydrogen bonds on fluorine modified silica would be much larger than these reported values. The internuclear distance, r_{HF}, for a hydroxyl group and a fluorine atom on neighboring silicon atoms using a simple model for silica is estimated to be 2.5 Å. The splitting for the divergences of the powder pattern of the dipolar spectrum for such a heteronuclear dipole pair would be 1.2 kHz with the shoulders having a separation of 2.4 kHz. This behavior was not apparent in the hydrogen spectra of fluorinated silica. VanderHart and Gutowsky (21) have described the powder pattern spectra which would be expected for isolated dipole pairs when the magnitude of the chemical shift anisotropy of the resonant spin approaches the magnitude of the separation between the divergences in the dipolar spectrum. Isolated hydrogen bonds formed between hydroxyl groups and fluorine atoms would have an NMR spectrum similar to the results of their calculations. Such fluorine and hydrogen NMR spectra were not observed at room temperature. Therefore, the room temperature NMR data does not verify the formation of hydrogen bonds between hydroxyl groups and fluorine for the modified silicas prepared for this investigation.

Magic-angle sample spinning techniques would contribute significantly to the understanding of fluorinated silicas. Use of these techniques would eliminate the dipolar broadening and broadening due to the chemical

shift anisotropy. The elimination of these effects would help to resolve the spectra of hydroxyl groups whose isotropic chemical shifts differ by only a few parts per million. Slight differences in the chemical bonding of the hydroxyl groups could be identified. The narrow line widths of the hydrogen spectra would allow narrowing of the spectrum at spinning rates of 2.5 kHz or less. Multiple-pulse techniques might be unnecessary since the homonuclear dipolar interaction is small. Magic-angle sample spinning could be used with the fluorine spectrum to determine the various types of fluorine present also.

The reason for the discrepancies between T_2 and T_2^+ needs to be understood. A study of the temperature dependence of the relaxation times is needed to determine if this behavior is due to motional phenomena. Spectra must be obtained at temperatures below 100 K if spectra without the effects of anisotropic motion or chemical exchange between different sites are to be observed.

References

1. Choudhary, V. R. Ind. Eng. Chem., Prod. Research Develop. 16, 12 (1977).
2. Peri, J. B., J. Phys. Chem. 72, 2917 (1968).
3. Chapman, I. D., and Hair, M. L., J. Catal. 2, 145 (1963).
4. Katsuo, T., Satohiro, Y., and Kimio, T., Bull. Jap. Petrol. Inst. 12, 136 (1970).
5. Sidorov, A. N., and Neimark, I. E., Russ. J. Phys. Chem. 38, 1518 (1964).
6. Golovanova, G. F., Ivanova, N. N., and others, Theor. Exp. Chem., USSR 9, 301 (1973).
7. "Silicon Compounds: Register and Review" (B. C. Arkles and W. R. Peterson, Jr., Eds.) p. 110. Petrarch Systems, Inc., Levittown, Pa., 1979.
8. Vaughan, R. W., Elleman, D. D., Stacey, L. M., Rhim, W. K., and Lee, J. W., Rev. Sci. Instrum. 43, 1356 (1972).
9. Meiboom, S., and Gill, D., Rev. Sci. Instrum. 29, 688 (1958).
10. Hughes, T. R., White, H. M., and White, R. J., J. Catal. 13, 58 (1969).
11. Hall, W. K., Leftin, H. P., Cheselke, F. J., and O'Reilly, D. E., J. Catal. 2. 506 (1963).
12. Schreiber, L. B., and Vaughan, R. W., J. Catal. 40, 226 (1975).
13. Freude, D., Muller, D., and Schmiedel, H., Surface Sci. 25, 289 (1971).
14. Oehme, W., Diplomarbeit, Karl-Marx-Universitat, Leipzig, 1970. from Ravkin, B., and Herak, J. W., Surface Sci. 51, 310 (1975).
15. Davydov, V. Y., Kiselev, A. V., and Zhuravlev, L.T., Trans. Faraday Soc. 60. 2254 (1964).
16. Abragam, A., "The Principles of Nuclear Magnetism", Oxford University Press, 1961.

17. Osborn, J. A., Phys. Rev. 67, 351 (1945).

18. Reimer, J. A., Vaughan, R. W., and Knights, J. C., Phys. Rev. Lett. 44, 193 (1980).

19. Reimer, J. A., Personal Communication.

20. O'Reilly, D. E., Leftin, H. P., and Hall, W. K., J. Chem. Phys. 29, 970 (1958).

21. VanderHart, D. L., and Gutowsky, H. S., J. Chem. Phys. 49, 261 (1968).

22. Emsley, J., and Phillips, L., in "Progress in Nuclear Magnetic Resonance" (J. W. Emsley, J. Feeney, and L. H. Sutcliffe, Eds.). Vol. 7, pp. 500-502. Pergamon Press, New York, 1971.

23. Haeberlin, U., "High Resolution NMR in Solids-Selective Averaging", in "Advances in Magnetic Resonance", Suppl. 1, (J. S. Waugh, Ed.). Academic Press, New York,1976.

24. Carr, H. Y., and Purcell, E. M., Phys. Rev. 94, 630 (1954).

25. Anderson, P. W., Phys. Rev. 82, 342 (1951).

26. Maciel, G. E., and Sindorf, D. W., J. Amer. Chem. Soc. 102, 7606 (1980).

27. Maciel, G. E., Sindorf, D. W., and Bartuska, V. J., J. Chromatog. 205, 438 (1981).

28. Mehring, M., "High Resolution NMR Spectroscopy in Solids, NMR-Basic Principles and Progress" (P. Diehl, E. Fluck, and R. Kosfeld, Eds.). Vol. 11, p.1. Springer-Verlag, New York, 1976.

29. Staudte, B., Z. Phys. Chem. (Leipzig) 255, 158 (1974).

30. Waugh, J. S., Humphrey, F. B., and Yost, D. M., J. Phys. Chem. 57, 486 (1953).

31. Van Hecke, P., Spiess, H. W., and Haeberlen, U., J. Magn. Resonance. 22, 93 (1976).

32. Van Hecke, P., Spiess, H. W., and Haeberlen, U., J. Magn. Resonance. 22, 103 (1976).

33. Deeley, C. M., and Richards, R. E., Trans. Faraday Soc. 50, 560 (1954).

Table 1

Hydrogen and Fluorine Concentrations

Fluorine Treatment	Calcining Temperature (K)	BET Surface Area (m^2/g)	Surface Concentrations ($10^{18}/m^2$) Hydrogen	Fluorine	Weight Percent Fluorine (%)
None	773	250 + 10	2.4+0.3	----	----
Light	573	255	2.8	2.1+0.3	1.7+0.2
	673	238	2.7	2.4	1.8
	773	256	1.8	2.4	2.0
	873	223	1.2	1.5	1.1
Moderate	573	232	2.1	6.9	5.1
	873	207	1.3	1.4	0.9

Table 2

Spin-Lattice Relaxation Times

Fluorine Treatment	Calcining Temperature (K)	T_1[a] Hydrogen (sec)	Fluorine (sec)
None	773	6.2	---
Light	573	8.4	41.
	673	12.	40.
	773	8.4	37.
	873	14.	21.
Moderate	573	17.	19.
	873	11.	28.
Heavy	773	---	9.9

[a] Relative standard deviation of 10%.

Table 3

Moments from Hydrogen Spectra

Flourine Treatment	Calcining Temperature (K)	External Field (kG)	Center of Mass[a] (ppm)	Full Width at Half Height (Hz)	Second Moment[b] (G^2)
None	773	13.2	0.+1	1500	0.06
		23.4	-3.	1800	0.05
Light	573	13.2	3.	2150	0.13
		23.4	5.	2600	0.19
	873	13.2	-8.	1200	0.03
		23.4	-1.	1600	0.03
Moderate	573	13.2	0.	1400	0.06
		23.4	-5.	2000	0.18
	873	13.2	-5.	1200	0.02
		23.4	-2.	1600	0.04

[a] Relative to tetramethylsilane

[b] $\pm$ 15%

Table 4

Moments from Fluorine Spectra

Fluorine Treatment	Calcining Temperature (K)	External Field (kG)	Center of Mass[a] (ppm)	Second Moment (G^2)
Light	573	14.1	-11.+2.	0.40+0.03
		22.5	-12.	0.66
	673	22.5	-11.	0.45
	773	22.5	-10.	0.51
	873	22.5	-10.	0.48
Moderate	573	14.1	-16.	0.34
		22.5	-10.	0.62
	873	14.1	-11.	0.24
		22.5	-8.	0.47
Heavy	773	22.5	-11.	0.53

[a] Relative to hexafluorobenzene

Table 5

Principal Components of ^{19}F Chemical Shift Tensors for Fluorinated Silica

Fluorine Treatment	Calcining Temperature (K)	σ_{xx} (ppm)	σ_{yy} (ppm)	σ_{zz} (ppm)	$\bar{\sigma}$ (ppm)	δ (ppm)	η
Light	573	-46.+3	-34.+3	49.+3	-10.+2	60.	0.21
	673	-41.	-35.	47.	-10.	57.	0.10
	773	-38.	-35.	50.	-7.	58.	0.05
	873	-43.	-38.	53.	-10.	63.	0.08
Moderate	573	---	---	---	---	---	---
	873	-38.	-35.	53.	-6.	60.	0.05
Heavy	773	-54.	-31.	52.	-11.	63.	0.36

Principal components and isotropic shifts are reported relative to hexafluorobenzene.

Table 6

Hydrogen Relaxation Times

Fluorine Treatment	Calcining Temperature (K)	T_2[a] (msec)	T_2^{IS}[b] (msec)	T_2^{+}[b] (msec)
None	773	0.33	0.41	0.63
				14.
Light	573	0.21	0.19	17.
	873	0.66	0.47	1.5
Moderate	573	0.48	0.27	10.
	873	0.74	0.25	19

[a] Relative Error of ± 20%

[b] Relative Error of ± 10%

Table 7

Fluorine Relaxation Times

Fluorine Treatment	Calcining Temperature (K)	T_2[a] (msec)	T_2^+[a] (msec)
Light	573	---	12.
	873	---	1.6
Moderate	573	0.26	8.3
	873	0.80	8.2

[a] Relative Error of ± 15%

Table 8

Low Temperature Hydrogen Data

Fluorine Treatment	Calcining Temperature (K)	Observation Temperature (K)	Center of Mass[a] (ppm)	Full Width at Half Height (kHz)	Second Moment[b] (G^2)
None	773	290	-3.+1	1.8+0.1	0.05+0.005
		220	-4.	2.0	0.05
		160	-6.	2.0	0.07
		105	-10.	2.0	0.08
Light	573	290	5.	2.8	0.19
		165	-5.	2.8	0.15
		140	-8.	3.0	0.26
		110	-9.	2.8	0.24
	873	290	-2.	1.6	0.03
		160	-6.	1.8	0.03
		110	-6.	2.2	0.06
Moderate	573	290	-5.	2.2	0.18
		141	5.	3.0	0.30
		115	-1.	2.4	0.22
	873	290	-2.	1.6	0.04
		160	-4.	1.4	0.02
		145	-7.	1.8	0.05
		110	-10.	1.4	----

[a] Relative to TMS
[b] Relative Error of ±15%

Table 9

Low Temperature Fluorine Chemical Shift Parameters

Fluorine Treatment	Calcining Temperature (K)	Observation Temperature (K)	Principal Components σ_{zz} (ppm)	σ_{xx} (ppm)	σ_{yy} (ppm)	δ (ppm)	η
Light	573	290	49.+5	-46.+3	-34.+3	60.	0.21
		115	50.	-45.	-40.	62.	0.09
	873	290	53.	-43.	-38.	63.	0.08
		110	49.	-50.	-42.	64.	0.14
Moderate	573	112	39.	-73.	-49.	67.	0.35

All values of the principal components are given in parts per million relative to hexafluorobenzene.

Figure Captions

Figure 1. Room temperature hydrogen FID spectrum of unmodified silica calcined at 773 K. The spectrum was obtained at 23.4 kG. Values of the chemical shift are reported relative to tetramethylsilane.

Figure 2. Room temperature hydrogen FID spectra of fluorinated silicas. The external field strength was 23.4 kG. At left are the fluorinated silicas prepared using a 5 mM F^- solution and calcined at (A) 573 K and at (B) 873 K. At right are the fluorinated silicas prepared with an 18 mM F^- solution and calcined at (C) 573 K and at (D) 873 K. Values of the chemical shift are reported relative to tetramethylsilane.

Figure 3. Room temperature fluorine FID spectra obtained at 22.5 kG of fluorinated silicas prepared using a 5 mM F^- solution and calcined at (A) 573 K, at (B) 773 K, and at (C) 873 K. Values of the chemical shift are reported relative to hexafluorobenzene.

Figure 4. Room temperature fluorine FID spectra obtained at 22.5 kG of fluorinated silicas prepared using an 18 nM F^- solution and calcined at (A) 573 K and at (B) 873 K. Values of the chemical shift are reported relative to hexafluorobenzene.

Figure 5. Room temperature fluorine FID spectra of fluorinated silica prepared using an 18 mM F^- solution and calcined at 573 K. The external magnetic field strengths used were (A) 22.5 kG and (B) 14.1 kG.

Figure 6. Comparison of the hydrogen Carr-Purcell-Meiboom-Gill (CPMG), 90^{o}-τ-80^{o}, and 90^{o}_{y}-τ-90^{o}_{x} decays of unmodified silica calcined at 773 K. Note the difference in the times scales between the CPMG and the two-pulse decays.

Figure 7. Comparison of the hydrogen T_2 decays as a function of sample preparation for the fluorinated silicas. At left are the decays of fluorinated silicas prepared using a 5 mM F^- solution and calcined at (A) 573 K and at (B) 873 K. At right are the decays of the fluorinated silicas prepared using an 18 mM F^- solution and calcined at (C) 573 K and at (D) 873 K.

Figure 8. Comparison of the hydrogen T_2^{IS} decays as a function of sample preparation for the fluorinated silicas. At left are the decays of fluorinated silicas prepared using a 5 mM F^- solution and calcined at (A) 573 K and at (B) 873 K. At right are the decays of the fluorinated silicas prepared using an 18 mM F^- solution and calcined at (C) 573 K and at (D) 873 K.

Figure 9. Comparison of the hydrogen CPMG (T_2^+) decays as a function of sample preparation. The top two decays are of fluorinated silicas prepared using a 5 mM F^- solution and calcined at (A) 573 K and at (B) 873 K. The bottom two decays are of fluorinated silicas prepared using an 18 mM F^- solution and calcined at (C) 573 K and at (D) 873 K.

Figure 10. Hydrogen FID spectra as a function of temperature of an unmodified silica calcined at 773 K. The temperatures at which the data were obtained are given beside each spectrum.

Values of the chemical shift are reported relative to tetramethylsilane.

Figure 11. Fluorine FID spectra as a function of temperature for a fluorinated silica prepared using a 5 mM F^- solution and calcined at 873 K. The spectra were obtained at (A) 290 K and at (B) 110 K. Values of the chemical shift are reported relative to hexafluorobenzene.

Figure 12. Fluorine FID spectra as a function of temperature for a fluorinated silica prepared using an 18 mM F^- solution and calcined at 573 K. The temperatures at which the data were obtained are given beside each spectrum. Values of the chemical shift are reported relative to hexafluorobenzene.

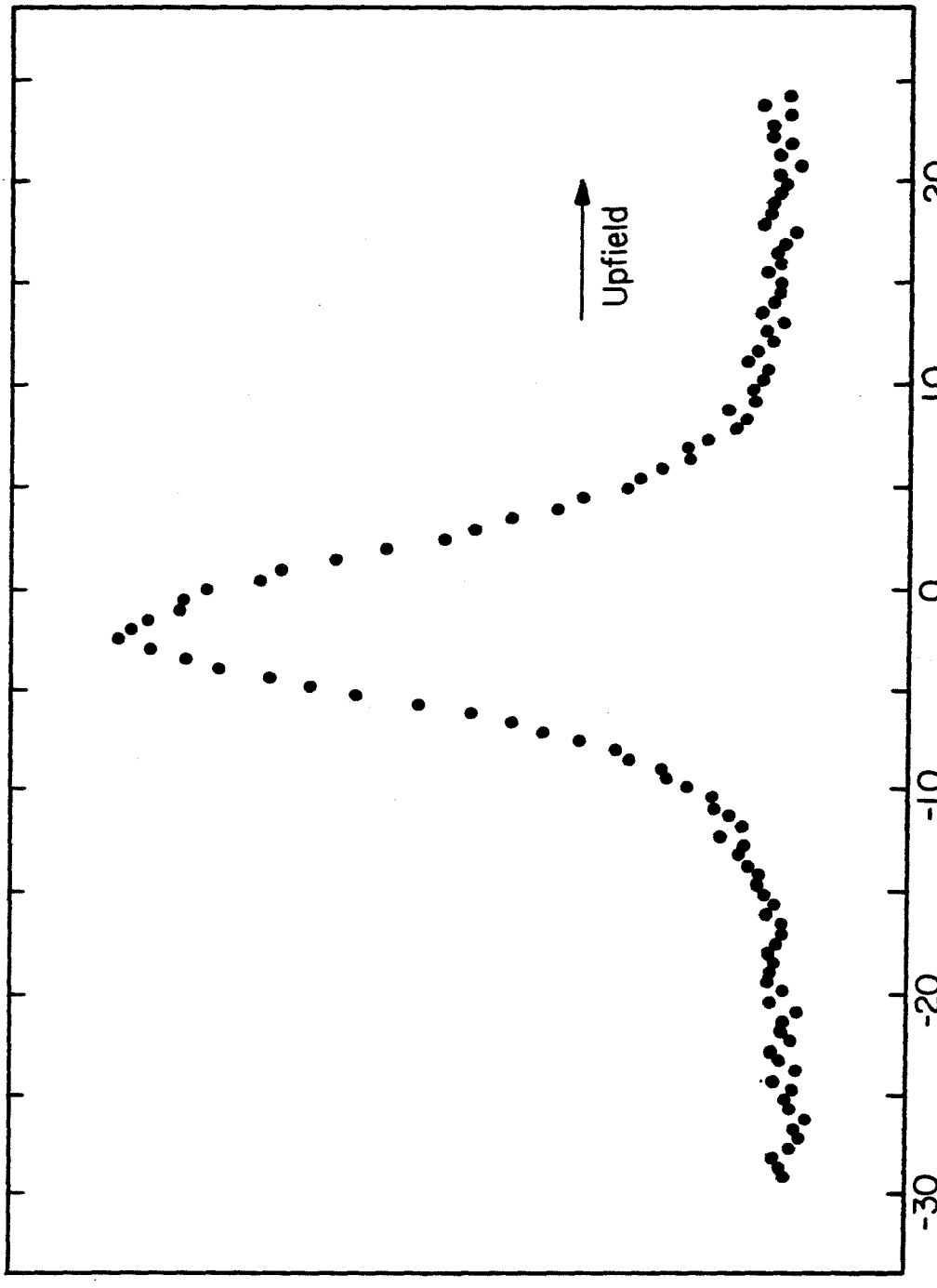

Figure 1

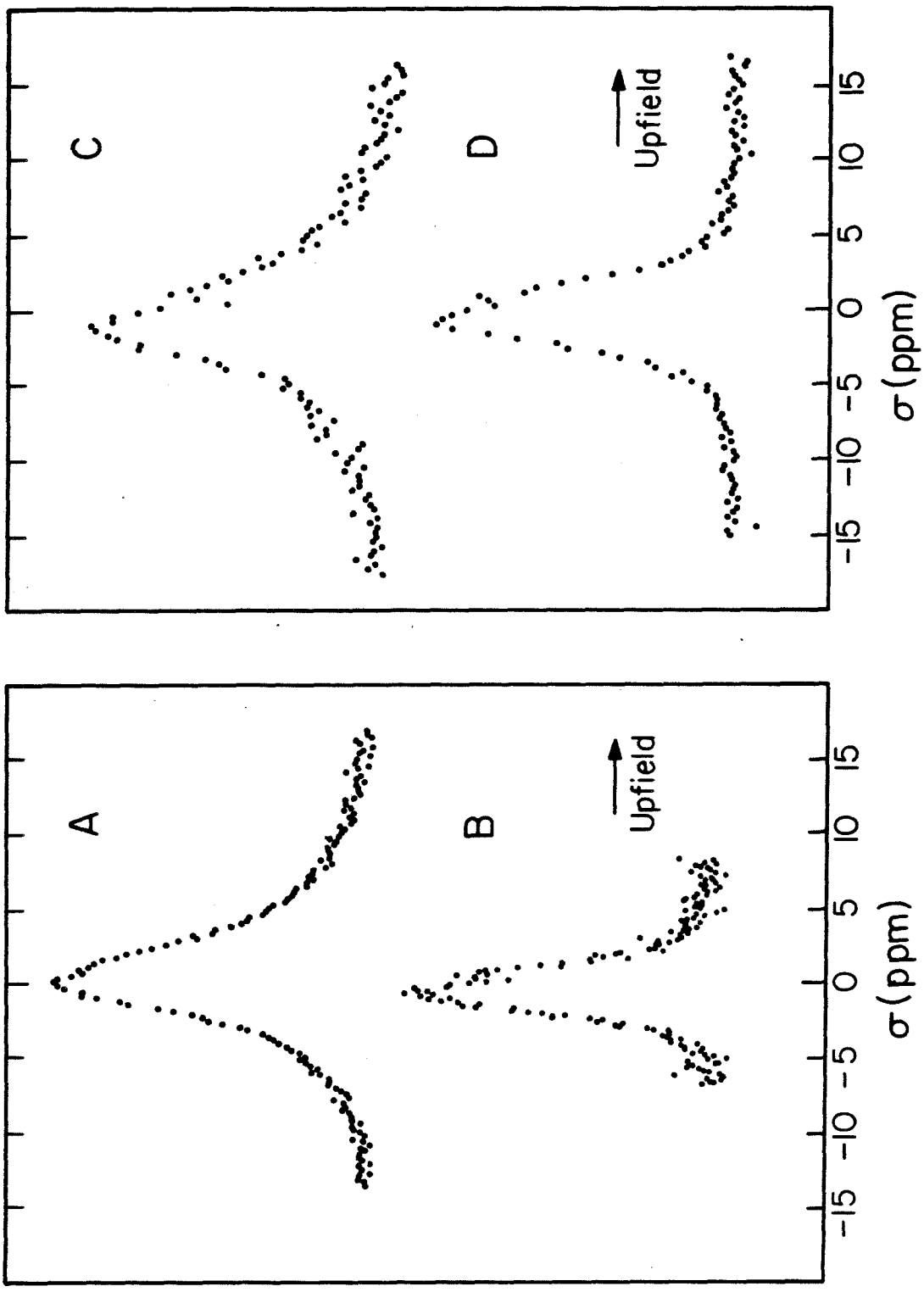

Figure 2

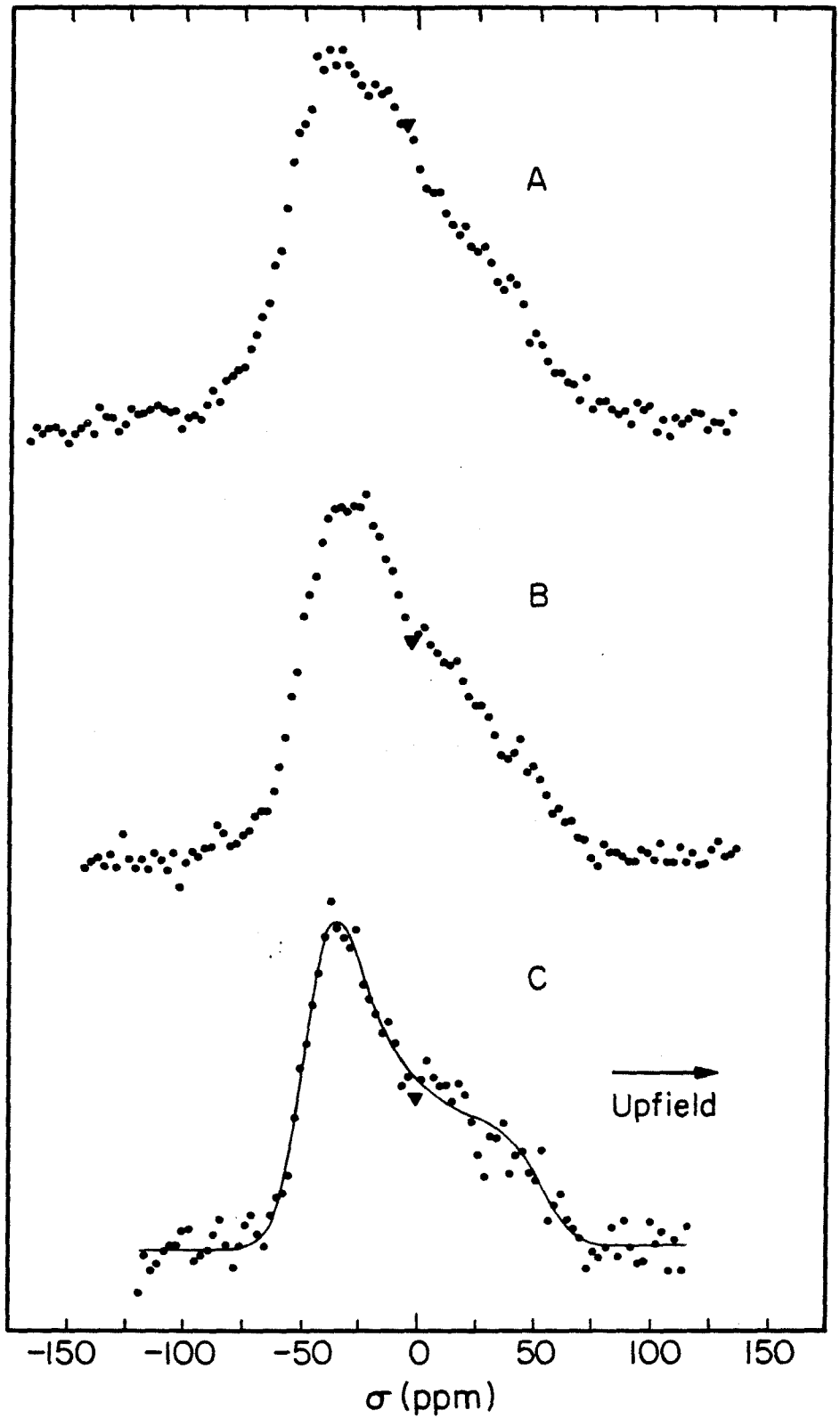

Figure 3

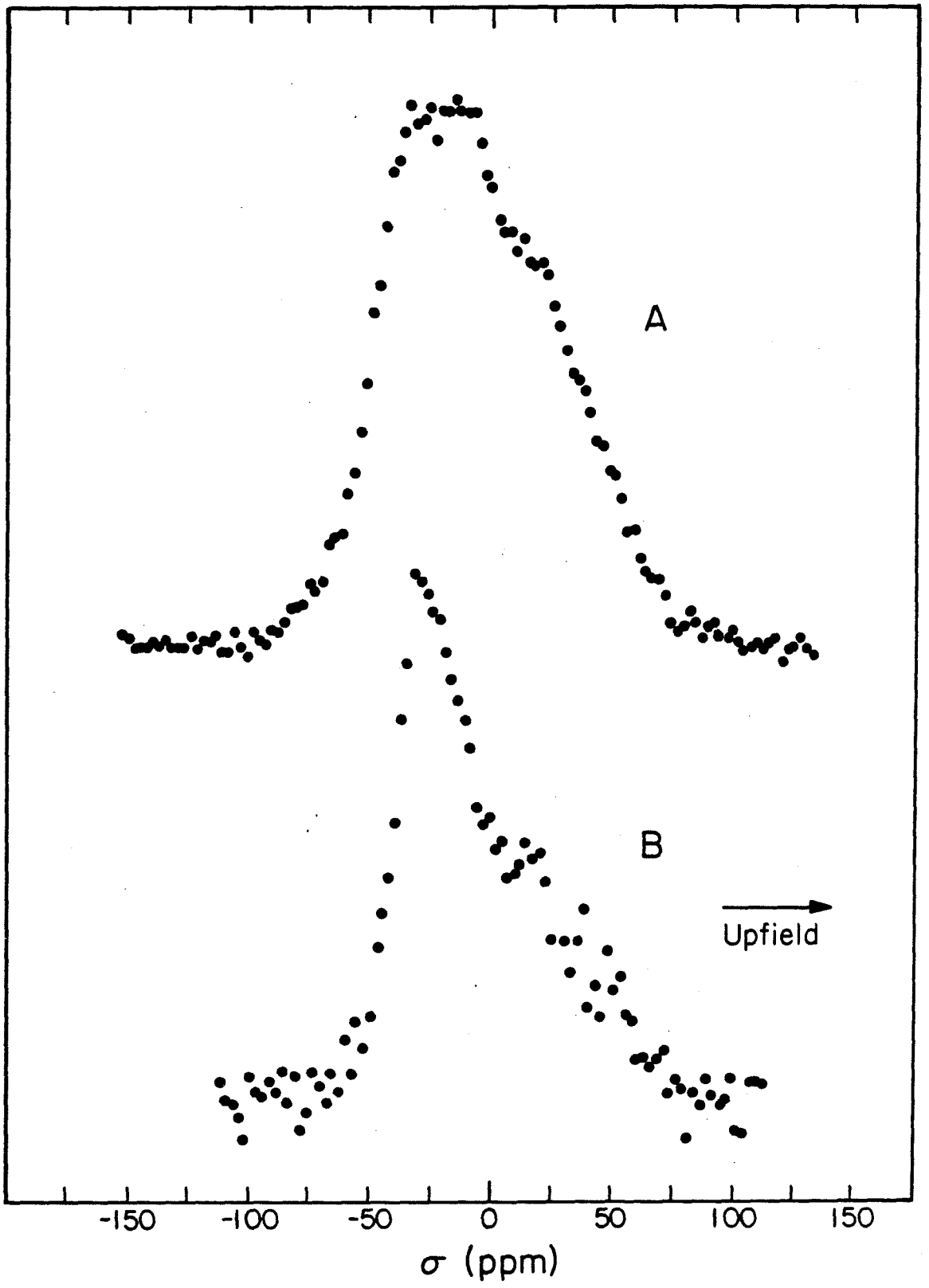

Figure 4

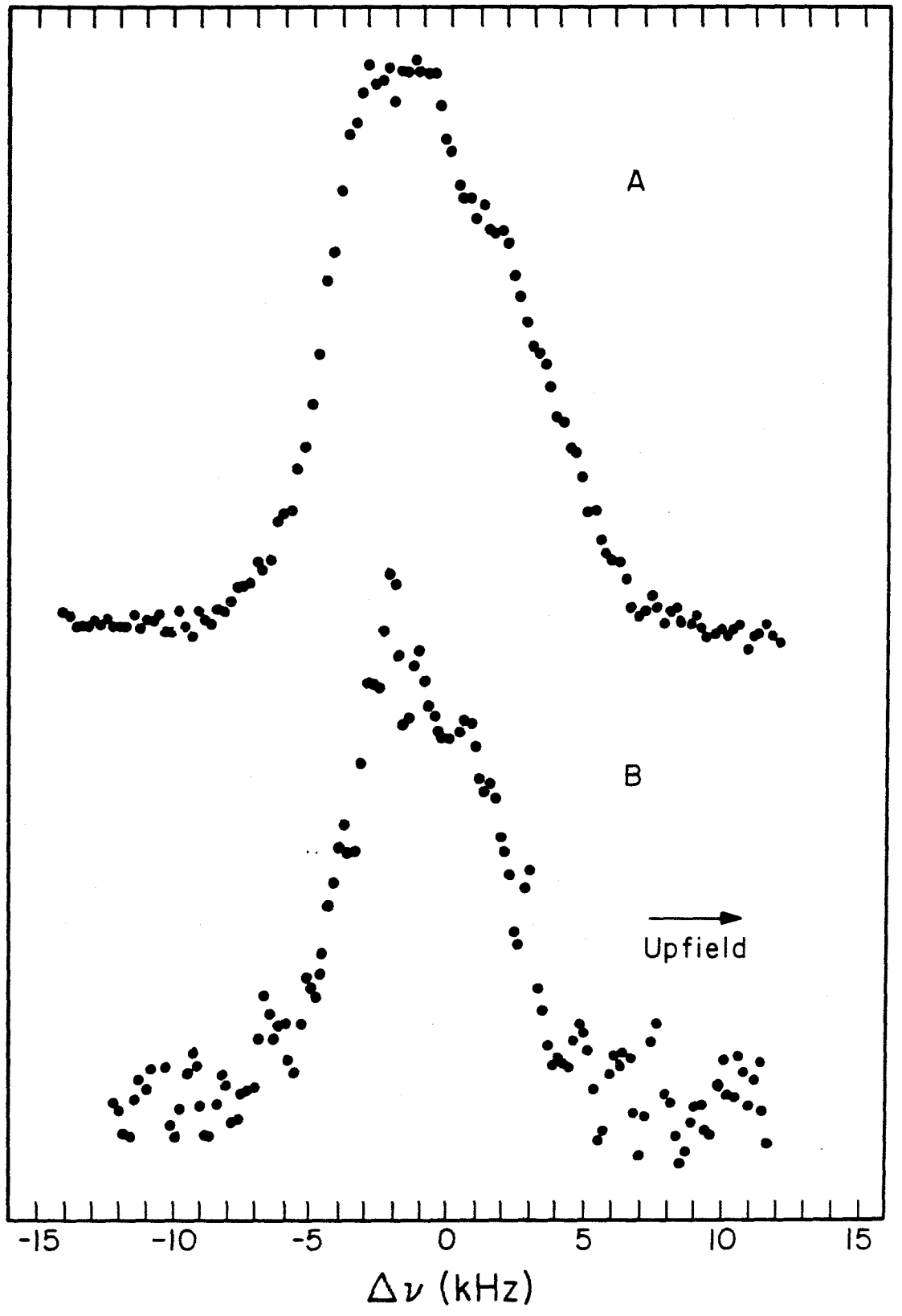

Figure 5

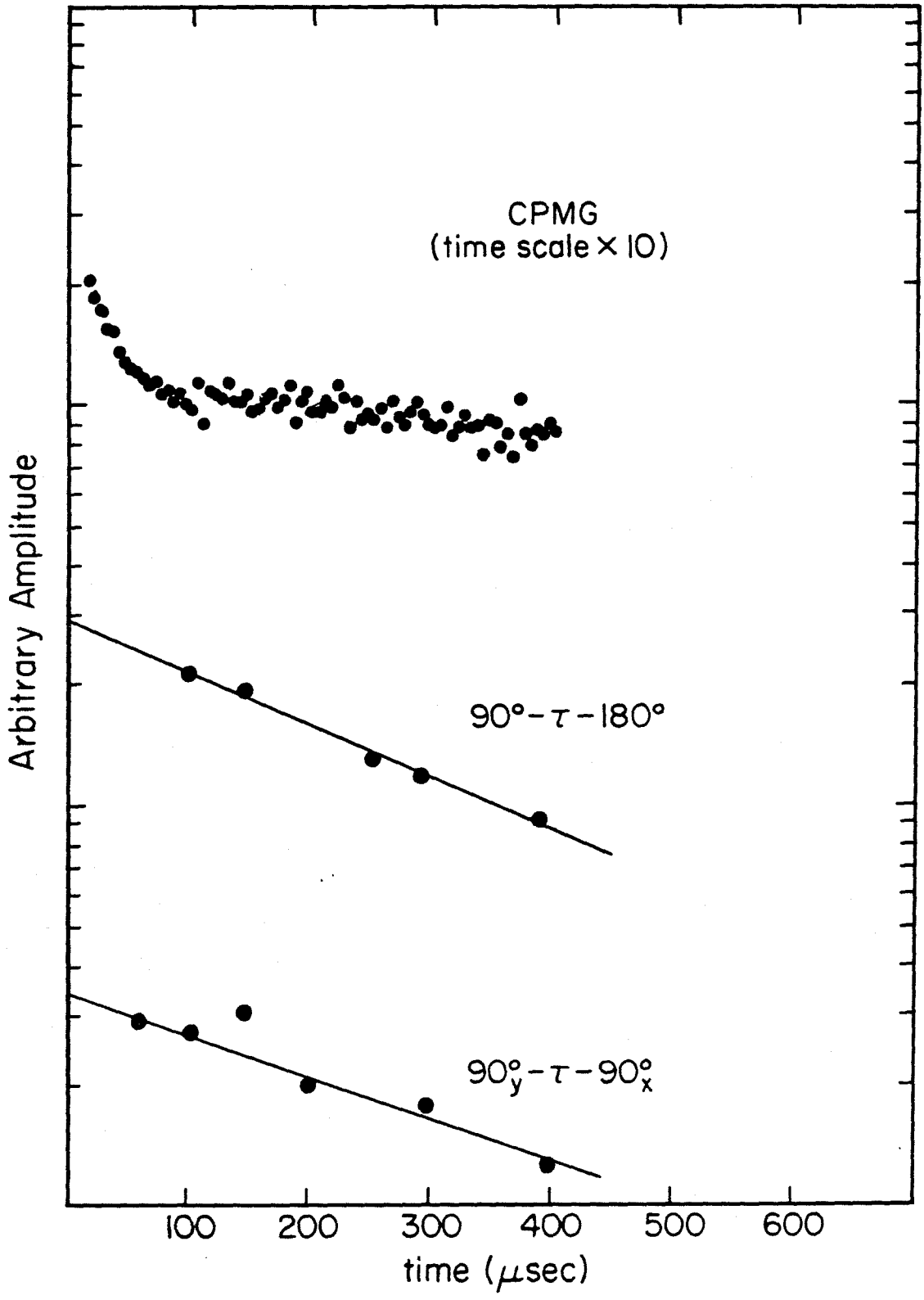
CPMG
(time scale × 10)
90°-τ-180°
90°y-τ-90°x
Arbitrary Amplitude
100
200
300
400
500
600
time (μsec)

Figure 6

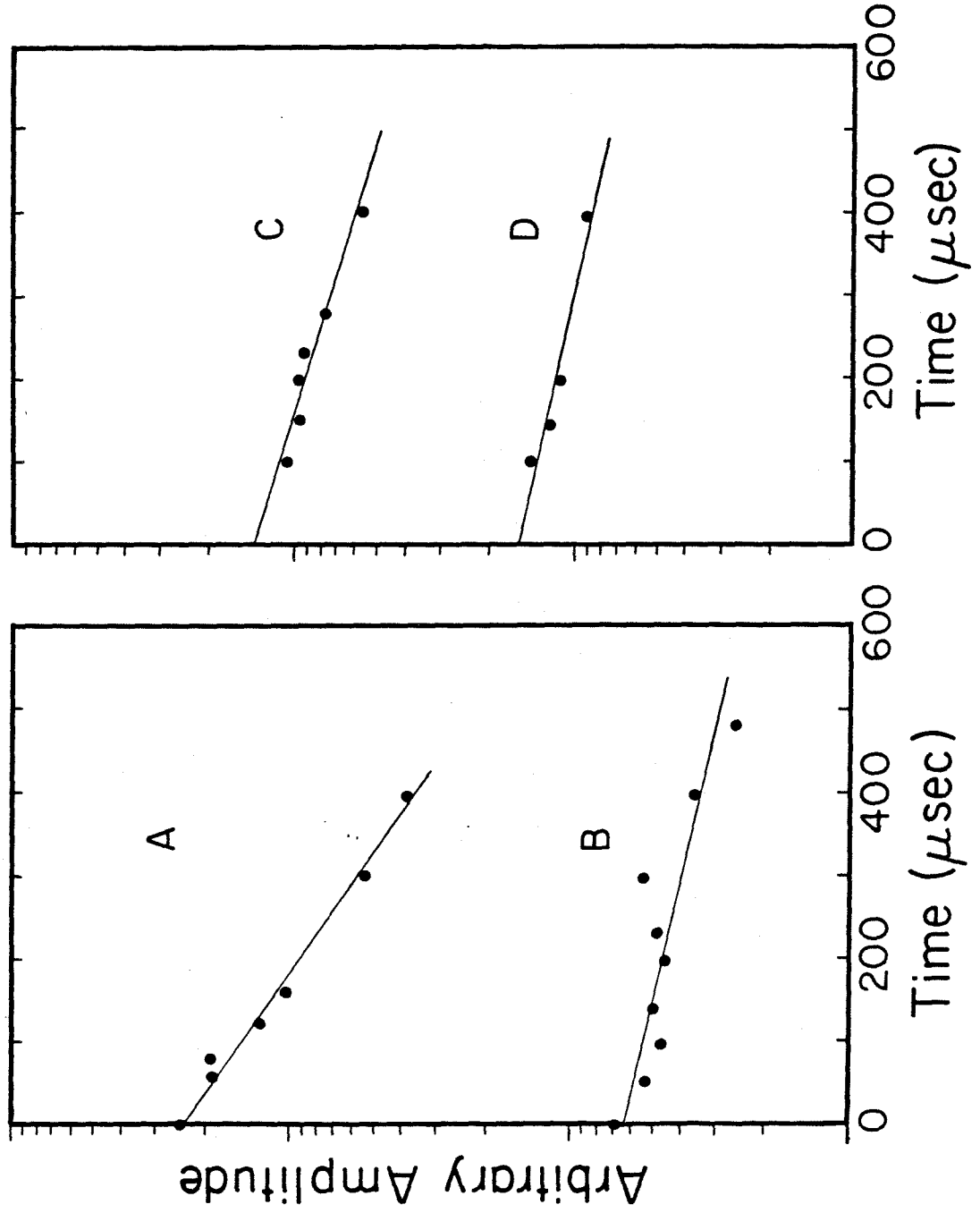
Arbitrary Amplitude
A
B
C
D
0
200
400
600
Time (μsec)
0
200
400
600
Time (μsec)

Figure 7

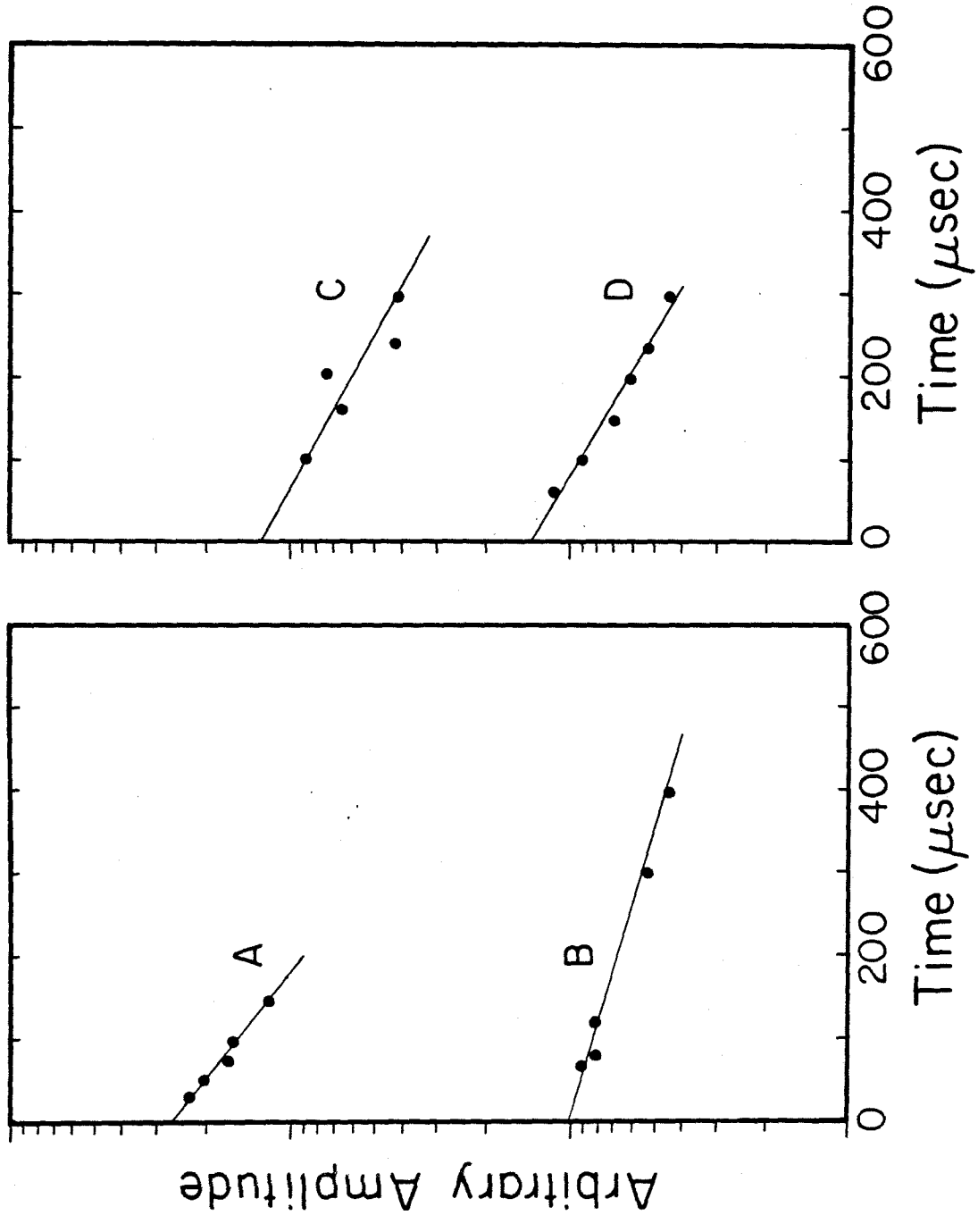
Arbitrary Amplitude
A
B
C
D
0
200
400
600
Time (μsec)
0
200
400
600
Time (μsec)

Figure 8

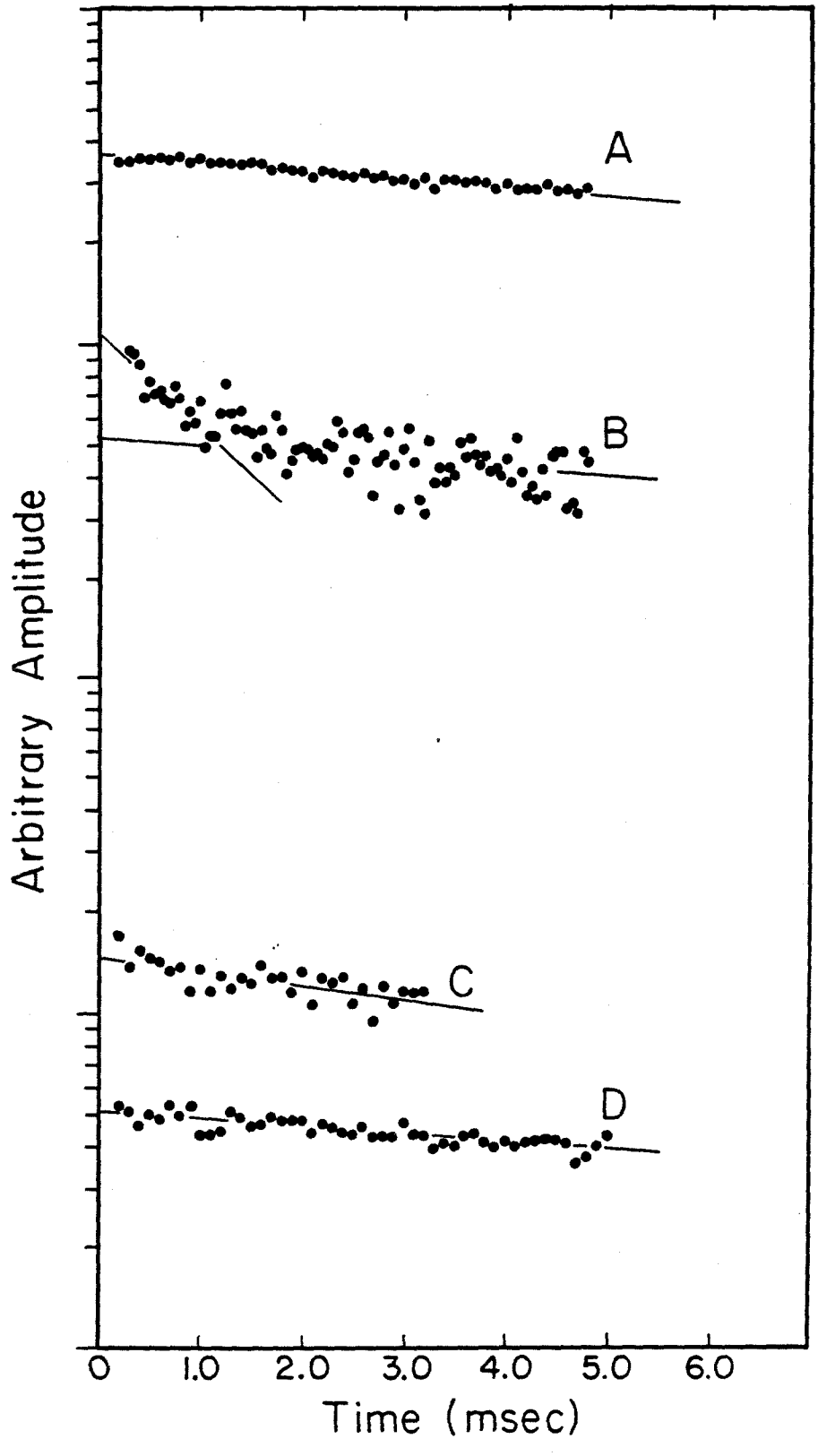

Figure 9

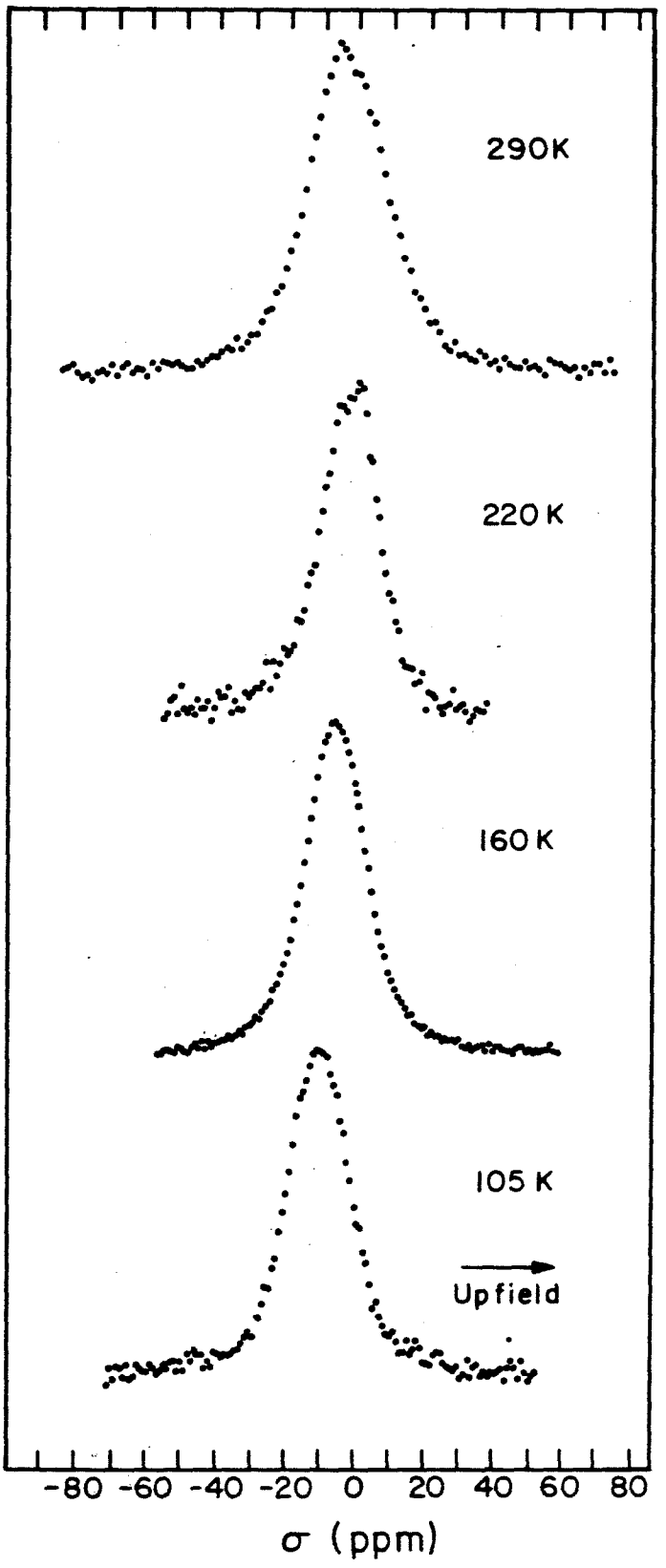

Figure 10

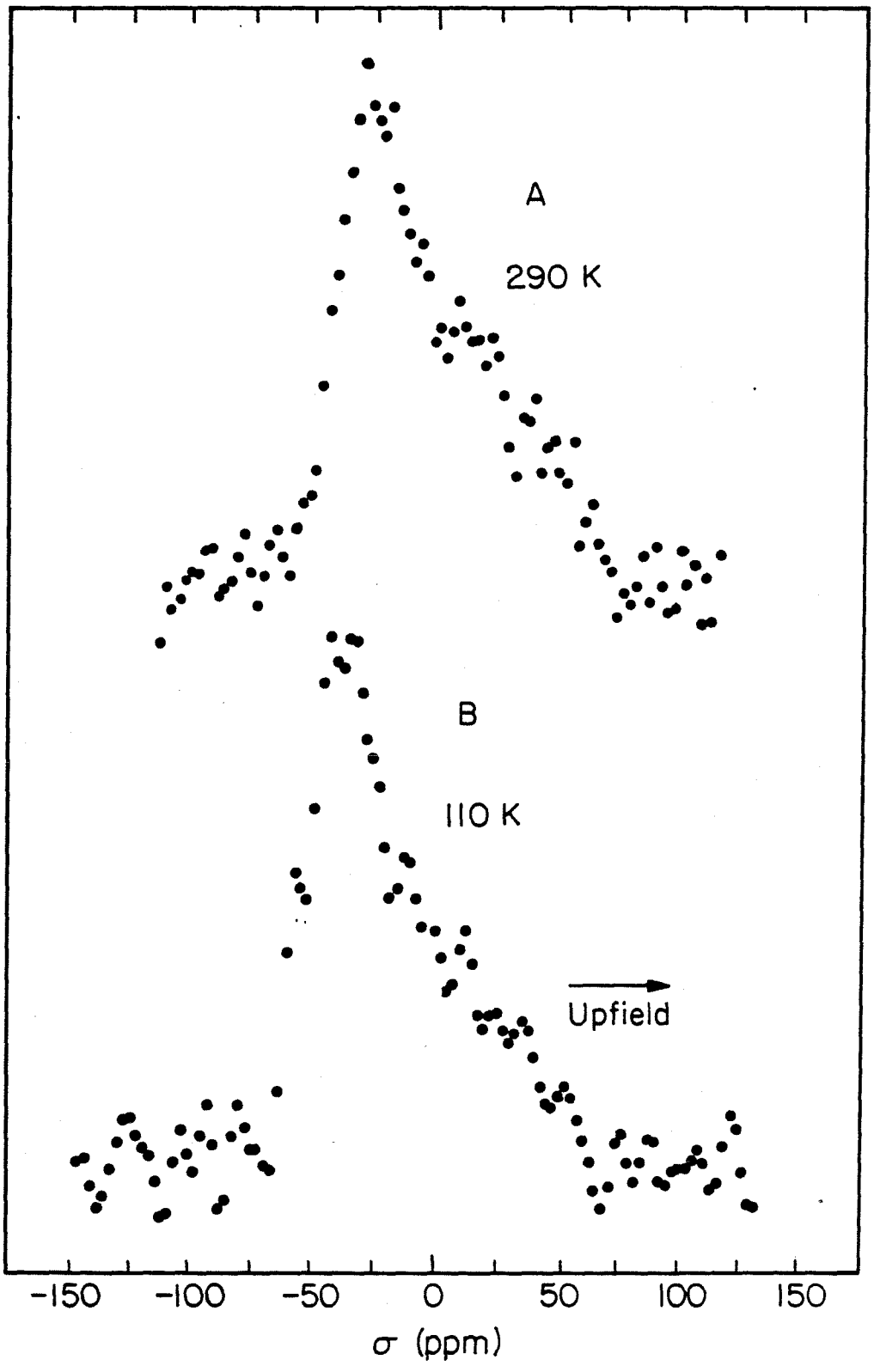

Figure 11

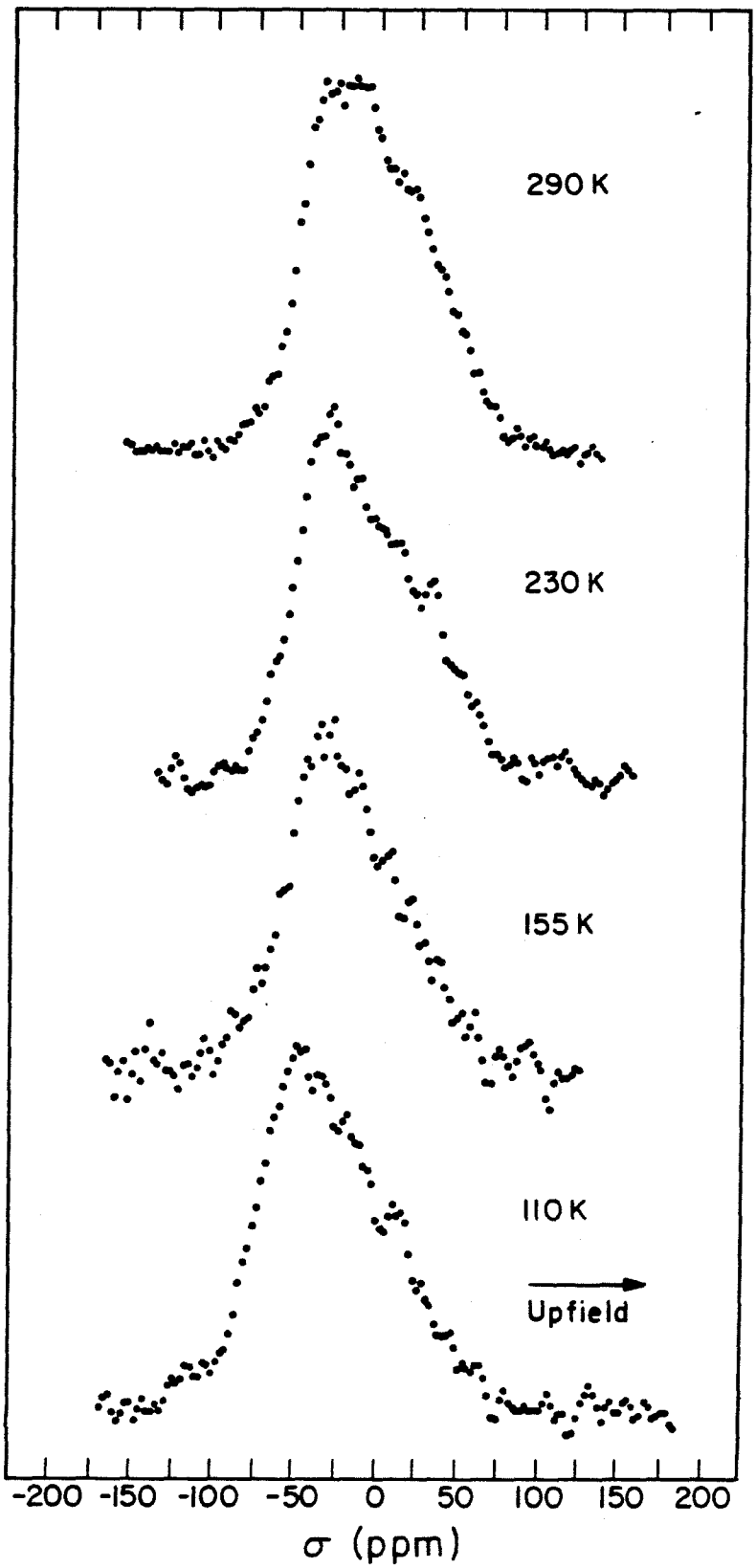
290 K
230 K
155 K
110 K
Upfield
-200 -150 -100 -50 0 50 100 150 200
σ (ppm)

Figure 12

CHAPTER IV

A NUCLEAR MAGNETIC RESONANCE INVESTIGATION OF FLUORINATED OXIDE CATALYSTS

Part 2: Fluorinated Alumina and Aluminosilicates

(Chapter IV is essentially an article by J. R. Schlup and R. W. Vaughan, entitled "A Nuclear Magnetic Resonance Investigation of Fluorinated Oxide Catalysts. Part 2: Fluorinated Alumina and Aluminosilicates." This article has been submitted to The Journal of Catalysis.)

INTRODUCTION

In an earlier paper (1), fluorinated silicas were investigated using hydrogen and fluorine nuclear magnetic resonance (NMR) sepctroscopy. Although silica is a useful model for an initial study of fluorinated catalytic oxides. The purpose of this investigation is to use Fourier transform NMR spectroscopy as a direct spectroscopic probe of fluorinated aluminas and aluminosilicates.

Fluorinated aluminas and aluminosilicates are important industrial catalysts, and their catalytic activity has been investigated extensively (2,3). The catalytic activity of these materials has been sutdied using a variety of reactions. Fluorination of alumina and alumino-silicates influences the activity of these oxide catalysts for polymerization (4, 7, 8), isomerization (4, 9, 10, 11, 12), and cracking (5, 6, 9, 13, 14, 15, 16) reactions. A maximum in catalytic activity is usually observed for catalysts with fluorine concentrations between 1 and 10 weight percent fluorine. Fluorination can cause changes in the selectivity of the catalysts for a given product (4, 10, 13, 16). A significant reduction in coke formation during cracking reactions has been reported also (13, 16).

Studying the reaction kinetics of these catalysts provides a useful description of the macroscopic behavior of fluorinated oxide catalysts. However, information concerning the catalysts at the molecular level can be obtained only indirectly from these data. It would be desirable to observe directly the changes that occur in the catalysts following fluorination.

Several attempts have been made to study the acid sites on fluorinated oxide catalysts (4, 5, 6, 17, 18, 19, 20). The results from these investigations have been ambiguous. The existence of Brönsted acid sites has not been established clearly. The changes in the number and in the strength of the acid sites following fluorination are unclear also.

Spectroscopic techniques should provide direct information concerning the environments of the fluorine atoms and the surface hydroxyl groups . The most widely used spectroscopic technique has been infrared spectroscopy (3, 8, 19, 21, 22, 23). Changes in the hydroxyl stretching frequencies have been reported as a function of the fluorine content and of the sample preparation. The differences in the infrared spectra of simple molecules adsorbed onto unmodified and fluorinated oxides have been studied also. However, SiF, SiOF, AlF, and AlOF vibrations have not been identified in the infrared spectra which have been reported.

X-ray photoelectron spectroscopy (XPS) has been applied to fluorinated aluminas (21, 24, 25). XPS demonstrated the presence of fluorine on the surface. By combining these results with X-ray diffraction patterns, the presence of aluminum trifluoride, aluminum hydroxyfluorides, and isolated surface fluorine atoms have been reported, depending upon the particular sample preparation.

Magnetic resonance techniques have been used as spectroscopic probes of fluorinated oxides also. Although electron spin resonance (ESR) has been used to study the behavior of organic free radicals adsorbed onto fluorinated alumina (26, 27), it cannot be used to observe directly the hydroxyl groups or fluorine atoms on the oxide surface. Hydrogen and fluorine NMR spectroscopy probe specifically the environments of the

hydrogen and fluorine atoms on the oxide.

O'Reilly (28) used fluorine NMR to study fluorinated alumina with fluorine concentrations ranging from 0.3 to 12.5 weight percent. He concluded that a bulk aluminum fluoride phase forms at fluorine concentrations greater than five weight percent. Golovanova and co-workers (29) obtained hydrogen and fluorine wide line NMR spectra of fluorinated aluminas. Spectra obtained at 80 K and at 300 K showed that the fluorine atoms were not mobile. Hydrogen was present even on aluminas containing 11 weight percent fluorine.

In this investigation, hydrogen and fluorine NMR were utilized to investigate further the chemical environment of the hydroxyl groups and fluorine atoms on fluorinated alumina. In addition, hydrogen and fluorine NMR spectra were obtained for several fluorinated aluminosilicates. Fourier transform NMR spectroscopy was used and the absorption curves of the frequency spectrum were obtained rather than the first derivative of the spectrum. The application of NMR techniques can furnish information concerning the concentration of the atoms, the nature of the bonding of the atoms, the interactions between neighboring atoms, and the motion of the atoms. Quantitative analysis of hydrogen and fluorine in catalytic oxides usually requires temperatures higher than 1200 K and results in sample destruction. Quantitative NMR is a nondestructive technique, and the initial amplitudes of the free induction decays were used for the hydrogen and fluorine analyses in this investigation.

The nature of the chemical bonding of hydrogen and fluorine to

alumina and aluminosilicates was investigated using the center of mass or the isotropic chemical shift of the Fourier transform of the free induction decay and the fluorine chemical shift anisotropy. The magnetic field at a nuclear site can be distorted by the electron distribution about the nucleus. The electronic environment about a nucleus is normally not isotropic. Therefore, the field experienced by a nucleus in a solid will have an angular dependence described by the chemical shift tensor. The spectra of the unmodified and fluorinated aluminas were obtained at temperatures as low as 110 K to provide motional information concerning the hydroxyl groups and fluorine atoms.

The centers of mass and chemical shift parameters for the spectra reported here are not corrected for the effects of bulk magnetic susceptibility. The volume susceptibility of these oxides has not been measured. An estimate of the necessary susceptibility correction can be made using an estimated volume susceptibility of -0.34×10^{-6} for alumina and -1.13×10^{-6} for silica. The sample can be approximated as an ellipsoid with b=c=0.5a, where a, b, and c are the semiaxes with the magnetic field along axis b. A bulk susceptibility correction of 0.34 ppm to higher field is estimated using the values tabulated by Osborn (30) for the demagnetizing factors and the volumetric susceptibility of alumina. Similarly, a correction factor of 1.1 ppm to higher field was estimated for silica samples (1). Both of these correction factors are less than or equal to the experimental error in the chemical shift data reported for fluorinated aluminas and aluminosilicates. Therefore, corrections for differences in the bulk magnetic susceptibility between the samples were negligible.

Only room temperature NMR relaxation data were obtained. A complete understanding of the NMR relaxation behavior of these materials was not the object of this investigation. However, the spin-lattice relaxation times (T_1's) at 290 K were needed to optimize the conditions for signal averaging. Since the magnetization observed during these NMR experiments depends upon the T_1 for the sample, the T_1 of the sample must be known if accurate an quantitative analysis using NMR is to be obtained. The relaxation times obtained from 90^{o}-τ-180^{o} and Carr-Purcell-Meiboom-Gill experiments provide information about the distances between hydroxyl groups and between fluorine atoms. The presence of fluctuations in the local magnetic field about a nucleus, such as those caused by diffusion, can be detected by comparing these two relaxation times.

EXPERIMENTAL DETAILS

Sample Preparation

The alumina samples were prepared from a commercial alumina catalyst, Alcoa F-20. The particle size specification was 80 to 270 mesh and the reported surface area was 210 m^2/g. The silica content was 0.09 wt% and the Na_2O content was 0.9 wt%. The alumina was initially calcined at 773 K under flowing oxygen for three hours.

Two fluorinated aluminas were prepared by impregation with NH_4F using an aqueous solution of ammonium fluoride with a fluoride concentration of 5.4 mM. After soaking the catalyst in this solution for three hours the excess solution was gently evaporated. Two samples were prepared from this material, one calcined at 573 K and one calcined at 873 K. All other aspects of their sample preparation were identical.

An unmodified alumina was prepared by treating the previously calcined alumina exactly as the fluorinated aluminas except that it was calcined at 773 K and was not treated with the fluoride solution.

The fluorinated aluminosilicates were prepared in an analogous fashion to the fluorinated aluminas. The unmodified aluminosilicates were prepared by Chevron Research Company. They were xerogel aluminosilicate catalysts coprecipitated with ammonia from sodium silicate and hydroxy aluminum chloride-acetic acid solutions. One aluminosilicate contained 48 weight percent alumina, and the other contained 11 weight percent alumina. Two fluorinated oxides were prepared from each aluminosilicate. The more heavily fluorinated samples were exposed for 70 hours to an aqueous ammonium fluoride solution that was 5.5 weight percent fluoride and were calcined at 773 K. The lightly fluorinated samples were prepared using a 5.4 mM F^- aqueous solution and were calcined at 873 K.

All of the unmodified and fluorinated samples were calcined in flowing oxygen for the three hours at the desired calcining temperature following the sample preparation discussed above. The samples were placed in quartz sample tubes and the tubes were plugged with quartz wool. The samples were evacuated on the BET apparatus, and the sample volumes were flushed with oxygen. The samples were calcined at the desired temperature for two hours under three psig of oxygen and then calcined under vacuum (10^{-2} torr) for one-half hour. Then the nitrogen BET surface areas were measured. After measuring the surface areas, the samples were calcined for another one and one-half hours under three psig of oxygen.

The samples were evacuated at their calcining temperatures to a pressure of 10^{-2} torr and the quartz sample tubes were sealed.

NMR Apparatus

The Fourier transform NMR spectrometers used in this investigation were the same as those used in the previous study of fluorinated silica (1). The spectrometers had field strengths of 13 kG and 24 kG. The sample probe and the low temperature equipment were the same as described in the study of fluorinated silica (1). The low signal-to-noise ratio of these samples required accumulating the signal from as few as 256 to as many as 4096 experiments in order to obtain the data reported.

RESULTS AND DISCUSSION

1. Fluorinated Aluminas

Spin-Lattice Relaxation Time (T_1) Measurements

The spin-lattice relaxation times obtained at 290 K are given in Table 1. The external field strengths were 21.2 kG for the hydrogen data and 22.5 kG for the fluorine data. The fluorine T_1 decreases as the calcining temperature increases. The hydrogen T_1's of the fluorinated aluminas double as the calcining temperature increases from 573 K to 873 K. The hydrogen T_1 decreases by at least a factor of three when the alumina is fluorinated.

Quantitative Analysis

The hydrogen and fluorine atom concentrations of the unmodified and

fluorinated aluminas are given in Table 2. The unmodified alumina has a surface hydrogen concentration of 13.6 hydrogen atoms per 100 $\AA^2$. Even at calcining temperatures as low as 573 K, the addition of fluorine caused a decrease in the hydrogen concentration by a factor of two. The hydrogen concentration of fluorinated alumina decreases as the calcining temperature increases. Hydrogen was present even after calcining at 873 K.

The fluorinated aluminas in this investigation were prepared using only a single type of fluoride treatment, an aqueous 5.4 mM F^- solution. The sum of the hydrogen and fluorine concentrations for the sample calcined at 573 K is equal to the hydrogen concentration of the unmodified alumina. The hydrogen and fluorine concentrations of the fluorinated aluminas are equal at both calcining temperatures.

The fluorinated alumina calcined at 573 K is 4.5 weight percent fluorine. Significant changes in the catalytic behavior of alumina have been observed with fluorination at this concentration. Calcining the sample at 873 K reduced the fluorine content to 2.4 weight percent. Materials having this fluorine concentration typically have catalytic activity similar to unmodified alumina. The changes in fluorine concentration of the fluorinated aluminas studied here are due to the calcining temperature and not to the fluorine treatment.

No volatile products formed during calcination. The disappearance of fluorine and hydrogen appears to result from the formation of hydrogen fluoride by the condensation of neighboring surface groups or by reaction to form *HF* and H_2O as the atoms diffuse on the surface at elevated calcining temperatures.

Gerberich, Lutinski, and Hall (9) studied the effects of fluoride

modification on alumina catalysts. Their catalysts were prepared using aqueous solutions of H_2F_2 and they were calcined at 873 K under dry nitrogen gas for 10-12 hours. In general, the samples investigated here contained higher hydrogen concentrations. In their calculation Gerberich and co-workers assumed 12.5 X 10^{18} sites per square meter, based on Peri's model (31) of an alumina surface. The surface fluorine atom concentration reaches a constant value of 12.5 X 10^{18} F^-/m^2 at 5 wt% fluorine. This agrees well with the initial number of hydroxyl groups observed on the unmodified alumina in this investigation and with the sum of the hydrogen and fluorine atom concentrations observed at 573 K for fluorinated alumina. The evolution of HF at elevated temperatures would form an oxygen bridge between neighboring aluminum atoms which would not be observed using hydrogen and fluorine NMR. Also, evolution of HF would result in equal surface concentrations of hydrogen and fluorine which were observed. The ratio of the surface concentration of fluorine to the weight percent fluorine observed in this investigation is consistent with that observed by Gerberich and co-workers. Their mechanism for the addition of fluorine to alumina using an aqueous solution is consistent with the data observed here. Differences in the data can be explained by the greater hydrogen content of the unmodified alumina used in this investigation.

Room Temperature Free Induction Decay (FID) Data

The hydrogen spectra of alumina and fluorinated alumina are broad with second moments ranging from 0.8 G^2 to 2.5 G^2 (see Table 3). The hydrogen spectra of these materials are shown in Figure 1. When the field strength is increased from 13.1 kG to 23.4 kG, the line widths remain constant which means that the line widths are dominated by dipolar

interactions. The calcining temperature has a marked effect on the second moment of the hydrogen spectra of fluorinated aluminas. The second moment of fluorinated alumina calcined at 573 K is reduced by a factor of two when the sample is calcined at 873 K. The center of mass and the line shape of the spectra are the same regardless of the calcining temperature.

Since the line widths are broad, the uncertainty of the center of mass is determined by the large frequency range represented by each point in the frequency spectrum (244.1 to 488.3 Hz per point). At external field strengths of 13.1 kG and 23.4 kG, an error of one point (488 Hz for this example) in the frequency spectrum corresponds to an error of 8.5 and 5.5 ppm, respectively. The centers of mass of the hydrogen spectra are consistent with the reported chemical shifts for alcoholic hydrogen within experimental error.

The centers of mass and second moments for the fluorine spectra are given in Table 4. The fluorine spectra are shown in Figure 2. The line shapes are neither Lorentzian nor Gaussian. It is symmetric at these field strengths. The fluorine spectra are much broader than the hydroxyl group spectra. However, the second moments of the fluorine spectra for these two fluorinated aluminas are the same regardless of the calcining temperature. Since the proton and fluorine concentration decrease as the calcining temperature increases, the observed second moments must be dominated by the chemical shift anisotropy and by the aluminum-fluorine dipolar interaction.

The center of mass for the room temperature fluorine spectrum appears to shift 10 ppm to higher field when the modified alumina is calcined at

873 K. However, each point in the frequency spectrum represents approximately 5 ppm, and the experimental error is sufficient to account for the observed shift. The observed centers of mass are too far upfield to be explained by an oxyfluoride species (-OF) or by a fluoride ion since -454 ppm $<\sigma_{OF}<$-210 ppm and -154 ppm $<\sigma_{F^-}<$-35 ppm. The fluorine isotropic chemical shift observed for fluorinated alumina is typical of covalent aluminum-fluorine bonds.

Relaxation Data

The decay constants obtained during hydrogen 90^{o}-τ-180^{o} (spin echo) and Carr-Purcell-Meiboom-Gill (32) experiments are given in Table 5 for unmodified and fluorinated aluminas. The hydrogen CPMG relaxation time, T_2^+, is 20 times longer than the spin echo relaxation time, T_2. The large value of T_2^+ means that the hydrogen-hydrogen homonuclear dipolar interactions are negligible. The discrepancy between T_2 and T_2^+ means that the hydroxyl groups are mobile on the surface or that the interactions between neighboring hydroxyl groups and fluorine atoms are time dependent. The relaxation time for the CPMG experiment was independent of the pulse specing for $2\tau \leq 100$ μsec.

The modified alumina calcined at 573 K has a hydrogen T_2 of 76 μsec. The envelope of the echo maxima for the hydrogen CPMG experiment can be described by two Lorentzian line shapes. Their relaxation times are 0.57 msec and 3.26 msec. The decay from the fluorine spin echo experiment cannot be described by either a Lorentzian or Gaussian line shape. The fluorine CPMG data can be described by two Lorentzian line shapes with decay constants of 1.1 and 4.5 msec.

The results of the spin echo and CPMG experiments for the fluorinated

alumina calcined at 873 K are similar to those for the sample calcined at 573 K. The hydrogen decay of the spin echo experiment is characteristic of a Lorentzian line shape with a decay constant of 0.20 msec. The hydrogen CPMG data are characteristic of a Lorentzian line shape with a decay constant of 1.7 msec. The decay of the fluorine CPMG experiment is described by assuming two Lorentzian line shapes having decay constants of 0.4 and 5.3 msec.

The spin echo and CPMG experiments show that the hydroxyl groups experience fluctuations in their local magnetic fields. The hydrogen T_2 after calcining at 873 K is over twice as large as that for a sample calcined at 573 K. Two dipolar environments exist for hydrogen on fluorinated alumina calcined at 573 K. The statistical theory developed by Anderson (33) to describe the absorption curve for a magnetically dilute material broadened by dipolar effects has been used to compare the average internuclear distances of two homonuclear dipolar environments observed in CPMG data (1). For fluorinated alumina calcined at 573 K, the initial slope represents hydroxyl groups which are 1.8 times closer to one another than those contributing to the latter part of the CPMG decay. The second component of the decay has the same relaxation time as the hydroxyl groups of the unmodified alumina. If the lattice structure of the unmodified and fluorinated aluminas are assumed to be the same, then the initial part of the CPMG decay of the fluorinated alumina calcined at 573 K represents hydroxyl groups which are 1.9 times closer to other hydroxyl groups than the hydroxyl groups of an unmodified alumina calcined at 773 K. Calcining the fluorinated alumina at 873 K removes the hydroxyl groups that have closer neighboring hydroxyl groups. Although the hydroxyl group concentration of the fluorinated alumina

calcined at 873 K is less than that of either the unmodified alumina or the fluorinated alumina calcined at 573 K, the hydrogen T_2^+ of this sample is one-half the value of the other alumina samples. Similarly, the unmodified alumina and the fluorinated alumina calcined at 573 K have the same hydrogen T_2^+, but their hydroxyl group concentrations differ by a factor of three. Therefore, fluorination and the calcining process cause rearrangement of the hydroxyl groups.

The fluorine CPMG data show that fluorine exists with two average fluorine internuclear distances with one being 1.6 times greater than the other when the sample is calcined at 573 K and 2.3 times greater than the other when calcined at 873 K. While calcining at 873 K seems to remove hydroxyl groups selectively from one homonuclear dipolar environment, both fluorine homonuclear dipolar environments are present after calcining at 873 K. Increasing the calcining temperature from 573 K to 873 K decreases the fluorine relaxation time for the initial part of the CPMG decay by a factor of two.

Low Temperature Spectra

The centers of mass, line widths, and second moments of the hydrogen spectra for the unmodified and fluorinated aluminas are given in Table 6. The errors in the center of mass correspond to one point in the frequency spectrum. The center of mass for each oxide is independent of the observation temperature within experimental error. The line shape broadens as the sample is cooled for the modified alumina calcined at 573 K. The spectrum of the unmodified alumina and the fluorinated alumina calcined at 873 K do not change as the sample temperature is

lowered.

The parameters of the low temperature fluorine spectra are given in Table 7. The low temperature fluorine spectra of fluorinated aluminas are shown in Figure 2. The fluorine spectrum of the fluorinated alumina calcined at 573 K shows a change in its center of mass of 7 ppm to higher field at 110 K. Although the room temperature spectrum is symmetric, an asymmetry appears downfield from the center of mass at 110 K. The center of mass of the fluorine spectra of the fluorinated alumina calcined at 873 K does not change as the observation temperature is lowered. For spectra obtained at temperatures below 200 K, the line width increases from 8.8 kHz to 10 kHz. The same asymmetry observed for the fluorinated alumina calcined at 573 K is observed in the spectrum of the fluorinated alumina calcined at 873 K for observation temperatures below 200 K.

The low temperature hydrogen spectra of these aluminas show that the hydroxyl groups are still mobile at 110 K. The changes in the fluorine spectra may be caused by several factors. The asymmetry of the low temperature fluorine spectra could be due to the fluorine chemical shift anisotropy. Anisotropic motion would cause motional averaging of the fluorine chemical shift tensor at room temperature. The second possibility is that the quadrupolar interaction at the aluminum nucleus is sufficiently large that the aluminum nucleus is not in a pure Zeeman state. Then heteronuclear dipolar interactions cannot be classified as being either secular or nonsecular. VanderHart (34) has calculated line shapes for the spectrum of a spin-½ nucleus which is coupled to a spin-5/2 nucleus. This phenomenom and the large chemical shift anisotropy of the fluorine nucleus could account for the observed asymmetry.

The last alternative considers the fluorine resonance to be the spectrum of an isolated aluminum-fluorine dipole pair. VanderHart and Gutowsky (35) have calculated possible powder pattern spectra for isolated dipole pairs where the chemical shift anisotropy of the resonant spin approaches the magnitude of the separation of the divergences of the powder pattern of the dipolar spectrum of the isolated dipole pair. Fluorine atoms bonded to surface aluminum atoms at low coverages would exhibit this behavior. VanderHart and Gutowsky define a parameter, P_1, which describes the relative magnitudes of the chemical shift and dipolar effects. A chemical shift tensor with axial symmetry along the internuclear vector between the aluminum and fluorine atoms will be assumed. In this situation P_1 would be defined as

$$P_1 = \frac{-(1/3)\gamma_F B_0(\sigma_{||} - \sigma_{\perp})}{(\frac{1}{2}\gamma_F \gamma_{Al} \hbar / r^3_{AlF})}$$

where γ_F and γ_{Al} are the gyromagnetic ratios of fluorine and aluminum, respectively; B_0 is the strength of the external magnetic field; $\sigma_{||}$ and $\sigma_{\perp}$ are the components of the axially symmetric chemical shift tensor; and, r_{AlF} is the length of the internuclear vector between the aluminum and the fluorine atoms.

Using the fluorine chemical shift anisotropy measured for fluorinated silica (1), P_1 for the aluminum fluorine dipolar pair is estimated to be

$$P_1 = \frac{-17966 \text{ rad/sec}}{20600 \text{ rad/sec}} = -0.87 \quad .$$

An internuclear distance of 1.65 Å was used in the calculation above. This shows that the spectrum of fluorine on fluorinated alumina must be

described as discussed by VanderHart and Gutowsky if there is no diffusion of the fluorine.

If it is assumed that the interpretation of the spectrum as an isolated dipole pair is applicable to this situation and that the spectrum is not complicated by contributions from the aluminum where the spin quantum number, m, has a value other than $\pm\frac{1}{2}$, an estimate of the fluorine chemical shift anisotropy can be obtained. The fluorine spectrum obtained at 110 K of the fluorinated alumina calcined at 873 K will be used for the calculation. The peak closest to the center of mass is upfield from the center of mass. Therefore, the chemical shift parameter, $\beta = -(1/3)\gamma_F B_o(\sigma_{\parallel} - \sigma_{\perp})$, is negative (35). The value of β is estimated to be -1500 rad/sec from the asymmetry of the line shape. Therefore, the fluorine chemical shift anisotropy, $\sigma_{\parallel} - \sigma_{\perp}$, is estimated to be 76 ppm. This estimate of the fluorine chemical shift anisotropy is 20% less than the 96 ppm anisotropy measured for fluorinated silica (1). This means there would be a more uniform electron distribution about the fluorine nuclei on alumina than on silica.

2. 11 weight percent alumina aluminosilicate

The spin-lattice relaxation times for these aluminosilicates are given in Table 1. The sample prepared using a 5.4 mM F^- solution has hydrogen and fluorine T_1's that are approximately the same as those observed for a similarly prepared modified silica (1). Further addition of fluoride decreases that T_1 measured for hydrogen by 50% and that measured for fluorine by more than a factor of seven.

The hydrogen and fluorine concentrations of these samples are given in Table 2. The hydrogen and fluorine atom concentrations of these

samples agree closely with the values obtained for fluorinated silica prepared in a similar manner. Hydrogen is still present after fluoride treatment using a 5.5 wt% F^- solution. The resulting fluorine atom concentration is 7.9 weight percent fluorine.

The hydrogen atom content of the fluorinated aluminosilicate calcined at 873 K was 4.5 X 10^{20} per gram. The relationship of the hydrogen atom concentration to the specific surface area is in excellent agreement with that reported by O'Reilly (28) for an unmodified aluminosilicate that was 12.5% alumina. This suggests that the hydrogen environment has not been disturbed by fluorination using an aqueous 5.4 mM fluoride solution.

The ratios of fluorine atoms to silicon atoms and hydrogen atoms to silicon atoms for an aluminosilicate treated with a 5.4 mM F^- solution are 0.038 and 0.05 , respectively. When a 5.5 wt% F^- solution is used for sample preparation, the fluorine atom to silicon atom ratio becomes 0.28 and the hydrogen atom to silicon atom ratio becomes 0.15 .

Quantitative analysis of the aluminosilicate fluorinated with the 5.5 wt% F^- solution must be interpreted carefully. A substantial reduction in the specific surface area occurs when the aluminosilicate is treated with an aqueous ammonium fluoride solution that is 5.5 wt% fluoride. The unmodified oxide had a surface area of 484 m^2/gm. An aqueous fluoride treatment using a 5.4 mM F^- solution caused a 22% reduction in specific surface area. Use of the higher ammonium fluoride concentration caused a surface area reduction of 68%. A volatile material was produced when the fluorinated aluminosilicate prepared using a 5.5 wt% F^- solution was calcined. Neutron activation analysis of the volatile

product showed that it is 52 wt% fluorine, 19 wt% silicon, and 290 ppm aluminum. If the remaining 29 wt% is assumed to be oxygen, the following molar ratios are obtained.

$$\frac{\text{moles Fluorine}}{\text{moles Silicon}} = 4.0 \qquad \frac{\text{Moles fluorine}}{\text{moles oxygen}} = 1.5$$

$$\frac{\text{moles oxygen}}{\text{moles silicon}} = 2.6$$

These ratios suggest the existence of a mixture of fluorinated silanes, siloxanes, and silicic acids. These species were observed in the mass spectrum of a similarly prepared fluorinated silica (1). These results demonstrate that fluorination of aluminosilicates using concentrated aqueous fluoride solutions results in selective removal of silica from the aluminosilicate lattice.

The spectral parameters for the room temperature hydrogen spectrum of the lightly modified sample are given in Table 3. The hydrogen spectrum is shown in Figure 3. The line shape is very symmetric and has a second moment of 0.044 G^2. The center of mass and second moment agree well with those measured for a fluorinated silica prepared in a similar manner (1). Similar line widths have been reported for an unmodified aluminosilicate 12.5 wt% alumina (28, 33).

The fluorine spectrum is shown in Figure 4. The center of mass and second moment are given in Table 4. The line shape can be described by an axially symmetric chemical shift tensor. The parameters describing the fluorine chemical shift tensor are

$\sigma_{\parallel}$ = 48 ppm

$\sigma_{\perp}$ = -39 ppm

$\bar{\sigma} = 1/3 \text{ tr } \underset{\approx}{\sigma} = -10$ ppm

$\Delta\sigma = \sigma_{\parallel} - \sigma_{\perp} = 87$ ppm

$\delta = \sigma_{zz} - \bar{\sigma} = 58$ ppm

All values are in parts per million relative to hexafluorobenzene. The chemical shift observed is the same as that for similarly prepared fluorinated silicas (1). Therefore, the chemical bonding of the fluorine on a fluorinated aluminosilicate that is 11 wt% alumina is the same as that for fluorinated silica.

The aluminosilicate fluorinated using a 5.5 wt% F^- solution has a line shape that can be described by an axially symmetric chemical shift tensor also. The observed chemical shift parameters relative to hexafluorobenzene are given below.

$\sigma_{\parallel}$ = 49 ppm

$\sigma_{\perp}$ = -46 ppm

$\bar{\sigma}$ = -14 ppm

$\Delta\sigma$ = 95 ppm

δ = 63 ppm

Therefore, the chemical bonding of the fluorine atoms to the aluminosilicate does not change with more severe fluorine treatment.

The total second moment of the fluorine spectrum will be defined as

$$\langle\Delta\omega^2\rangle_T = \langle\Delta\omega^2\rangle^{cs} + \langle\Delta\omega^2\rangle^{dip}$$

where $\langle\Delta\omega^2\rangle^{cs}$ and $\langle\Delta\omega^2\rangle^{dip}$ are the contributions to the total second moment ($\langle\Delta\omega^2\rangle_T$) due to the chemical shift and dipolar interactions, respectively. It has been shown (36) that

$$\langle\Delta\omega^2\rangle^{cs} = (1/15)(\omega_0\delta)^2(3+\eta^2)$$

The contribution from the chemical shift interaction to the second moment is then 0.34 G^2 (using the parameters for the axially symmetric tensor measured for the aluminosilicate treated with a 5.4 mM F^- solution). The contributions to the second moment due to dipolar interactions are then 0.20 G^2 for the sample treated with a 5.4 mM F^- solution and 0.70 G^2 for

the sample treated with a 5.5 wt% F^- solution.

The dipolar effects could result from either hydrogen-fluorine, fluorine-fluorine, or aluminum-fluorine dipolar interactions. The relaxation time for the fluorine Carr-Purcell-Meiboom-Gill experiment (T_2^+) of the aluminosilicate treated with the 5.4 wt% F^- solution is 10. msec. The fluorine homonuclear dipolar interaction would have a full width at half height of 32 Hz and makes a negligible contribution to the total line width. Therefore, $\langle \Delta\omega^2 \rangle^{dip}$ results from the hydrogen-fluorine and aluminum-fluorine dipolar interactions. The fluorine T_2^+ is at least an order of magnitude longer than the fluorine T_2 measured for this sample. Therefore, fluctuations are occurring in the local fields of the fluorine nuclei. This behavior was reported for fluorinated silica prepared in a similar manner (1).

3. 48 Weight Percent Alumina Aluminosilicates

The room temperature hydrogen and fluorine spin-lattice relaxation times are given in Table 1. The hydrogen T_1 measured for these fluorinated aluminosilicates increases by fifty percent when the oxide is fluorinated using a 5.5 wt% F^- solution rather than the 5.4 mM F^- solution. The fluorine T_1 value decreases by a factor of three for the sample treated with a 5.5 wt% F^- solution.

The Fourier transform of the spin echo envelopes for hydrogen and fluorine give a two component line shape. Figure 4 shows the fluorine spectrum, and Figure 3 shows the hydrogen spectrum of the aluminosilicate treated with the 5.4 mM F^- solution. From Figure 4, it is clear that the narrow component of the fluorine spectrum is identical to the

fluorine spectrum of fluorinated silica (1) and a fluorinated 11 wt% alumina aluminosilicate prepared in the same manner. The same is true for the hydrogen spectrum. Therefore, the narrow component is the contribution from isolated fluorine atoms and hydroxyl groups bonded to silicon atoms, i.e., SiF and SiOH. Figure 5 compares the fluorine spectra of this fluorinated aluminosilicate with those of fluorinated alumina and with aluminum trifluoride ($AlF_3 \cdot xH_2O$). The broad component of the fluorine spectrum can be associated with fluorine bonded to aluminum atoms (AlF groups). The broad component of the hydrogen spectrum is explained by hydroxyl groups bonded to the aluminum atoms (see Figures 1 and 3).

The SiF concentration can be obtained by extrapolating the behavior of the FID at long times to the origin as shown in Figure 6. The difference between this intercept and the total amplitude is a measure of the AlF concentration. The intercept for the total amplitude was obtained by subtracting the extrapolation of the long time behavior of the FID from the observed amplitudes in the short time region and extrapolating this difference to zero time. A similar procedure was followed to determine the hydroxyl group concentrations. The aluminosilicate treated with a 5.4 mM F^- solution has average surface concentrations of 2.5 F /100 $\AA^2$ and 1.6 OH/100 $\AA^2$. The ratio of SiF groups to silicon atoms is 0.045, and the ratio of SiOH groups to silicon atoms is 0.039. The ratios of AlF groups and AlOH groups to aluminum atoms are 0.015 and 0.021, respectively. X-ray photoelectron spectroscopy data obtained prior to fluorination showed that the ratio of silicon to

aluminum atoms on the surface is the same as that for the bulk aluminosilicate (37).

The fluorine spin echo behavior shows that the fluorine dipolar environments of fluorinated aluminosilicates prepared using aqueous solutions with fluoride concentrations of 5.4 mM and 5.5 wt% are significantly different. Figures 7 and 8 show the fluorine echo envelops at different pulse intervals for samples prepared using 5.4 mM F^- and 5.5 wt% F^- solutions, respectively. The fluorinated aluminosilicate prepared using a 5.5 wt% F^- solution clearly has two fluorine homonuclear dipolar environments. The Fourier transform of the FID (τ=0) has a two component spectrum. The Fourier transform of the data where τ=40 μsec beginning with $t = 2\tau$ has only the narrow component of the fluorine spectrum characteristic of SiF groups. The broad component represents the fluorine atoms bonded to aluminum. The homonuclear dipolar coupling between the fluorine atoms bonded to aluminum is much greater than that between the SiF groups since $T_2^{Al} < T_2^{SiF}$. The large difference in the amplitudes of the two decays at time zero demonstrates that the concentration of the AlF groups is much higher than the SiF group concentration.

All spin echo envelopes for the sample prepared using the 5.4 mM F^- solution can be described by a single Gaussian line shape. The decay of the echo amplitudes can be described by a single decay constant with $T_2 \sim 1.8$ msec. If the second moment is measured from the echo envelopes, no change is observed in the second moment for $2\tau \leq 100$ μsec. However, the second moment increases from 1.5 G^2 to 2.5 G^2 for $2\tau = 400$ μsec. The change in the second moment indicates that there are two or more

components in the fluorine spectrum. However, the various fluorine environments have similar contributions from the fluorine homonuclear dipolar interaction. The separation between neighboring fluorine atoms are the same regardless of the particular fluorine species. The results of the fluorine Carr-Purcell-Meiboom-Gill experiment can be described by two Lorentzian decays. The initial decay constant is the same as T_2^+ within experimental error. The second decay constant is 14 msec. The ratio between the observed values of T_2^+ shows that the average internuclear distance in the second dipolar environment is 2.4 times longer than in the dipolar environment responsible for the initial decay. The fact that T_2 is approximately equal to the initial T_2^+ indicates that the local fields experienced by the fluorine nuclei are constant. The spin echo data were not obtained at sufficiently large pulse separations to observe the long time behavior of the fluorine homonuclear dipolar interaction.

CONCLUSIONS

Fluorination using an aqueous solution of ammonium fluoride (5.4 mM F^-) resulted in fluorine atoms directly replacing hydroxyl groups

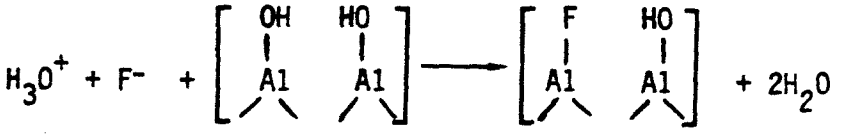

or in disruption of the oxide bridges of the surface by the ammonium fluoride solution

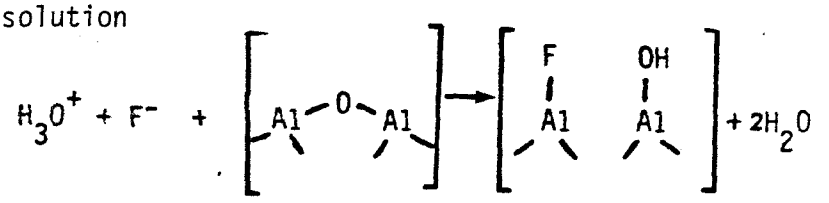

The unmodified alumina had all of its surface sites occupied by hydroxyl groups based upon the models of a alumina surface developed by Gerberich et al. (9) and Peri (31). All the surface sites of the fluorinated alumina calcined at 573 K were occupied by an hydroxyl group or a fluorine atom. The fluorine content of the catalyst was reduced when the catalyst was calcined at 873 K. This can be explained by condensation reactions between neighboring surface groups to form HF or H_2O or by reaction between fluorine atoms and hydroxyl groups during surface diffusion.

The fluorine concnetrations of the aluminas studied in this investigation lie in the range where changes in the catalytic activity are known to occur. Nuclear magnetic resonance T_1 data (28) and X-ray diffraction data (25, 38) have shown that an aluminum trifluoride (AlF_3) phase does not form at these fluorine concentrations. The fluorine spectra of fluorinated alumina at low fluorine concentrations is quite different from that of $AlF_3 \cdot xH_2O$. The second moments of the spectra of fluorinated alumina are a factor of five smaller than that of $AlF_3 \cdot xH_2O$. The line shape of the fluorine spectra of $AlF_3 \cdot xH_2O$ is a broad Gaussian while those of fluorinated alumina are asymmetric, especially when observed at 110 K (see Figures 2 and 5).

The CPMG data demonstrate that two fluorine homonuclear dipolar environments exist regardless of the calcining temperature. Calcining at 873 K causes a rearrangement of the fluorine atoms as evidenced by the reduction in T_2^+ for the initial part of the CPMG decay. The hydrogen CPMG data show that two hydrogen homonuclear dipolar environments exist when the sample is calcined at 573 K, but the hydroxyl groups which are closer to neighboring hydroxyl groups are removed upon calcining at 873 K.

The low temperature fluorine spectra show that either molecular motion or chemical exchange between two or more sites is occurring at room temperature. This motion would also account for the discrepancies between T_2 and T_2^+ for both the hydrogen and fluorine data. It is not possible to explain the temperature dependent phenomena on the basis of the data presented here. Use of magic angle sample spinning techniques and of temperature dependent relaxation time studies are needed to gain a better understanding of these phenomena.

The fluorine spectrum of the 11 wt% alumina aluminosilicate and the narrow component of the fluorine spectrum of the 48 wt% alumina aluminosilicate are identical to the fluorine spectrum of similarly prepared fluorinated silicas (1). Therefore, the chemical bonding of the fluorine atoms is the same in each case. The hydrogen spectra are similar for fluorinated silica (1), the fluorinated 11 wt% alumina aluminosilicate, and the narrow component of the fluorinated 48 wt% alumina aluminosilicate also.

The interpretation of the hydrogen and fluorine NMR data of fluorinated aluminosilicates requires an understanding of the atomic organization of the unmodified aluminosilicates. X-ray diffraction data (39, 40) has shown that aluminosilicates containing less than 30 percent alumina have a silica-like structure with isomorphic substitution of aluminum atoms. For alumina contents between 30% and 50%, an η-alumina phase begins to appear. As the alumina content increases from 50% to 80%, a structure similar to mullite appears. Similar results have been reported based upon X-ray photoemission data (41). Hall and co-workers have reported (42) that the results of differential hydrogen analysis of an aluminosilicate containing 12% alumina is unique compared with those of silica, alumina, or a mechanical mixture of silica and alumina.

Schreiber and Vaughan (43) reported that AlOH groups were not observed by NMR spectroscopy for aluminosilicates with less than 25%. The data reported here show that AlOH groups are not present in the spectrum of a fluorinated aluminosilicate containing 11 wt% alumina. AlF groups were not detected in the fluorine spectra of this aluminosilicate even with sample treatment using a 5.5 wt% F^- solution. However, SiOH, SiF, AlOH and AlF groups were present on aluminosilicates containing 48 weight percent alumina. Therefore, an alumina phase is required in the unmodified aluminosilicate if AlOH or AlF groups are to be present on the fluorinated catalyst.

The hydrogen and fluorine relaxation time data leave several questions unanswered. Nuclear magnetic resonance studies of the hydroxyl groups in decationated X and Y zeolites (44, 45) show that the line widths are constant at observation temperatures below 373 K. The hydrogen and fluorine atoms of the fluorinated alumina and the fluorinated aluminosilicates with 11 wt% alumina have fluctuations in their local magnetic fields as evidenced by the discrepancies between T_2 and T_2^+. Preliminary relaxation time data suggest that the fluctuations observed in these two fluorinated oxides are not present in the fluorinated aluminosilicate containing 48 wt% alumina.

No evidence was observed for the existence of hydrogen bonds between the hydroxyl groups and the fluorine atoms. The characteristic powder pattern for such an isolated dipole pair as described by VanderHart and Gutowsky (35) would differ little from that predicted for fluorinated silica (1). The most important change in the parameters describing such

a spectrum would be in the length of the internuclear vector between the hydrogen and fluorine atoms. Resolution of the features of this spectrum would be more difficult because of the heteronuclear dipolar broadening between the resonant spin and the neighboring aluminum atoms.

If the catalytic activity of fluorinated oxides is to be understood, the composition and the chemical nature of the oxides must be known. Pulsed Fourier transform NMR has been a useful probe of the hydroxyl group and fluorine atom environments of fluorinated alumina and aluminosilicates. Quantitative NMR has been used to study the composition of the fluorinate oxide catalysts as a function of sample preparation. NMR techniques have shown that the surface species undergo diffusion or anisotropic motion at 290 K. NMR has been used to determine whether the hydroxyl groups and fluorine atoms are chemically bonded either to aluminum or to silicon atoms. The chemical nature of fluorinated aluminosilicates has been shown to be distinctly different for catalysts containing 11 wt% alumina and 48 wt% alumina and it depends upon both the alumina content of the unmodified oxide and the fluoride treatment.

References

1. Schlup, J. R., and Vaughan, R. W., J. Catal., submitted.
2. Choudhary, V. R., Ind. Eng. Chem., Product Res. and Develop. 16, 12 (1977).
3. Antipina, T. V., Bulgakov, O. V., and Uvarov, A. V., in "Proceedings of the Fourth International Congress on Catalysis (Moscow), 1968" (J. W. Hightower, Ed.). Vol. 4, p. 1387. Rice University Printing and Reproduction Dept., Houston, 1969.
4. Holm. V. C. F., and Clark, A., Ind. Eng. Chem., Product Res. and Develop. 2, 38 (1963).
5. Covini, R., Fattore, V., and Giordano, N., J. Catal. 7, 126 (1967).
6. Sano, M., Hosino, T., Yotsuyanagi, T., and Aomura, K., Kogyo Kogaku Zasshi 73, 2541 (1970).
7. Holm. V. C. F., and Clark, A., J. Catal. 8, 286 (1967).
8. Peri, J. B., J. Phys. Chem. 72, 2917 (1968).
9. Gerberich, H. R., Lutinski, F. E., and Hall, W. K., J. Catal. 6, 209 (1966).
10. Orkin, B. A., Ind. Eng. Chem., Product Res. and Develop. 8, 154 (1969).
11. Choudhary, V. R., and Doraiswamy, L. K., J. Catal. 23, 54 (1971).
12. Finch, J. N., and Clark, A., J. Catal. 19, 292 (1970).
13. Plank, C. J., Sibbett, D. J., and Smith, R. B., Ind. Eng. Chem. 49, 742 (1957).
14. Hall, W. K., Lutinski, F. E., and Gerberich, H. R., J. Catal. 3, 512 (1964).

15. Holm, V. C. F., and Clark, A., Ind. Eng. Chem., Product Res. and Develop. 2, 38 (1963).

16. Komarov, V. S., Varlanov, V. I., Semyachko, R. Ya., and others, Russ. J. Phys. Chem. 45, 41 (1971).

17. Webb, A. N., Ind. Eng. Chem. 49, 261 (1963).

18. Hirschler, A. E., J. Catal. 2, 428 (1963).

19. Hughes, T. R., White, H. M., and White, R. J., J. Catal. 13, 58 (1969).

20. Chernov, V. A., and Antipina, T. V., Kinet. Katal. 7, 739 (1966).

21. Scokart, P. D., Selim, S. A., Damon, J. P., and Rouxhet, P. G., J. Coll. Interf. Sci. 70, 209 (1979).

22. Antipina, T. V., Chukin, G. D., and Kirina, O. F., Russ. J. Phys. Chem. 46, 1663 (1972).

23. Antipina, T. V., and Bulgakov, O. V., Dokl. Akad. Nauk SSSR 179, 845 (1968).

24. Evans, H. E., Ph.D. thesis, California Institute of Technology, 1980.

25. Kerkhof, F. P. J. M., Moulijn, J. A., Thomas, R., and Oudejans, J. C., in "Preparations of Catalysts II, Studies in Surface Science and Catalysis" (B. Delmon, P. Grange, P. Jacobs, and G. Poncelet, Eds.) Vol. 3, p. 77. Elsevier Scientific Publishing Co., New York, 1979.

26. Brouwer, D. H., J. Catal. 1, 372 (1962).

27. Evreinov, V. I., Lunina, E. V., and Golubev, V. B., Russ. J. Phys. Chem. 47, 578 (1973).

28. O'Reilly, D. E., in "Advance in Catalysis" (D. D. Eley, H. Pines, and P. B. Weisz, Eds.). Vol 12, p. 31. Academic Press, New York, 1960.

29. Golovanova, G. F., Kvlividze, V. I., and Kiselev, V. F., Kinet. Katal. 16, 761 (1975).

30. Osborn, J. A., Phys. Rev. 67, 351 (1945).

31. Peri, J. B., J. Phys. Chem. 69, 220 (1965).

32. Meiboom, S., and Gill, D., Rev. Sci. Instrum. 29, 688 (1958).

33. Anderson, P. W., Phys. Rev. 82, 342 (1951).

34. VanderHart, D. L., Ph.D. thesis, University of Illinois, 1968.

35. VanderHart, D. L., and Gutowsky, H. S., J. Chem. Phys. 49, 261 (1968).

36. Haeberlen, U., "High Resolution NMR in Solids-Selective Averaging", in "Advances in Magnetic Resonance", Suppl. 1, (J. S. Waugh, Ed.). Academic Press, New York, 1976.

37. Hickson, D., Personal Communication.

38. Reitsma, H. J., and Boelhouwer, C., J. Catal. 33, 39 (1974).

39. Leonard, A. J., Ratnasamy, P., Declerck, F. D., and Fripiat, J. J., Discuss. Faraday Soc. 52, 98 (1971).

40. Ratnasamy, P., and Leonard, A. J., in "Catalysis Reviews" (H. Heinemann, Ed.). Vol. 6, p. 293. Marcel Dekker, Inc., New York, 1972.

41. Defosse, C., Canesson, P., Rouxhet, P. G., and Delmon, B., J. Catal. 51, 269 (1978).

42. Hall, W. K., Leftin, H. P., Cheselske, F. J., and O'Reilly, D. E., J. Catal. 2, 506 (1963).

43. Schreiber, L. B., and Vaughan, R. W., J. Catal. 40, 226 (1975).

44. Mesdagh, M. M., Stone, W. E., and Fripiat, J. J., J. Phys. Chem. 76, 1220 (1972).

45. Freude, D., Oehme, W., Schmeidel, H., and Staudte, B., J. Catal. 32, 137 (1974).

TABLE 1

Spin-Lattice Relaxation Times

Oxide	Fluoride Treatment	Calcining Temperature (K)	Hydrogen T_1 (sec)	Fluorine T_1 (sec)
Alumina	None	773	33.	----
	5.4 mM	573	5.	22.±2
		873	11.	15.
Aluminosiliate	5.4 mM	873	13.	23.
(11 wt% Alumina)	5.5 wt%	773	7.	3.(±0.4)
Aluminosilicate	5.4 mM	873	12.	13.
(48 wt% Alumina)	5.5 wt%	773	18.	4.(±.7)

TABLE 2

Hydrogen and Fluorine Concentrations

Oxide	Fluoride Treatment	Calcing Temperature (K)	Specific Surface Area (m^2/g)	Surface Hydrogen Concentration[a] ($10^{18}/m^2$)	Fluorine Concentration Surface ($10^{18}/m^2$)	Fluorine Concentration wt%[b]
Alumina	None	773	156	14+2.	-----	---
	5.4 mM	573	207	6.7+0.2	7.0+1	4.6
		873	173	4.4+0.6	4.4+0.2	2.4
Aluminosilicate	5.4 mM	873	379	1.1+0.1	0.9+0.2	1.1
(11 wt% Alumina)	5.5 wt%	773	156	0.9+0.1	16.+2	8.

[a] One standard deviation

[b] Relative error of 10%

TABLE 3

Centers of Mass and Second

Moments of Hydrogen

Free Induction Decay Spectra

Oxide	Fluoride Treatment	Calcining Temperature (K)	External Field (kG)	Center of Mass[a,b] (ppm)	Second Moment[c] (G^2)
Alumina	None	773	13.2	4.0	0.82
			23.4	-1.0	1.1
	5.4 mM	573	23.4	-4.	2.5
		873	13.2	12.	1.5
			23.4	-3.	1.3
Aluminosilicate (11 wt% Alumina)	5.4 mM	873	23.4	-1.8±0.3	0.044

[a] Relative to tetramethylsilane;

[b] ±3 ppm

[c] Relative error of 15%

TABLE 4

Centers of Mass and Second Moments

Of Fluorine Free Induction Decay Spectra

Oxide	Fluoride Treatment	Calcining Temperature (K)	External Field (kG)	Center of Mass[a] (ppm)	Second Moment[b] (G^2)
Alumina	5.4 mM	573	22.5	1.03 ± 5	5.6
		873	14.1	11.4	6.0
			22.5	13.	4.9
$AlF_3 \cdot xH_2O$	----	----	22.5	-7.	29.
Aluminosilicate	5.4 mM	873	22.5	-8.	0.54
(11 wt% alumina)	5.5 wt%	773	14.1	-3.	0.54
			22.5	-11.	1.0

[a] Relative to hexafluorobenzene

[b] Relative error of 20%

TABLE 5

Hydrogen and Fluorine Relaxation Times

Oxide	Fluoride Treatment	Calcining Temperature (K)	Hydrogen T_2[a] (msec)	Hydrogen T_2^+[b] (msec)	Flourine T_2^+[b] (msec)
Alumina	None	773	0.17	3.8	
	5.4 mM	573	0.076	0.57	1.1
				3.3	4.5
		873	0.20	1.7	0.41
					5.3

[a] Relative Error of 20%

[b] Relative Error of 15%

TABLE 6

Parameters from Low Temperature Hydrogen Spectra of the Alumina Samples

Fluorine Treatment	Calcining Temperature (K)	Observation Temperature (K)	Center of Mass[a] (ppm)	Full Width at Half Height[c] (kHz)	Second Moment (G^2)
None	773	290	-1.0	8.0	1.1
		110	-9.8	10.4	2.0
5.4 mM	573	290	-4.5	15.4	2.5
		110	2.4	20.0	4.2
5.4 mM	873	290	-2.9	10.8	1.3
		115	-6.4	13.2	2.2

[a] ± 2 ppm

[b] Relative error of ± 15%

[c] ± 0.3 kHz

TABLE 7

Parameters from Low Temperature Fluorine Spectra of Fluorinated Alumina

Calcining Temperature (K)	Observation Temperature (K)	Center of Mass[a] (ppm)	Full Width at Half Height[b] (kHz)	Second Moment[c] (G^2)
573	290	1.0	20.4	5.6
	110	20.0	20.4	6.8
873	290	13.	17.6	4.9
	140	9.6	18.6	5.0
	110	1.9	20.2	6.3

[a] ± 5 ppm

[b] ± 0.5 kHz

[c] Relative error of 15%

Figure Captions

Figure 1. Room temperature hydrogen spectra of (A) unmodified alumina calcined at 773 K, of (B) fluorinated alumina calcined at 573 K, and of (C) fluorinated alumina calcined at 873 K. The spectra were obtained at 23 kG. Values of the chemical shift are reported relative to tetramethylsilane.

Figure 2. Fluorine spectra of fluorinated aluminas obtained at 23 kG. At left are the spectra of samples calcined at 573 K and observed at (A) 290 K and at (B) 110 K. At right are the spectra of samples calcined at 873 K and observed at (C) 290 K and at (D) 110 K. Values of the chemical shift are reported relative to hexafluorobenzene.

Figure 3. Room temperature hydrogen spectra of fluorinated aluminosilicates obtained at 23 kG. The aluminosilicates contain (A) 11 wt% alumina and (B) 48 wt% alumina. Values of the chemical shift are reported relative to tetramethylsilane.

Figure 4. Room temperature fluorine spectra of fluorinated silicas containing varying amounts of alumina. The oxides contain (A) 48 wt% alumina, (B) 11 wt% alumina, and (C) 0 wt% alumina. Values of the chemical shift are reported relative to hexafluorobenzene.

Figure 5. Room temperature fluorine spectra of (A) aluminum trifluoride, of (B) fluorinated alumina calcined at 873 K, and of (C) a fluorinated aluminosilicate containing 48 wt% alumina and

calcined at 873 K. The external field strength was 23 kG and the values of the chemical shift are reported relative to hexafluorobenzene.

Figure 6. Semi-logarithmic plot of the fluorine free induction decay for a fluorinated aluminosilicate containing 48 wt% alumina. The intercepts of both parts of the decay have been extrapolated to zero time.

Figure 7. Plots of the fluorine FID (o) and the fluorine 90^{o}-τ-180^{o} echo envelope with τ=200 μsec (Δ) for a fluorinated aluminosilicate containing 48 wt% alumina and prepared using a 5.4 mM F^- solution. The calcining temperature was 873 K. The time scale has been adjusted so that zero time for the spin echo envelope is at 2τ.

Figure 8. Plots of the fluorine FID (●) and the 90^{o}-τ-180^{o} echo envelopes with pulse separations (τ) of 15 μsec (▲), 25 μsec (■), and 40 μsec (o). The time scale has been adjusted so that zero time for each envelope as shown is at 2τ.

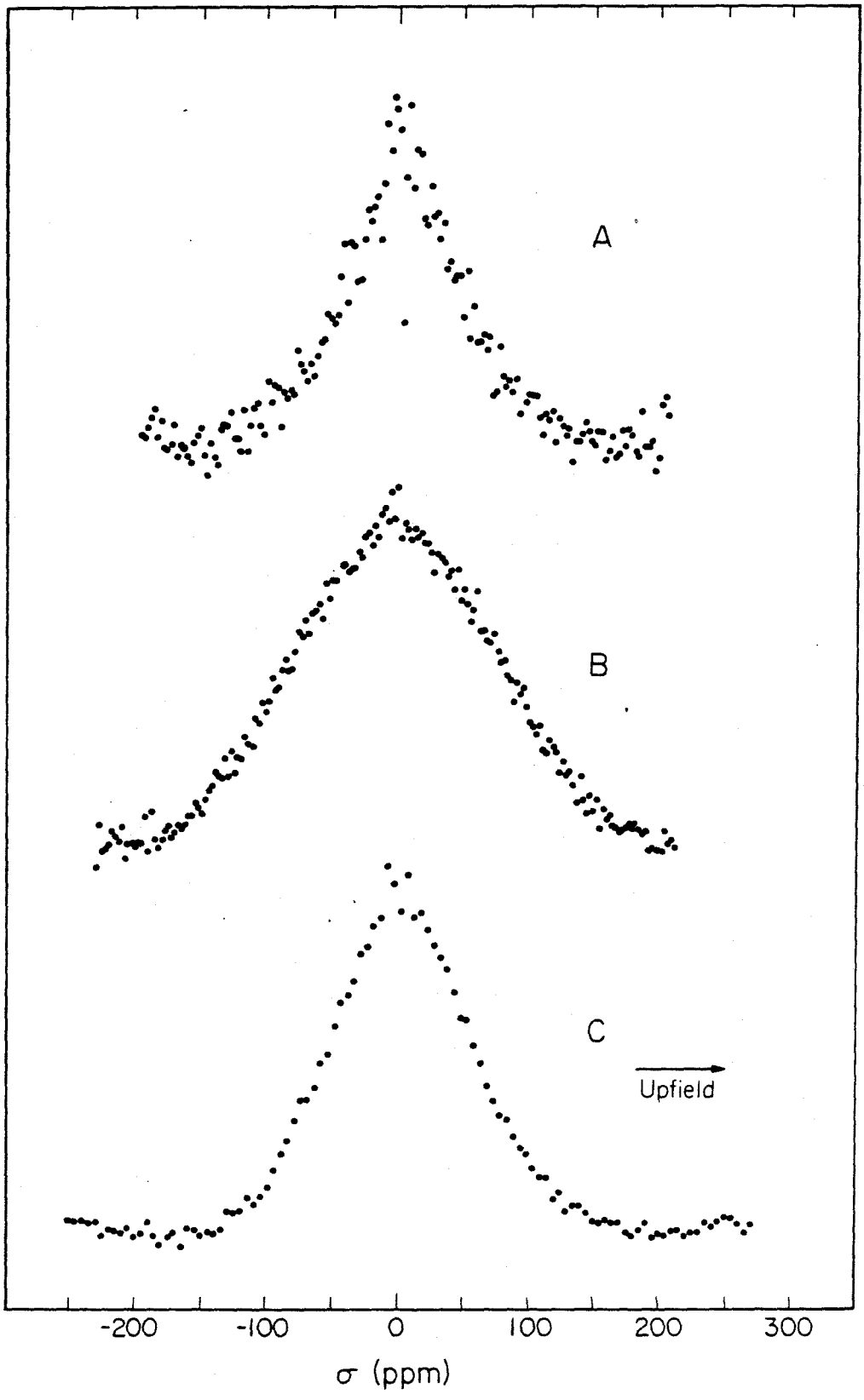

Figure 1

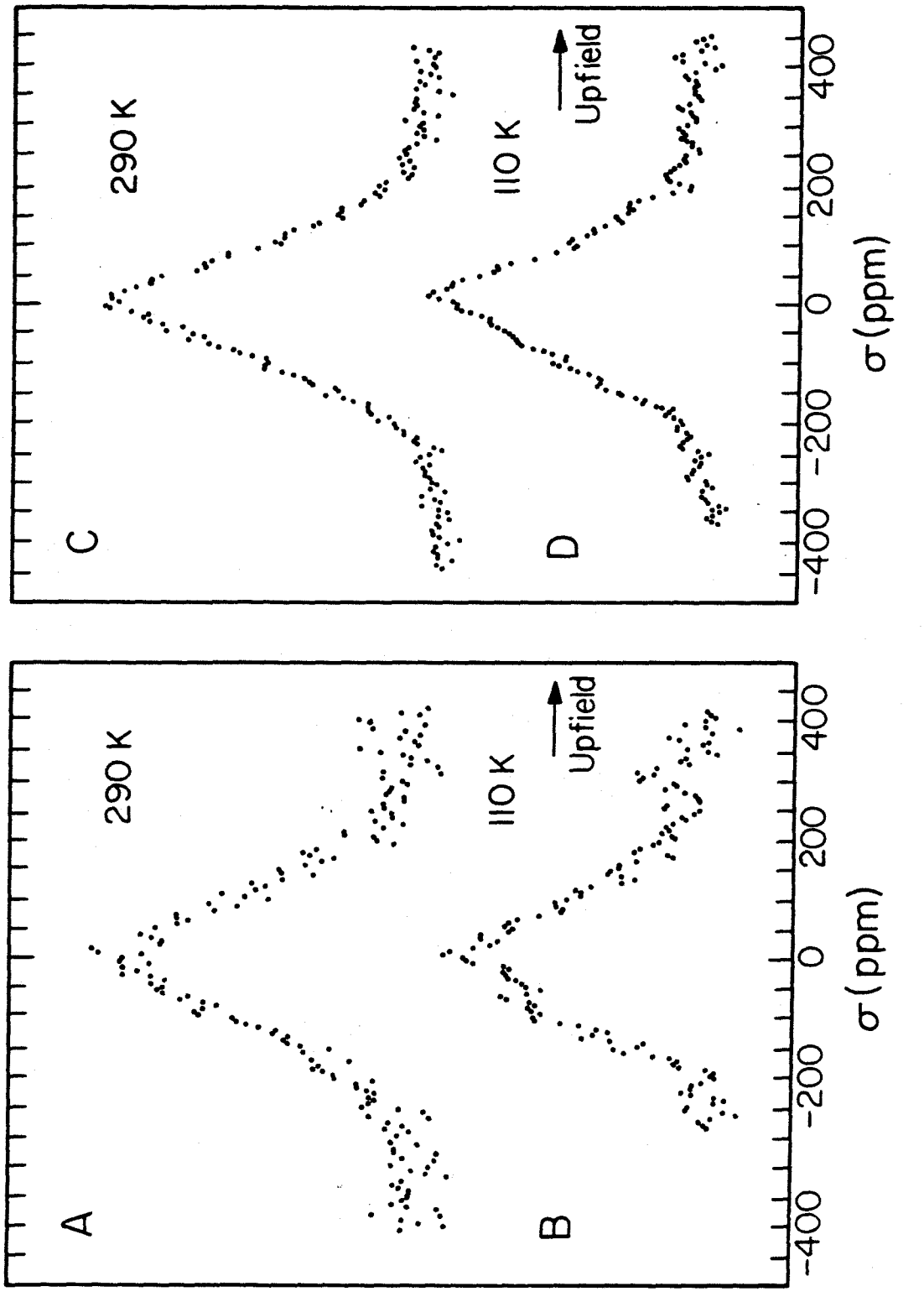
A
290 K
B
110 K
Upfield
C
290 K
D
110 K
Upfield
-400
-200
0
200
400
σ (ppm)

Figure 2

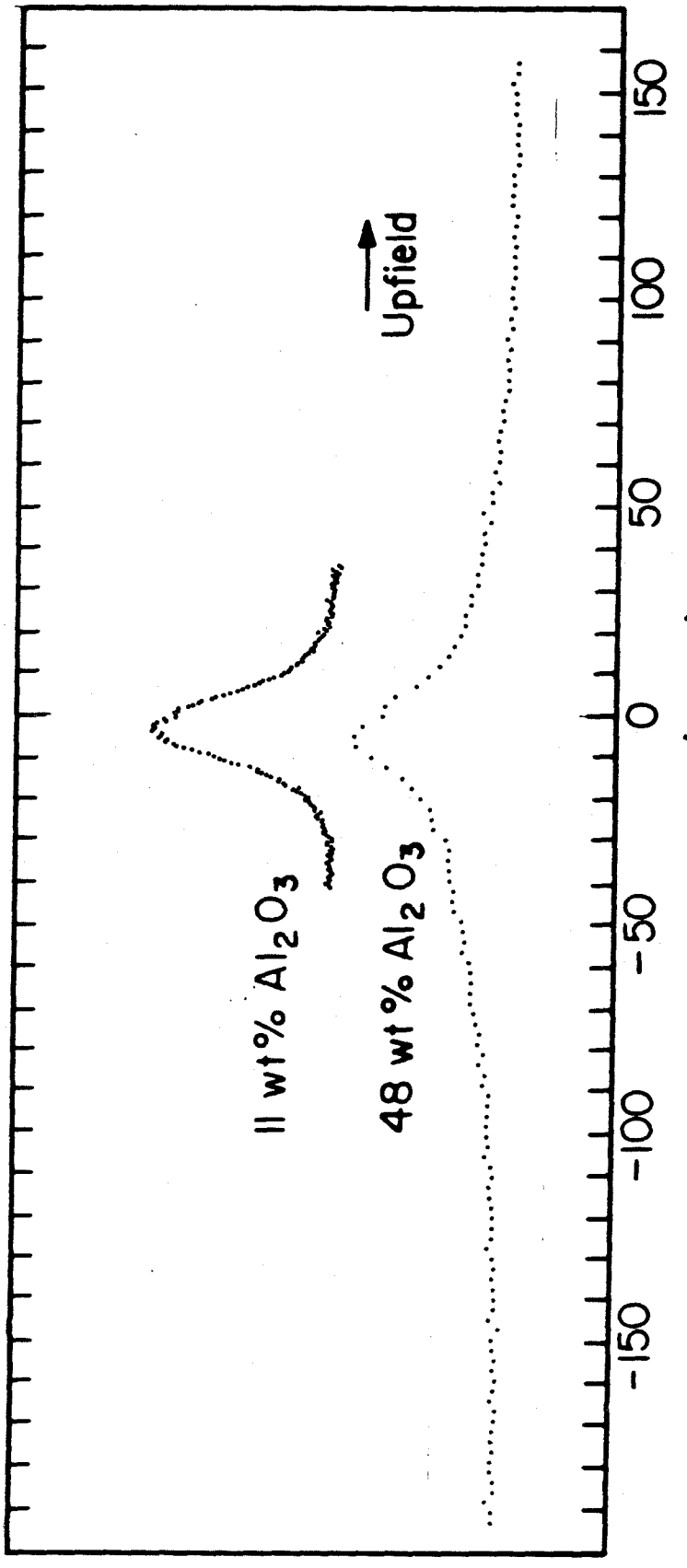

Figure 3

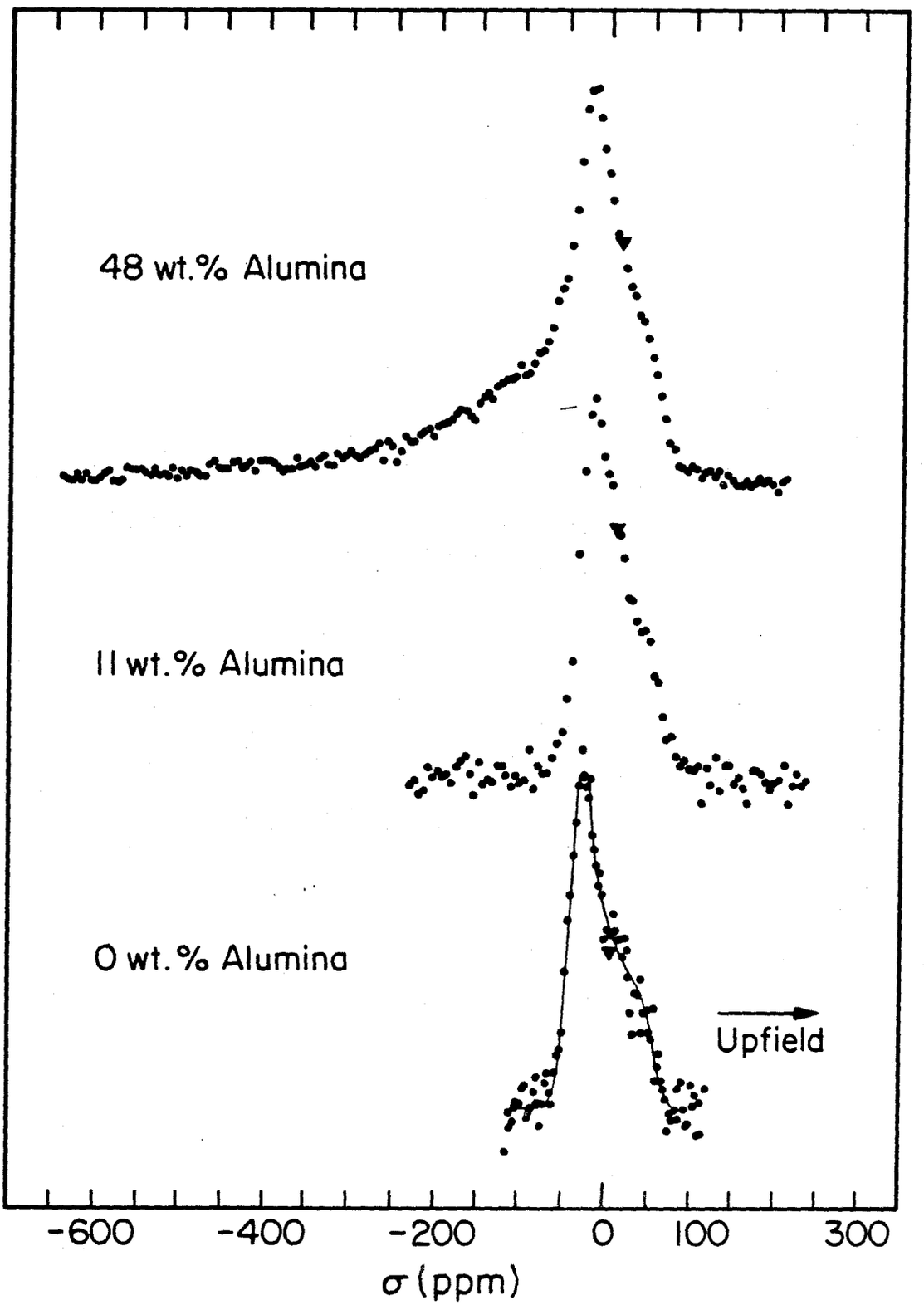
48 wt.% Alumina
11 wt.% Alumina
0 wt.% Alumina
Upfield
-600
-400
-200
0
100
300
σ (ppm)

Figure 4

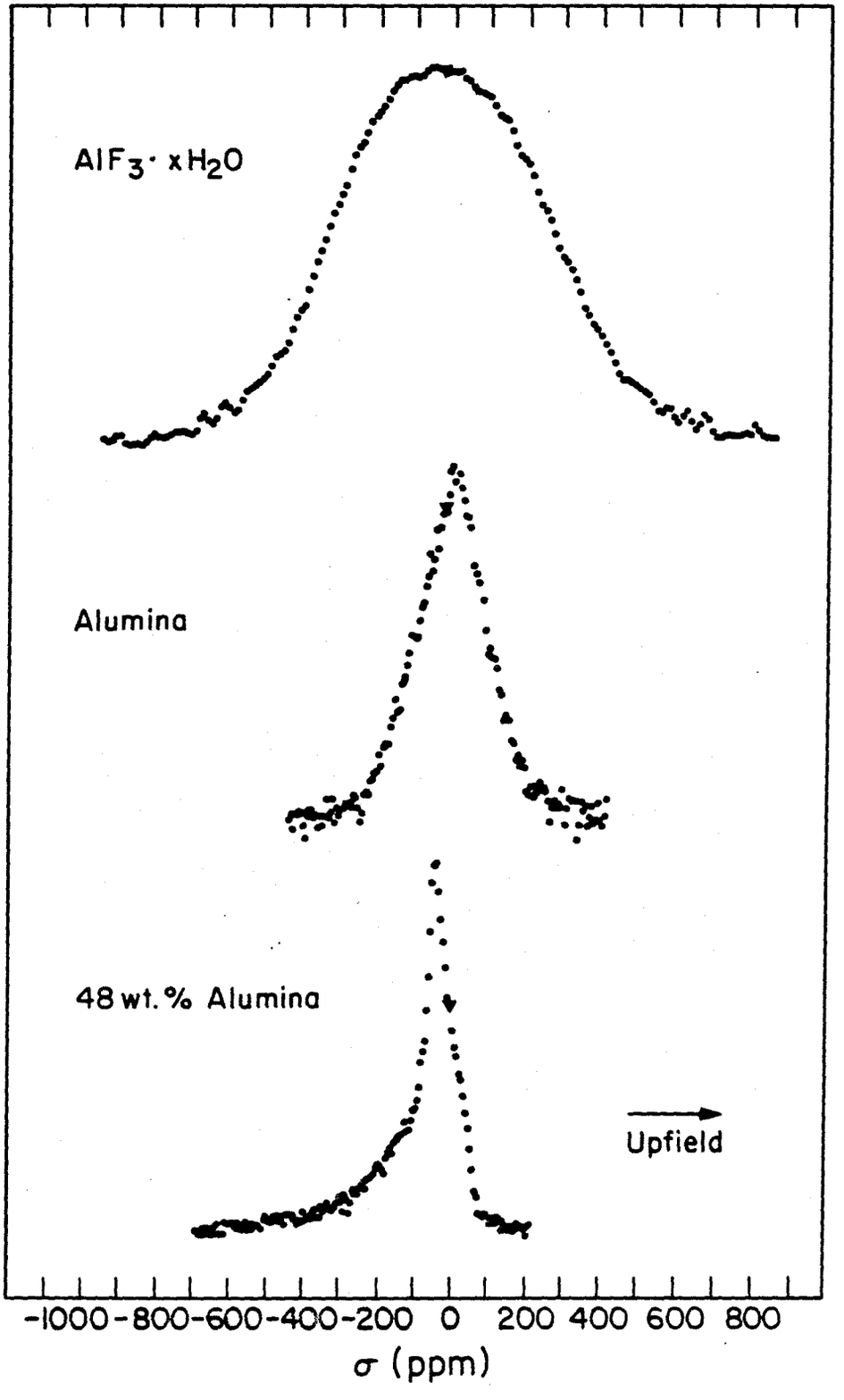
$AlF_3 \cdot xH_2O$
Alumina
48 wt.% Alumina
Upfield
-1000 -800 -600 -400 -200 0 200 400 600 800
σ (ppm)

Figure 5

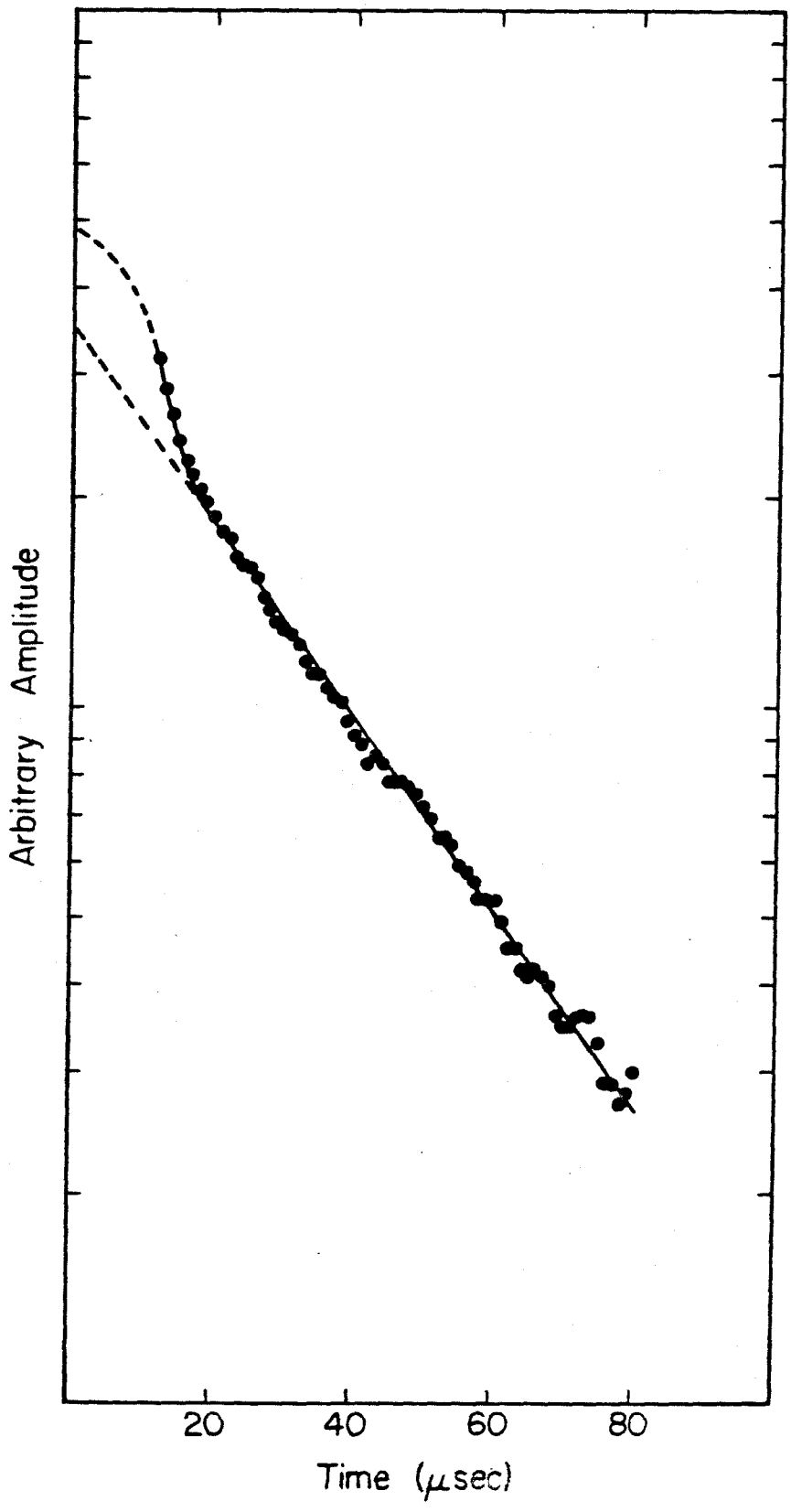

Figure 6

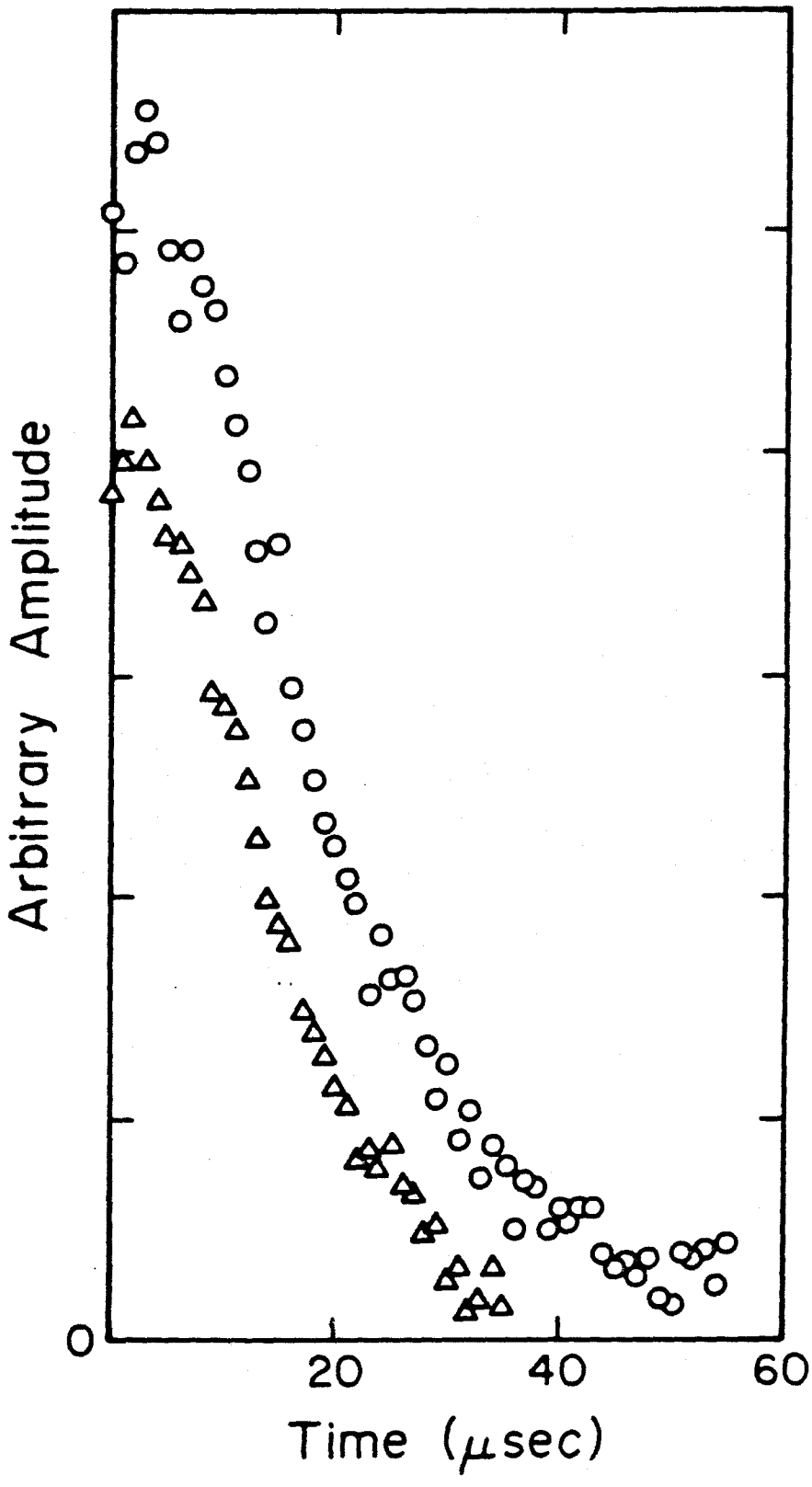

Figure 7

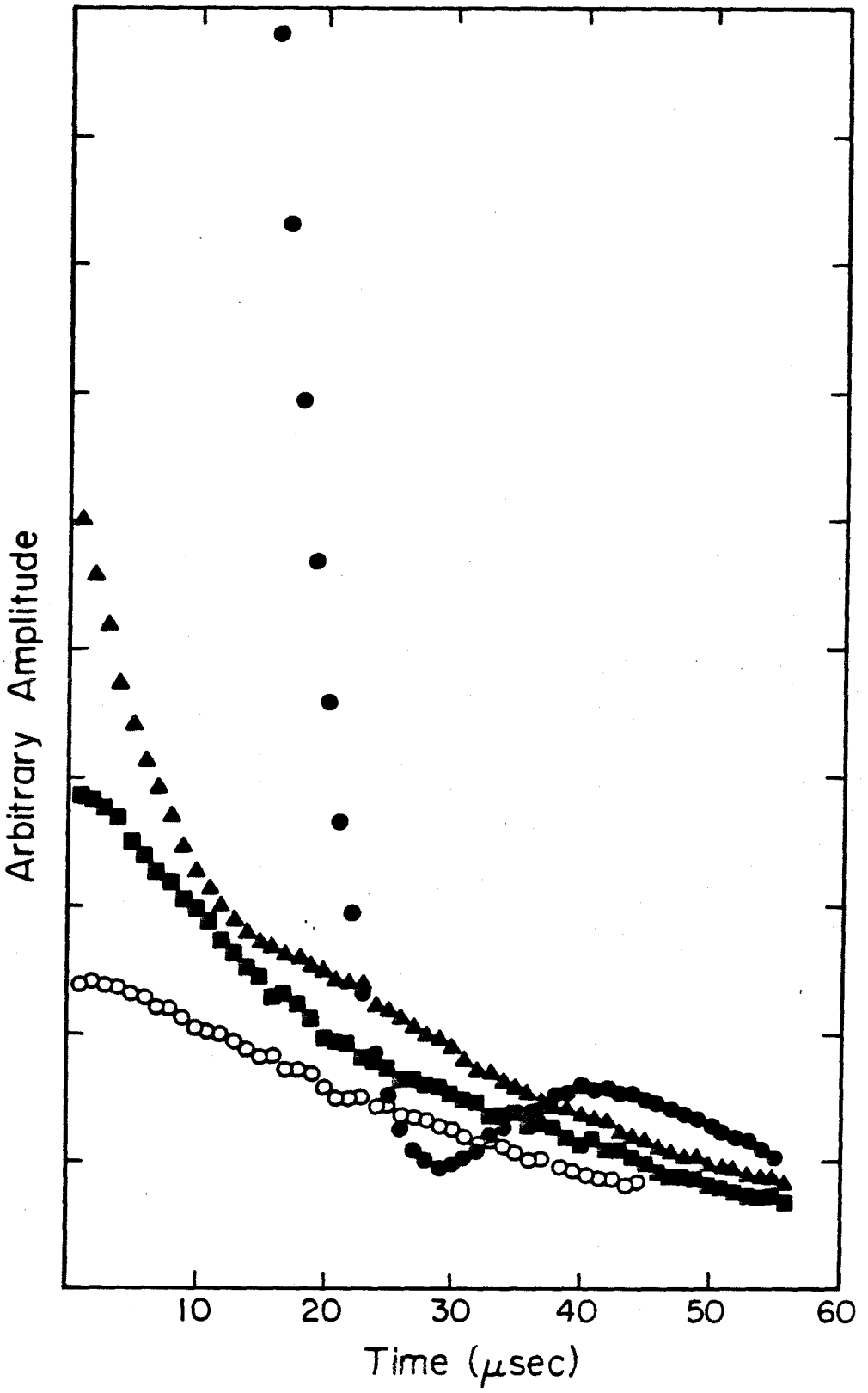

Figure 8

CHAPTER V

Conclusions

The object of this investigation has been to demonstrate the usefulness of solid state nuclear magnetic resonance as a direct spectroscopic probe of fluorinated oxide catalysts. Several questions are basic to understanding a catalyst at the molecular level. In particular, the geometry and chemical nature of the surface must be known as well as the concentration of the chemical species of interest. The most direct probe for an investigation of a given catalyst would be a spectroscopic probe that is specific for the local environment of the chemical species of interest. The usefulness of a specific spectroscopic technique will depend upon the catalytic system being investigated.

The local environments of the hydroxyl groups and fluorine atoms of fluorinated oxides have not been understood previously. Solid state NMR has been shown by this investigation to be well suited for investigating these chemical species. The results have been discussed in Chapters 3 and 4 of this thesis. In this chapter a brief review of these results will be given. Possible contributions from further NMR data will be discussed also.

Fluorinated silica, alumina, and aluminosilicate catalysts can be prepared reproducibly using aqueous ammonium fluoride solutions with fluoride concentrations at the millimolar level. The final composition of the catalysts depends upon both the fluoride treatment and the calcining temperature. Hydrogen is present on these fluorinated oxides even when calcined at temperatures up to 873 K. Oxides containing silica and prepared using a five weight percent fluoride solution form volatile

silicon-fluorine compounds during calcination. This sample preparation results in selective removal of the silicon from the oxide lattice.

Fluorine forms covalent bonds to the silicon and aluminum atoms. If the aluminosilicate contains 11 wt% alumina, the hydroxyl groups and fluorine atoms form bonds only with silicon atoms. Aluminosilicates containing 48 wt% alumina have hydroxyl groups and fluorine atoms chemically bonded to both aluminum and silicon atoms. The chemical bonding between silicon and fluorine atoms is independent of the fluoride treatment and the alumina-to-silica ratio of the aluminosilicate. The identification of SiF, SiOH, AlF, and AlOH species on fluorinated aluminosilicates has not been reported previously.

The ability to differentiate between hydroxyl groups and fluorine atoms forming chemical bonds with silicon and aluminum atoms is very useful. In Chapter 4 of this thesis the concentrations of SiF, SiOH, AlF, and AlOH could be determined for fluorinated aluminosilicates having various compositions. The use of spin echo experiments have shown that the distribution of fluorine atoms bonded to silicon and to aluminum atoms for a fluorinated aluminosilicate with a given alumina-to-silica ratio depends upon the fluoride treatment of the sample. This information has not been available previously.

Carr-Purcell-Meiboom-Gill (CPMG) data have shown that the hydroxyl groups of these fluorinated oxides are isolated from each other. The same is true of the fluorine atoms. Two populations of fluorine atoms having different *fluorine-fluorine* distances exist on the fluorinated aluminas.

Although the fluorine spectrum of fluorinated silicas calcined at 873 K remained unchanged for observation temperatures as low as 110 K, the line shapes of the hydrogen and fluorine spectra of several samples depended upon the observation temperature. The temperature dependences of the line shapes of the hydrogen spectrum of unmodified silica, of the fluorine spectrum of fluorinated silica prepared using an 18 mM F^- solution and calcined at 573 K, and of the fluorine spectra of both fluorinated aluminas are particularly interesting. The hydrogen spectrum of the unmodified silica has a downfield shift in its center of mass and an increase in its second moment for observation temperatures below 160 K. The line shape of the fluorine spectrum of fluorinated silica prepared using an 18 mM F^- and calcined at 573 K solution observed at 290 K cannot be described by chemical shift anisotropy alone. At 110 K the spectrum can be adequately described by a chemical shift powder pattern. The fluorine spectra of both fluorinated aluminas are symmetric at room temperature, but they acquire an asymmetry downfield from their center of mass for observation temperatures below 200 K.

The NMR data obtained to date have not exhausted the capabilities of the techniques. The number of different hydroxyl group sites could be determined using magic angle sample spinning techniques. The information obtained by performing sample spinning experiments at several temperatures could detect the presence of chemical exchange between two or more sites. This information would be important in understanding the changes in the line shape of the hydroxyl group spectra as a function of temperature.

The discrepancy observed between the relaxation times T_2 and T_2^+

needs to be explained. This discrepancy is caused by fluctuations in the local magnetic fields of the nuclei. Understanding the source of these fluctuations would determine if diffusion, chemical exchange, or anisotropic motion of the hydroxyl groups or fluorine atoms is occurring. More extensive hydrogen and fluorine T_2 data over a wider range of pulse intervals are needed. The changes in the CPMG decay rates as a function of the interval between 180^0 pulses is necessary. The temperature dependence of these relaxation times would be very informative.

The use of NMR spectroscopy as a probe of catalyst surfaces is limited by three factors. The chemical species of interest must possess nuclear spin. Observation of fewer than 10^{18} atoms requires extensive signal averaging because NMR lacks the sensitivity of optical spectroscopies. The NMR spectrum can become a broad featureless resonance as the concentration of the chemical species and the number of their interactions with neighboring nuclei increase. However, these limitations are not as severe as they may seem at first glance. Many catalytically important materials contain hydrogen, fluorine, carbon, sodium, boron, phosphorus, or other nuclei possessing nuclear spin. The detection limits of NMR can be improved by recent developments in NMR instrumentation. The availability of higher magnetic fields (63 kG or higher) is one example. Another advantage of solid state multiple-pulse NMR spectroscopy is the availability of various techniques (CPMG, heteronuclear decoupling, and magic angle sample spinning experiments for example) which selectively remove various molecular interactions. Detailed information about specific interactions have been obtained using these techniques.

Nuclear magnetic resonance will not provide a complete picture of any catalytic material. No one spectroscopic tool will accomplish this. However, solid state multiple-pulse NMR data are a valuable addition to data obtained from other spectroscopic techniques and from measurements of the catalytic activity.

APPENDIX A

Evaluation of the Catalytic Activity of a Heavily Fluorinated Aluminosilicate for the Isomerization of 1-Butene

The importance of understanding the properties of a particular catalyst at the molecular level was underscored in the ChE 126 laboratory in 1978. Fluorinated aluminosilicates were prepared as catalysts for butene isomerization. The unmodified aluminosilicate was a commerical catalyst, Strem 14-715. The composition of this catalyst was 87.3 wt% SiO_2, 12.4 wt% Al_2O_3, and 0.25 wt% Na_2O. Three catalyst samples were prepared. One was left unfluorinated. Two fluorinated catalysts were prepared using aqueous ammonium fluoride solutions. One solution had a fluoride concentration of 18 mM and the other had a fluoride concentration of 5.5 wt%. All of the catalysts were calcined in the reactor under flowing oxygen for two hours at 623 K prior to obtaining kinetic data. The preparation of a fluorinated aluminosilicate catalyst using a 5.5 wt% fluoride solution was similar to other sample preparations reported for fluorinated silica (1), fluorinated alumina (2), and fluorinated aluminosilicates (3).

A schematic of the reactor system is given in Figure 1. The details of the gas chromatography procedures have been discussed elsewhere (4). A schematic diagram of the catalyst bed and its surroundings is shown in Figure 2. The reactant stream contained 1-butene with helium as a diluent. The purpose of the broken quartz glass was to ensure mixing of the 1-butene and helium and to establish plug flow in the reactant stream. A more detailed description of the apparatus and procedures can be obtained in the ChE 126 report by Croes and Findley (5).

The catalytic behavior of the aluminosilicate prepared using the 5.5 wt% fluoride solution is discussed here. The catalytic data were

taken and analyzed by undergraduates Bart Croes and Jim Findley. They reported their results in their ChE 126b report, "Evaluation of Highly Fluorinated Silica-Alumina as a Catalyst for the Isomerization of 1-Butene" (5).

Haag and Pines (6) reported that the isomerization reactions of butene are reversible and that the reaction network shown below can be used to describe the reaction.

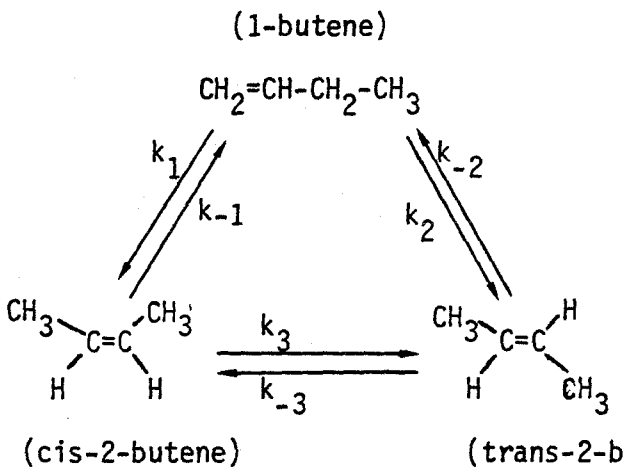

The following rate equations for the formation of cis-2-butene and trans-2-butene can be shown to apply for the situation where the data are obtained at short residence times and for a reactant stream containing only 1-butene diluted with helium.

$$\left.\frac{d[cis]}{dt}\right|_{t\to o} = k_1\,[1\text{-butene}] \qquad \left.\frac{d[trans]}{dt}\right|_{t\to o} = k_2\,[1\text{-butene}]$$

where

[cis] = final concentration of cis-2-butene

[trans] = final concentration of trans-2-butene

[1-butene] = initial concentration of 1-butene

This approach was used by Haag and Pines for analysis of their activity

data. Integration of the simplified rate equations yields the following expressions for the rate constants

$$k_1 = \frac{[\text{cis}]}{[\text{1-butene}]_o \, t_r} \qquad \text{and} \qquad k_2 = \frac{\text{trans}}{[\text{1-butene}]_o \, t_r}$$

where

$$t_r = \frac{(\text{volume of the catalyst bed})}{\left(\begin{array}{c}\text{volumetric flow rate of reactant} \\ \text{in the reactor}\end{array}\right)}$$

$$= \text{residence time.}$$

Croes and Findley studied the rate constants k_1 and k_2 in the temperature range from 530 K to 630 K. They obtained the following expressions for these rate constants assuming an Arrhenius temperature dependence.

$$k_1 = (7315/\text{sec})\exp((-11 \text{ kcal/gm-mol})/RT)$$

$$k_2 = (21400/\text{sec})\exp((-12 \text{ kcal/gm-mol})/RT)$$

The temperature range at which isomerization occurred was much higher than that observed for the unmodified aluminosilicate (7). Data for the unmodified aluminosiliate were obtained at 400 K. At that temperature the reaction rate was controlled by the reaction kinetics. The higher reaction temperatures required for the fluorinated aluminosilicate can be understood from the data reported in Chapter 4 of this thesis.

Nuclear magnetic resonance (NMR) data have shown that the fluorine atoms bond only to the silicon atoms for aluminosilicates which have this alumina-to-silica ratio. No aluminum-fluorine species are observed regardless of the concentration of the fluoride solution used to prepare the catalyst. When the fluorinated aluminosilicate catalyst was

prepared using a 5.5 wt% fluoride solution, volatile silicon-fluorine compounds formed during the calcining process which removed selectively the silicon from the lattice. A white sublimate collected at the cool end of the reaction tube. Analysis of the sublimate using neutron activation analysis showed that its composition was 19 wt% silicon, 52 wt% fluorine, and 290 ppm aluminum. Therefore, the calcining process increases the alumina-to-silica ratio of the catalyst, and the catalyst can be transformed into an alumina-like catalyst.

If the silicon content of the catalyst were reduced substantially, the catalytic behavior of the catalyst should be similar to that of alumina. Turkevich and Smith studied the catalytic activity of several oxides for butene isomerization (8). They reported that isomerization of butene using an alumina catalyst required a reactor temperature of approximately 560 K or higher. This is the temperature range in which catalytic activity was observed by Croes and Findley for the fluorinated aluminosilicate.

The fluorinated aluminosilicate catalyst had not been heated to temperatures above 623 K prior to obtaining the isomerization data. Isomerization data taken at temperatures below 623 K reflect the activity of the catalyst as calcined. However, the catalytic activity of the catalyst began to decline for reaction temperatures above 663 K (see Figure 3). Equilibrium conversion had not been obtained at that temperature. When the reaction temperature was lowered, lower conversions of 1-butene were observed when compared with the data obtained as the reactor temperature was being increased to 663 K. Calcining at 623 K under flowing oxygen did not restore the original activity of the catalyst.

The deactivation of the catalyst can be understood using the fluorine NMR data and the analysis of the sublimate. Calcining the fluorinated aluminosilicate formed volatile silicon-fluorine compounds. The alumina-to-silica ratio was increased as the silicon was removed from the aluminosilicate lattice during calcination. The resulting oxide required the higher reaction temperatures for isomerization to occur. When the catalyst was used at reaction temperatures higher than the temperature at which it was calcined, volatile silicon-fluorine products were formed again. This process further increased the alumina-to-silica ratio. The catalyst behavior became more similar to that of an alumina catalyst.

Since the deactivation was due to structural changes in the oxide, the activity of the catalyst after heating at 663 K was that of the transformed oxide. Calcining at 623 K would not affect the structure of this oxide. Therefore, the deactivation of the catalyst was irreversible.

An understanding of the catalyst structure and composition at the molecular level is necessary if catalytic activity data are to be interpreted properly. In this investigation, the reasons for the deactivation of a fluorinated aluminosilicate were not known based upon a study of the reaction kinetics alone. Neutron activation analysis of the sublimate clarified the changes that were occurring in the catalyst at elevated temperatures. Nuclear magnetic resonance was useful in describing the composition of the catalyst at the molecular level. By knowing the composition of the catalyst, the irreversible deactivation of the catalyst and the requirement of higher reactor temperatures could be explained.

Acknowledgments

The author would like to thank Bart Croes and Jim Findley for obtaining the kinetic data. The neutron activation analysis was performed by General Activation Analysis, Inc. of San Diego, California.

References

1. Chapman, I. D., and Hair, M. L., J. Catal. 2, 145 (1963).
2. Holm, V. C. F., and Clark, A., Ind. Eng. Chem., Product Res. and Develop. 2, 38 (1963).
3. Plank, C. J., Sibbett, D. J., and Smith, R. B., Ind. Eng. Chem. 49, 742 (1957).
4. Kaler, K.-E., ChE 126a laboratory report, November 1976.
5. Croes, B., and Findley, J., ChE 126b laboratory report, March 1978.
6. Haag, O., and Pines, H., J. Amer. Chem. Soc. 82, 2488 (1960).
7. Kim, S., and Lee, W.-H., ChE 126b laboratory report, March 1978.
8. Turkevich, J., and Smith, R. K., J. Chem. Phys. 16, 466 (1948).

Figure Captions

Figure 1. Schematic diagram of the experimental apparatus.

Figure 2. Schematic diagram of catalyst bed and its surroundings.

Figure 3. Plot of mole fraction of 1-butene and reaction products as a function of reactor temperature.

	Increasing Reactor Temperature	After Re-calcining
1-butene	○	⊙
cis-2-butene	□	⊡
trans-2-butene	▽	▽

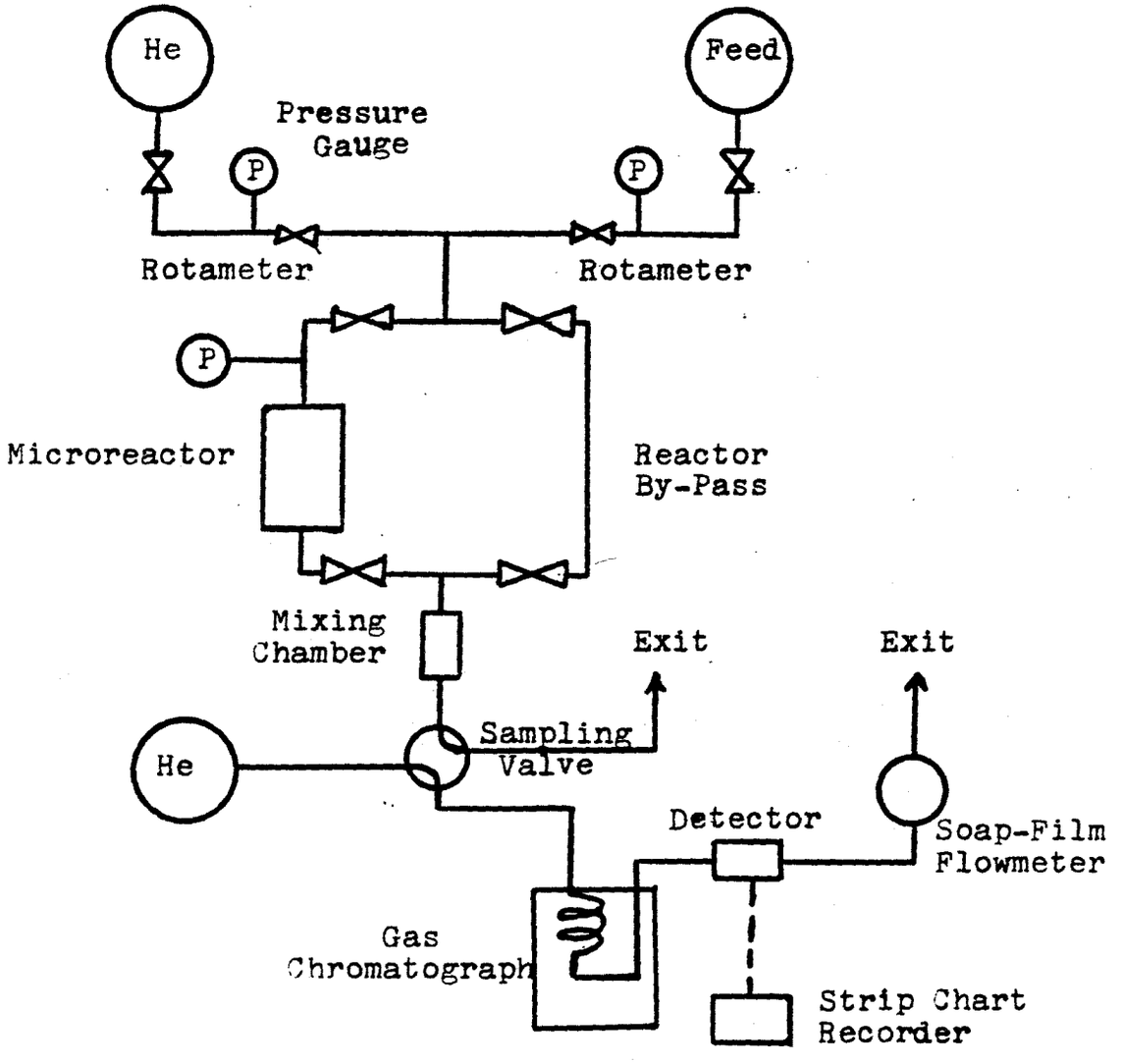
He
Feed
Pressure
Gauge
P
P
Rotameter
Rotameter
P
Microreactor
Reactor
By-Pass
Mixing
Chamber
Exit
Exit
He
Sampling
Valve
Detector
Soap-Film
Flowmeter
Gas
Chromatograph
Strip Chart
Recorder

Figure 1

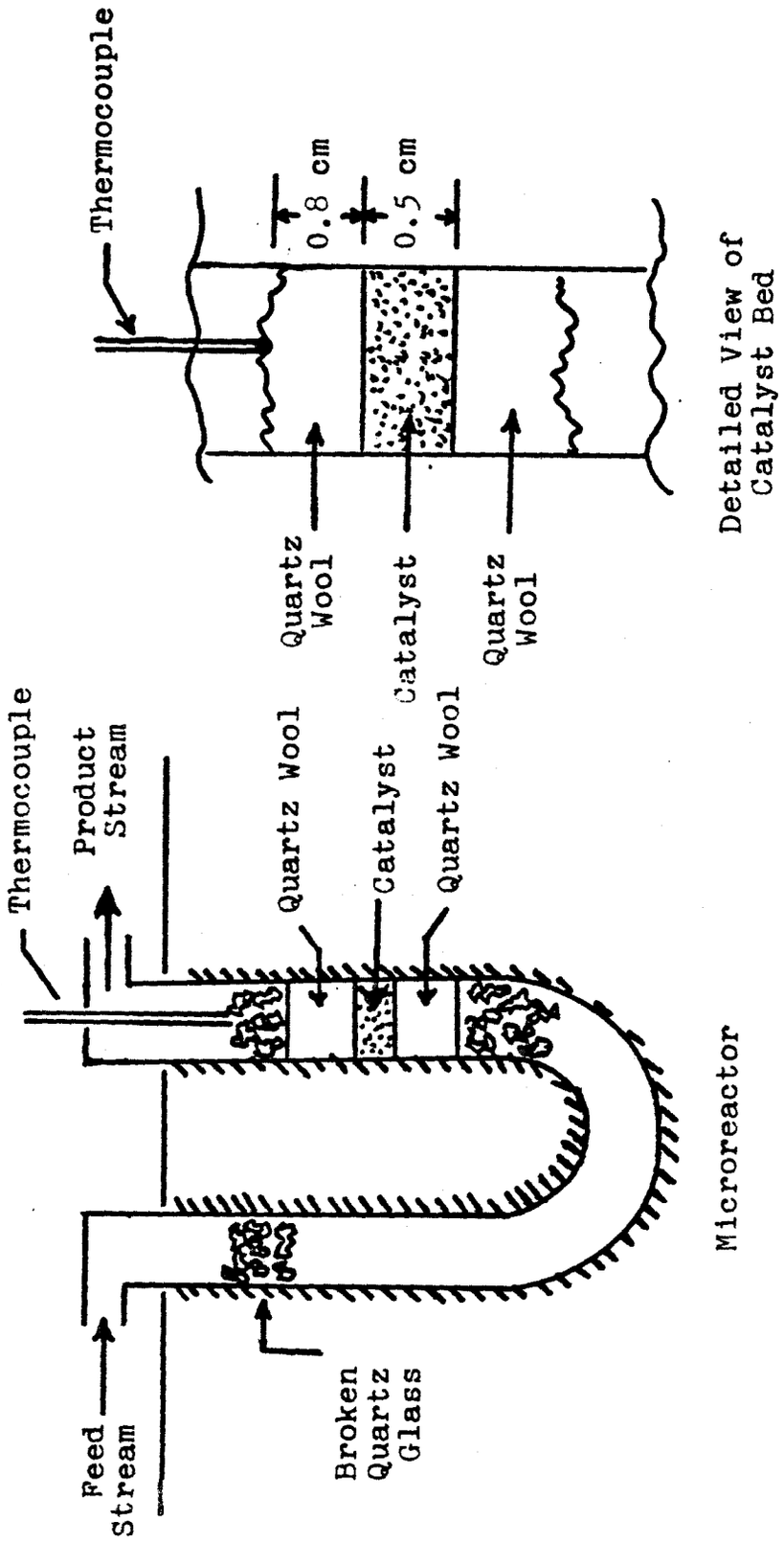
Thermocouple
Product Stream
Quartz Wool
Catalyst
Quartz Wool
Thermocouple
Feed Stream
Broken Quartz Glass
Microreactor
Thermocouple
0.8 cm
0.5 cm
Quartz Wool
Catalyst
Quartz Wool
Detailed View of Catalyst Bed

Figure 2

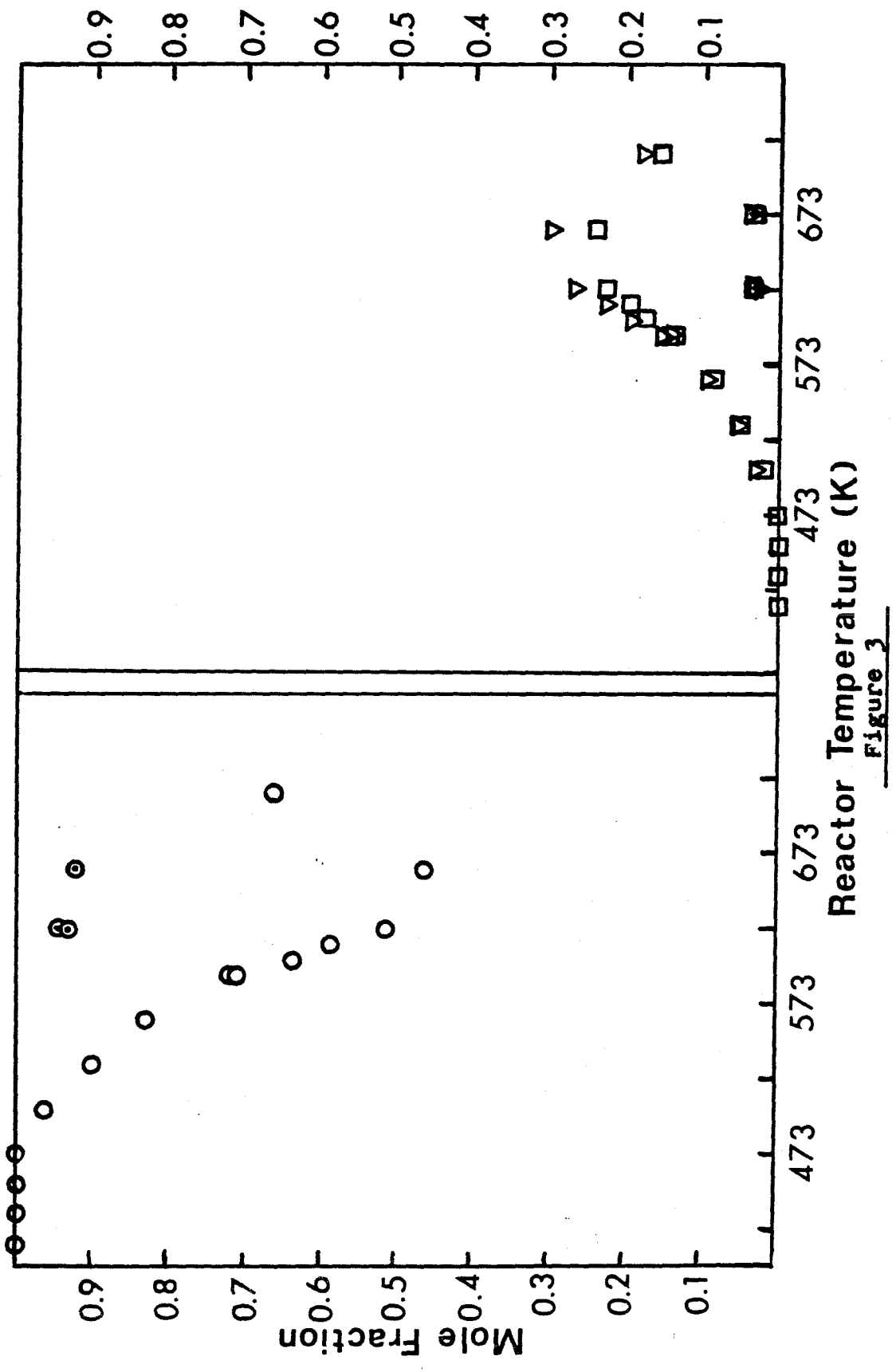
Mole Fraction
0.9
0.8
0.7
0.6
0.5
0.4
0.3
0.2
0.1
473
573
673
Reactor Temperature (K)

Figure 3

APPENDIX B

The Nature of Fluorine Modified Oxide Surfaces: An NMR Study

(Appendix B is an article by J. R. Schlup and R. W. Vaughan entitled "The Nature of Fluorine Modified Oxide Surfaces: An NMR Study." This article is to be published in Nuclear and Electron Resonance Spectroscopies Applied to Materials Science (G. K. Shenoy and E. N. Kaufmann, Eds.). North-Holland Publishing Co., 1981.)

Introduction

The addition of fluorine to oxide catalysts has been shown to drastically change the properties of oxide catalysts. During the last twenty years, these properties have been demonstrated with a wide variety of reactions, catalysts, and reactor conditions (1). Research on fluorine modified oxide catalysts has focused on improving product yields and selectivity and on obtaining a better understanding of the unmodified oxide catalysts as changes due to the addition of fluorine are observed.

Fluorine modified oxide catalysts have been studied by measuring the rates of a variety of reactions and by measuring the surface acidity. Spectroscopic techniques have included infrared spectroscopy, nuclear magnetic resonance, x-ray photoemission spectroscopy, x-ray diffraction, and inelastic electron tunneling spectroscopy. In general, the object has been to understand these catalysts by monitoring changes in their chemical behavior and in their adsorption of small molecules after the addition of fluorine. It is hoped the observed changes in behavior may then provide insight into changes at the catalytically active sites. Although this approach has provided much information about the catalysts, one would like to have a direct spectroscopic probe of the local environment of the hydroxyl groups and fluorine atoms.

In the past infrared spectroscopy has been most widely used as a spectroscopic probe. However, since the fluorine atom vibrations are buried among the bands due to the lattice vibrations, one is limited to observing only the hydroxyl group stretching vibrations. Even then, past research has focused on the perturbations in these vibrations that result

from modifying the surface or from the adsorption of small molecules. However, nuclear magnetic resonance provides a very specific probe of the local environments of hydrogen and fluorine atoms. The chemical shift interactions provide information on the electronic environment while the dipole-dipole interaction yields information about the location of neighboring atoms. NMR is also a useful tool for quantitative analysis.

Several key questions arise as one investigates fluorine modified oxides. The type of bonding present must be understood. The existence of fluorine-hydroxyl group hydrogen bonds has also been proposed (2, 3). The focus of the present discussion is the quantitative analysis of the modified oxide after various pretreatment conditions and the nature of the fluorine and proton bonding on various fluorine modified oxide catalysts.

Experimental

The NMR measurements were performed with a pulse NMR spectrometer described previously (4), operating at 16 kG and at 25 kG. All measurements were made at room temperature. The experiments reported herein were either free induction decays or spin echoes (90-τ-180).

The silica samples were prepared using a commercial dessicant silica gel (Grace Davison Grade 62). The alumina samples were prepared from Alcoa alumina F-20. The aluminosilicates used in this study were xerogel aluminosilicate catalysts prepared by Dr. D. A. Hickson at Chevron Laboratories in Richmond, California. The fluorine modified materials were prepared by soaking the catalysts in aqueous ammonium fluoride solutions (5.4 mM and 17.9 mM NH_4F). The suspensions were gently heated

to dryness and then calcined under flowing oxygen in a tube furnace. Nitrogen BET surface area data were taken and then the samples were again calcined under oxygen. The sample tubes were then evacuated and sealed. The surface areas of all of the samples were greater than 125 m^2/g with the fluorine modified silicas having surface areas of 225 m^2/g.

Quantitative Analysis

Numerous problems exist in obtaining proton and fluorine concentrations of fluorine modified oxides. Precision of 10% is very difficult to obtain for samples with low fluorine concentrations. Many quantitative techniques require preparations which cause irreversible changes in the sample. Vibrational spectroscopic measurements rely on knowledge of the oscillator strengths of the vibrations being considered. NMR is a good quantitative tool for determining proton and fluorine atom concentrations and it is a non-destructive technique. The signal intensity is directly proportional to the number of spins present. Precision of 5% has been demonstrated on samples containing as few as 5×10^{18} spins.

The presence of hydroxyl groups and fluorine atoms as a function of sample preparation is an important question. The relative number of hydroxyl groups and fluorine atoms needs to be known and yet values reported in the literature do not present a clear picture of their relationship. The results of counting the proton and fluorine spins are found in Table I. Protons are present on all the samples regardless of the pretreatment temperature. With silica samples at higher fluorine concentrations no protons were detected. Silica samples with higher fluorine concentrations also decompose to form a volatile silicon-fluorine compound.

The proton concentrations decrease as the sample pretreatment temperature is increased. The fluorine and proton concentrations after pretreatment at 600°C are the same regardless of the fluorine preparation (for this range of fluorine concentrations). The fluorine concentration is equal to the proton concentration for both silica and alumina after pretreatment at 600°C.

Spectra of Various Modified Oxides

Various fluorine modified silicas, aluminas, and aluminosilicates have been prepared. In all cases the fluorine spectra has a center of mass which corresponds to fluorine covalently bound to the metal atom of the oxide. Fluorine ions and oxyfluoride species were not detected. The nature of the fluorine-silicon and fluorine-aluminum bond did not change with the sample pretreatment temperature.

Figure 1 compares the ^{19}F spectra of fluorine modified aluminosilicates with varying alumina contents. The fluorine modified silica exhibits a lineshape resulting from the chemical shift anisotropy and the center of mass is consistent with that of fluorine bound covalently to silicon. The sample containing 11 wt% alumina exhibits an identical spectrum. This means that the fluorine exists in environments identical to those of a fluorine modified silica. However, the ^{19}F spectrum of an aluminosilicate containing 48 wt% alumina has two components. The narrow component is identical to that of fluorine bound covalently to silicon. The width of the broad component suggests that there are contributions from aluminum-fluorine dipole-dipole interactions.

Figure 2 contains ^{19}F spectra taken from spin echo experiments with

$AlF_3 \cdot xH_2O$, fluorine modified alumina, and a fluorine modified aluminosilicate which was 48 wt% alumina. The ^{19}F spectrum of aluminum trifluoride is a Gaussian line broadened by dipolar interactions between the neighboring fluorine, aluminum, and hydrogen atoms. The spectra for the fluorine modified alumina is not easy to interpret. It is asymmetric and the asymmetry is not due to chemical shift anisotropy. The spectrum of the fluorine modified aluminosilicate clearly has two components. As was shown in the previous figure, the narrow component results from fluorine bonded to silicon atoms. The center of mass of the broad component is consistent with fluorine bound covalently with aluminum. Therefore, fluorine binds to both silicon and aluminum in aluminosilcates with higher alumina concentrations. The hydroxyl groups of these samples exhibit similar behavior, which is consistent with data reported previously (5).

Conclusions

Fourier transform NMR has been shown to be a valuable tool for investigating fluorine modified oxide catalysts. It provides a precise, non-destructive tool for obtaining fluorine atom and proton concentrations. It has been shown that fluorine forms covalent bonds with the metal atom in silica, alumina, and aluminosilicates. In aluminosilicate materials with low alumina content, the fluorine bonds preferentially to the silicon atoms. Fluorine bonds with aluminum as the alumina content of the aluminosilicate increases.

References

1. V. R. Choudhary, Ind. Eng. Chem., Product Res. and Develop. 16, 12 (1977).
2. A. N. Sidorov and I. E. Neimark, Russ. J. Phys. Chem. 38, 1518 (1964).
3. R. W. Vaughan, D. D. Elleman, L. M. Stacey, W.-K. Rhim, and J. W. Lee, Rev. Sci. Instrum. 43, 1356 (1972).
4. L. B. Schreiber and R. W. Vaughan, J. Catal. 40, 226 (1975).

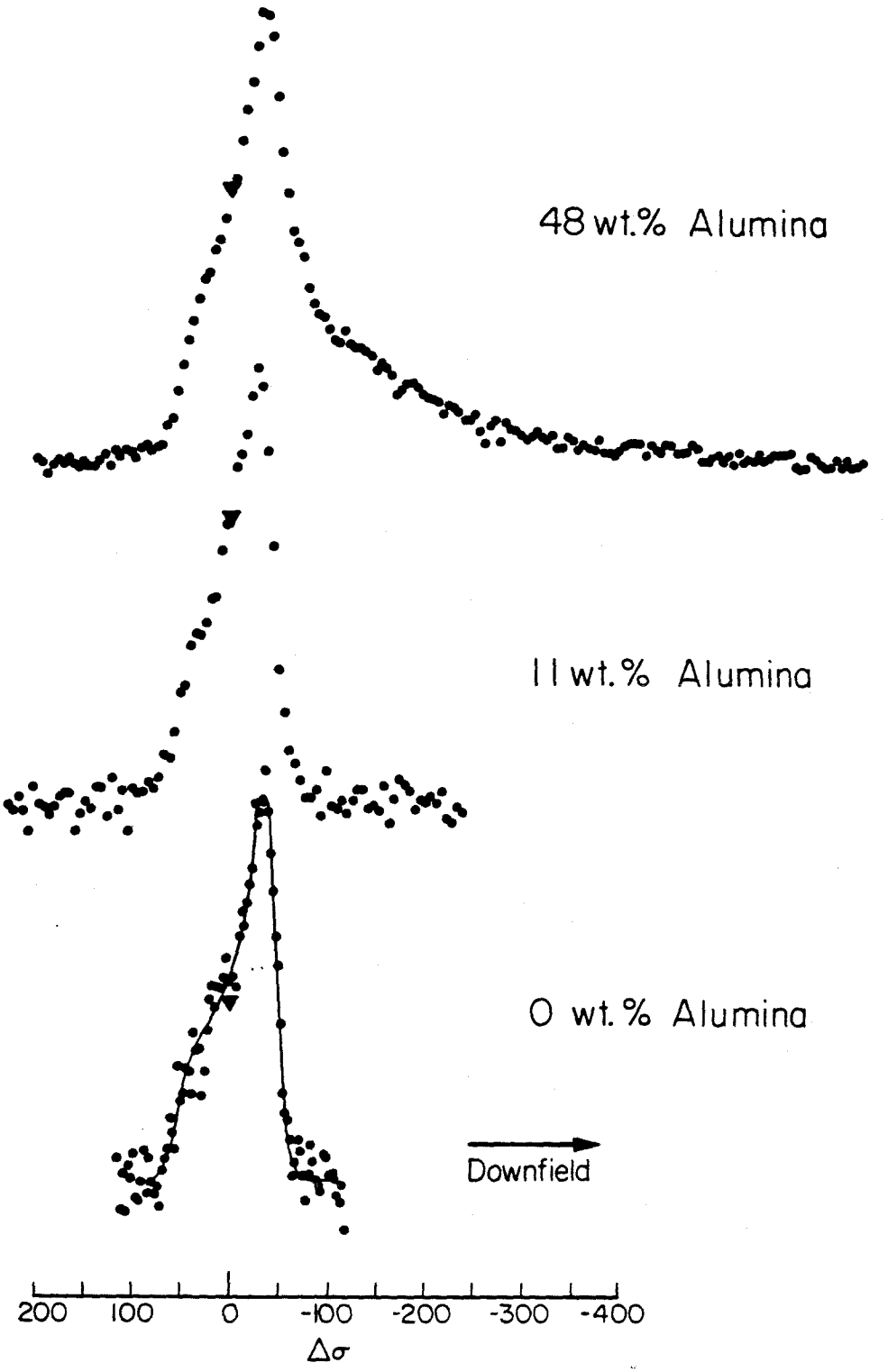

Fig. 1 ^{19}F powder patterns of fluorine modified oxides with varying alumina content. The signal amplitude is plotted versus chemical shift (ppm) relative to hexafluorobenzene.

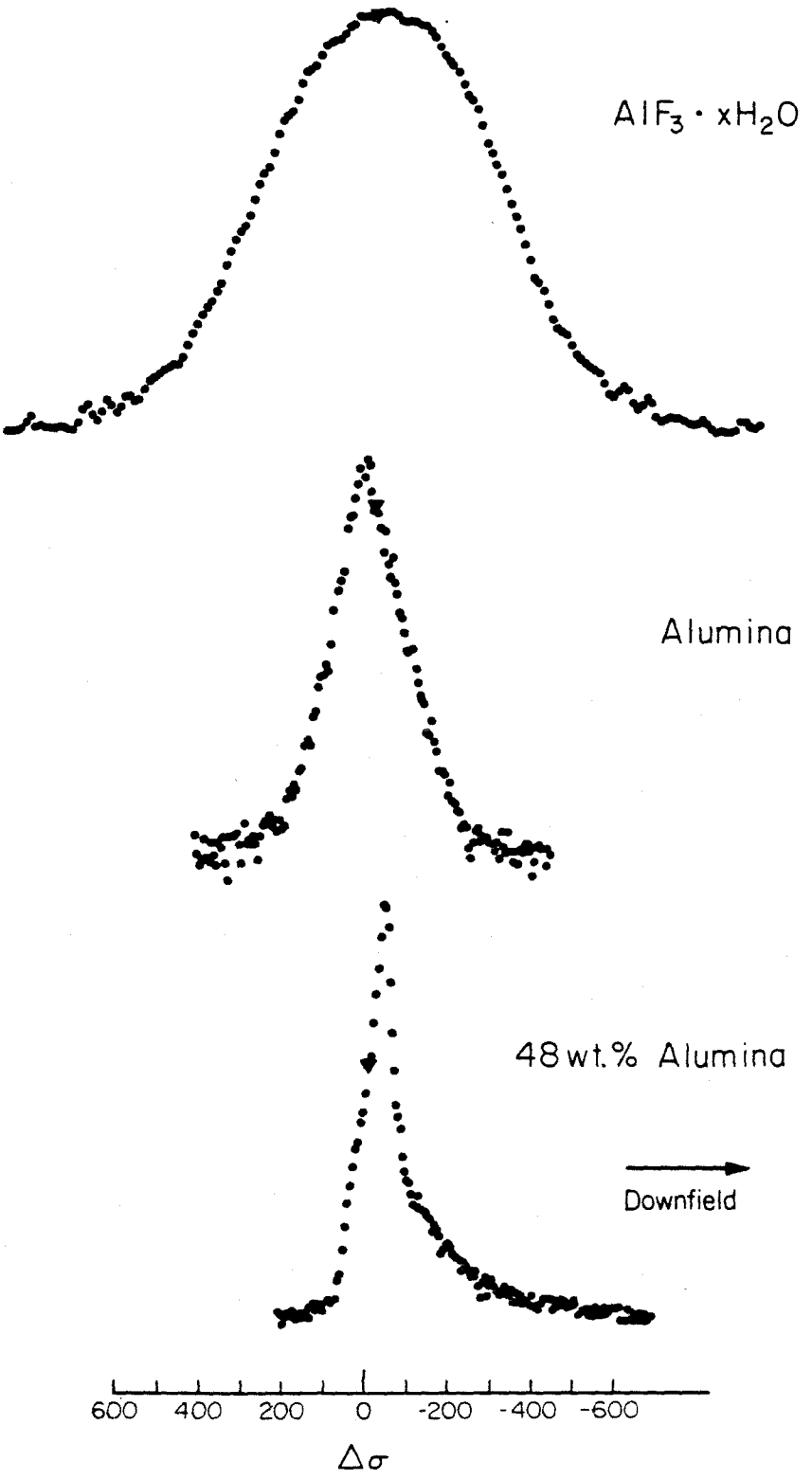

Fig. 2 ^{19}F powder patterns of materials with aluminum-fluorine interactions. The signal amplitude is plotted versus chemical shift (ppm) relative to hexafluorobenzene.

TABLE 1

PROTON AND FLUORINE CONCENTRATIONS FROM NMR DATA

	FLUORINE TREATMENT	PRETREATMENT TEMPERATURE (°C)	PROTONS PER 100 Å^2	FLUORINE ATOMS PER 100 Å^2	WEIGHT PERCENT FLUORINE
SILICA	LIGHT	300°	3.2	2.3	1.7
		400°	2.9	2.4	1.7
		500°	2.2	2.4	1.7
		600°	1.2	1.5	1.1
	HEAVY	300°	2.3	7.9	5.6
		600°	1.3	1.4	0.9
ALUMINA	LIGHT	300°	12.8	6.7	4.2
		600°	4.5	4.7	2.5